Development of new chromatographic methods for the characterization of the chemical composition distribution of ethylene propylene diene terpolymers

From the Department of Chemistry

at the Technischen Universität Darmstadt

submitted in fulfilment of the requirements for the

degree of Doctor of Engineering

(Dr.-Ing.)

Doctoral thesis

by Subrajeet Deshmukh

First Reviewer: Prof. Dr. Markus Biesalski

Second Reviewer: Prof. Dr. Rudolf Pfaendner

Darmstadt 2023

Development of new chromatographic methods for the characterization of the chemical composition distribution of ethylene propylene diene terpolymers

by Subrajeet Deshmukh

Thesis written in: Darmstadt, Technische Universität Darmstadt

Day of the viva voce: 19 June 2023

Date of submission: 3 April 2023

Year thesis published in TUprints: 2023

Dedicated to my Parents

for their constant support and encouragement

Acknowledgements

I would like to pay my sincere thanks to my research supervisor Prof. Dr. Markus Biesalski for giving me the opportunity to be a part of the doctoral program at TU Darmstadt. I would also like to thank Dr. Biesalski for his significant suggestions and critical inputs to my PhD presentations. I am grateful to Dr. Rudolf Pfaendner for being a part of my thesis committee, for his encouragement and helping me expedite the administrative process for our manuscript submission. A very special thanks to the thesis examiners, Dr. Christian Hess and Dr. Marcus Rose of TU Darmstadt for agreeing to be a part of the committee. I sincerely appreciate the alacrity with which they communicated with me while finalizing the date and time for the thesis defense.

The research during my doctoral thesis has been thoroughly enjoyable, which is largely a result of the interaction that I have had with my colleagues. I would like to take this opportunity to express my sincere and heartfelt gratitude to Dr. Robert Brüll for accepting me at Fraunhofer LBF. I still remember the first online meeting with him and the discussion about the possibilities of my research career in his group. He believed in me and gave me the opportunity to get a PhD in his research group. I truly appreciate his support, encouragement and guidance in various stages of my professional and personal life. I am grateful for the scientific knowledge and experience that I acquired and his contribution towards that achievement. For many people, these last few years have been very challenging both emotionally and mentally, especially because of the Covid-19 pandemic. I would like to thank Dr. Robert Brüll for his care and guidance in these tough times. A special thanks to Prof. Dr. Sampat Singh Bhati for recommending me to Dr. Robert Brüll and guiding me to carry out my PhD at Fraunhofer.

My special thanks to Dr. Tibor Macko and Dr. Jan Hendrik Arndt who were involved in each step of my doctoral research work, for their guidance and theoretical and technical training during the entire period of my stay at Fraunhofer LBF. Particularly their personal support and encouragement in writing publications have proved invaluable in my research activities. I can wholeheartedly say that I would not have been able to smoothly finish my PhD without their support and guidance. I would also like to thank Dr. Jan Hendrik Arndt who made life easier by helping me with German translation whenever I needed. I would like to thank Dr. Macko for his infectious enthusiasm which made my stay at Fraunhofer very memorable. I appreciate our engaging scientific discussions and his help with fixing instruments in our lab.

I wish to extend my gratitude to my colleagues in the department of Materials Analysis and Characterization starting with David Kot for making my transition to Fraunhofer LBF easy and helping me to acclimatize to the working culture in our lab. I would like to thank Dr. Frank Malz for his support with NMR measurements and his expert inputs in my research project. I would also like to thank Dr. Bastian Barton and Dr. Guru Geertz for their support and guidance in the field of Raman and Infrared spectroscopy respectively. I sincerely appreciate the scientific inputs from Dr. Guru Gertz during various stages of my PhD study. I would like to extend my regards to Dr. Jonas Keller for helping me with the SAP process and I eagerly look forward to collaborating with him. A big thank you to the administrative staff at Fraunhofer LBF for their invaluable assistance with my visa process and extensions and also taking care of the paperwork.

I am very grateful to our colleagues at Arlanxeo Netherlands B.V. for their financial support, for providing invaluable time and attention, and more importantly for their constant encouraging words. I would like to thank Dr. Gerard van Doremaele for taking immense interest in the research project, for his extremely useful critique on our manuscripts and for keeping our meetings very engaging. A special thanks to Dr. Raffaele Bernardo for being just a phone call away if I needed any help, for his invaluable inputs during our meetings, and for his help with improving the quality of our manuscripts. I would also like to thank him for taking care of the approval and administrative process thus making my life easier. I also take this opportuning to thank Niessen Sanders for his expert opinion and keeping a keen eye on the details when it came to reviewing the reports and manuscripts. I would also like to thank Dr. Victor Quiroga for his significant inputs and comments on the PhD project.

I would also like to take this opportunity to thank my colleagues from the National Chemical Laboratory, Pune, India, especially Dr. Guruswamy Kumaraswamy for his continuous support and encouragement during my stay at NCL. I sincerely thank him for his kind support when I needed it the most in my professional career. I would also like to thank him for believing in my potential and always pushing me to pursue excellence. I would also like to thank my group members at NCL Dr. Saurabh Usgaonkar, Dr. Bipul Biswas, Dr. Aakash Sharma, Prashant Yadav, Dr. Prophesar Kamdi and Dr. Nirmalya Bachhar for the engaging research discussions and making my stay at NCL extremely enjoyable and memorable.

I also take this opportunity to thank all the friends I made at my Alma Mater IIT Roorkee and UMass Amherst who made life very interesting and entertaining. A thank you is also due to Dr. Yuvraj Singh Negi, Dr Sanjay Palsule and Dr. Sujay Chattopadhyay for their support and encouragement.

Most importantly, I am ever so grateful to my dearest Mom, Dad, sister Nivi for their moral support, endless love, trust, and understanding throughout my life. Their motivational nature, enthusiasm and unwavering support in both good and difficult times will remain in my memory. Words cannot do justice to what I owe them and I would not have been here without their encouragement. I would also like to thank my cousin brother Aniket for being my closest friend and for our engaging discussions on science, philosophy and life.

During my PhD, I met and married the most important person in my life, my wife Saee. It was a rollercoaster of an experience getting married in times of Covid-19 pandemic. I cannot thank her enough for being my bestest friend and I will forever be indebted to her for her unconditional love, for her emotional support and being there for me anytime I needed. In the end, to put some philosophy in the Doctor of Philosophy, I borrow a quote ‘‘*It is neither the journey nor the destination that is important, it is the company*’’.

Die hier vorgestellten Untersuchungen sind das Ergebnis von Arbeiten die in der Zeit von Januar 2020 bis Dezember 2022 am Fraunhofer-Institut für Betriebsfestigkeit und Systemzuverlässigkeit LBF, Darmstadt unter der Leitung von Prof. Dr. Markus Biesalski und Dr. Robert Brüll durchgeführt wurden. This study is a result of the work carried out from January 2020 to December 2022 at Fraunhofer Institute for Structural Durability and Systems Reliability LBF, Darmstadt under the supervision of Prof. Dr. Markus Biesalski and Dr. Robert Brüll

Dieses Forschungsprojekt wurde durch ARLANXEO Netherlands B.V. finanziert und bildet Teil einer Kooperation zwischen der Abteilung Materialanalytik und Charakterisierung des Fraunhofer LBF und ARLANXEO Netherlands B.V, Geleen, The Netherlands.

Publications

1. Separation of Ethylene-Norbornene Copolymers using High Performance Liquid Chromatography
   Subrajeet Deshmukh, Tibor Macko, Jan-Hendrik Arndt, Frank Malz, Gerard van Doremaele, Raffaele Bernardo, Robert Brüll

   Journal of Chromatography A, 2021, 1652, 462367

2. Characterization of ethylene-propylene-diene terpolymers using high-temperature size exclusion chromatography coupled with an ultraviolet detector
   Subrajeet Deshmukh, Robert Brüll, Tibor Macko, Jan-Hendrik Arndt, Raffaele Bernardo, Sander Niessen

   Polymer, 2022, 242, 124585

3. Solvent selection for liquid adsorption chromatography of ethylene-propylene-diene terpolymers by combining structure-retention relationships and Hansen Solubility Parameters

   Subrajeet Deshmukh, Tibor Macko, Jan-Hendrik Arndt, Bastian Barton, Raffaele Bernardo, Gerard van Doremaele, Robert Brüll

   Industrial and Engineering Chemistry Research 2022, 61, 5672–5683

4. Critical conditions for liquid chromatography of statistical polyolefins: Evaluation of diene distribution in EPDM terpolymers
   Subrajeet Deshmukh, Tibor Macko, Jan-Hendrik Arndt, Frank Malz, Raffaele Bernardo, Sander Niessen, Gerard van Doremaele, Robert Brüll

   Analytica Chimica Acta 2023, 1246, 340856

5. Characterization of Unsaturated Polymers using High-Temperature Size Exclusion Chromatography coupled with Ultraviolet-Evaporative Light Scattering Dual Detection
   Subrajeet Deshmukh, Jan-Hendrik Arndt, Tibor Macko, Robert Brüll

   Macromolecular Symposia (In print)

6. Monitoring the chemical composition of polyolefins along the molar mass axis with high-temperature size exclusion chromatography coupled with an infrared detector (HT SEC-IR5)

   Hamza M. Aboelanin, **Subrajeet Deshmukh**, Tibor Macko, Jan-H. Arndt, Stepan Podzimek, Robert. Brüll

   Macromolecular Symposia (In print)

7. Separation of amorphous and semicrystalline parts of LLDPE with high-temperature interactive liquid chromatography

   Tibor Macko, Jan-Hendrik Arndt, **Subrajeet Deshmukh**, Frank Malz, Youlu Yu, Masud Monwar, Robert Brüll

   (Submitted to Journal of Applied Polymer Science, Wiley)

Conference Presentations (Virtual)

1. Separation of Ethylene-Norbornene Copolymers using High Performance Liquid Chromatography *Society of Plastics Engineers International Polyolefins Conference 2021*
2. Separation of ethylene-propene-diene and ethylene-norbornene copolymers using high temperature high performance liquid chromatography (HT-HPLC). *Asian Polyolefin Workshop 2021*
3. Characterization of Polyolefins using High-Temperature Size Exclusion Chromatography Coupled with an Ultraviolet Detector. *POLY-CHAR 2022*
4. Monitoring the chemical composition of polyolefins along the molar mass axis with high-temperature size exclusion chromatography coupled with an infrared detector. *POLY-CHAR 2022*
5. Solvent Selection for Liquid Adsorption Chromatography of EPDM Copolymers by Combining Structure-Retention Relationships and Hansen Solubility Parameters. *Society of Plastics Engineers International Polyolefins Conference 2023*
6. A novel approach for evaluating the suitability of non-chlorinated solvents for liquid adsorption chromatography of polyolefin elastomers. *International Conference on Polyolefin Characterization 2023*
7. Application of high-temperature size exclusion chromatography coupled with dual detection for measuring the distribution of unsaturation in EPDM terpolymers. *International Conference on Polyolefin Characterization 2023*

Published Posters

1. Characterization of ethylene-propylene-diene terpolymers using high-temperature size exclusion chromatography coupled with an ultraviolet detector

   November 30, 2022 (DOI: https://doi.org/10.54985/peeref.2211p1950002)
2. Characterization of Polyolefins using High-Temperature Size Exclusion Chromatography Coupled with an Infrared Detector (HT-SEC-IR5)

   December 06, 2022 (DOI: https://doi.org/10.54985/peeref.2212p1310865)

List of Contents

1 Summary

Ethylen-Propylen-Dien-Terpolymere (EPDM) gehören zur Klasse der Polyolefinelastomere und sind, dem Volumen nach, die wichtigsten Elastomere für Anwendungen abseits von Reifen. In EPDM-Terpolymeren werden die Monomere statistisch eingebaut, was zu ihrem amorphen und elastischen Charakter führt. Die extrem vielseitigen Endverwendungseigenschaften, wie Elastizität, Füllstoffakzeptanz, Ozon- und UV-Resistenz, werden durch ein gutes Kosten/Performance-Verhältnis ergänzt. Diese Vorzüge treiben die Verwendung von EPDM in einer Reihe von neuartigen und vielfältigen Anwendungsgebieten voran. Die beschriebene Vielseitigkeit kann erreicht werden, da die molekularen Heterogenitäten durch Fortschritte im Bereich der Katalysator- und Prozesstechnologie gesteuert werden können. Gleichzeitig bedingt sie aber auch die Entwicklung umfassender, präziser Analysetechniken zu deren molekularer Charakterisierung.

Die am häufigsten eingesetzten Diene sind 5-Ethyliden-2-Norbornen (ENB), Dicyclopentadien (DCPD) und Vinylnorbornen (VNB). Wenn sie durch Koordinationspolymerisation in die Polymerkette eingebaut sind, stellen sie eine Doppelbindung zur Verfügung die es dann erlaubt das Material nach der Polymerisation zu vulkanisieren (z.B. mit Schwefel, Peroxiden oder phenolischen Harzen). Ihrer kommerziellen Bedeutung nach lassen sich die Diene folgendermaßen ordnen: ENB > DCPD > VNB. ENB ist das Dien mit der weitesten Verbreitung da es sich aus kommerzieller Sicht am effizientesten mittels Schwefel vulkanisieren lässt. VNB zeigt eine herausragende Peroxidvulkanisierungseffizienz, während DCPD, das günstigste aller nichtkonjugierten Diene die bei der EPDM-Produktion eingesetzt werden, eine geringfügig höhere Effizienz bei Peroxidvulkanisation als ENB zeigt.

Die Größenausschlusschromatografie (*size exclusion chromatography*, SEC) ist ein wichtiges Werkzeug zur Bestimmung der Molmassenverteilung (*molar mass distribution*, MMD) und kann, unter Verwendung eines geeigneten Detektors, auch dazu verwendet werden, die Verteilung eines Comonomers entlang der Polymermolmasse zu bestimmen. Die Ergebnisse können Einblicke in den Polymerisationsmechanismus gewähren und dabei helfen ein Verständnis von Struktur-Eigenschaftsbeziehungen zu entwickeln. Wie in verschiedenen Arbeiten gezeigt, konnte der Einfluss der Katalysatorstruktur auf die Comonomerverteilung in linearem Polyethylen geringer Dichte durch die Kopplung von SEC und FTIR aufgeklärt werden. SEC-FTIR von EPDM wurde ebenso bereits vorgestellt. SEC-IR ist eine Standardmethode zur Bestimmung des EP-Verhältnisses, jedoch nicht für die Bestimmung des Diengehalts geeignet. Der LC-Transform-Ansatz für SEC-IR ist grundsätzlich zur Bestimmung

des Doppelbindungs-Gehalts geeignet, der Einsatz ist jedoch mühsam und nicht in einem Routine-Kontext denkbar. Dies eröffnet eine technologische Lücke die potenziell durch -SEC-UV geschlossen werden könnte.

Soweit bekannt gibt es nur sehr wenige Untersuchungen zur UV-Absorption von Polymeren die isolierte und nicht-konjugierte Doppelbindungen enthalten. Im ersten Kapitel wird gezeigt, wie ein mit der SEC gekoppelter UV-Detektor verwendet werden kann, um das Verhalten von EPDM-Terpolymeren zu untersuchen. Zu diesem Zweck wird der Einfluss wichtiger experimenteller Parameter auf die UV-Absorption von Ethylidennorbornen (ENB), Vinylnorbornen (VNB) und Dicyclopentadien (DCPD) bewertet. Die Ergebnisse werden dann verwendet, um den ENB-Gehalt entlang der MMD zu bestimmen.

Die Eigenschaften von Polyolefinen können durch Variation der mittleren Molmasse (MM) und der chemischen Zusammensetzung (CC), sowie Variation der den beiden Größen zu Grunde liegenden Verteilungen (MMD und CCD), angepasst werden. Die CCD von Polyolefinen wurde in der Vergangenheit häufig mittels Kristallisations-basierter Methoden wie Elutionsfraktionierung unter Temperaturerhöhung (*temperature rising elution fractionation*, TREF), analytischer Kristallisationsfraktionierung (*crystallization analysis fractionation*, CRYSTAF) und Kristallisationselutionsfraktionierung (*crystallization elution fractionation*, CEF) bestimmt. Diese Methoden basieren auf der Kristallisation von Makromolekülen aus einer verdünnten Lösung, die wiederum mit der Polymerzusammensetzung in Zusammenhang steht, und können daher nicht für amorphe Polymere angewendet werden. Die Flüssigadsorptionschromatografie (*liquid adsorption chromatography*, LAC) hat sich, unter Verwendung von porösem grafitischem Kohlenstoff (*porous graphitic carbon*, PGC) als stationärer Phase, zu einer zuverlässigen Methode für die Bestimmung der CCD von Polyolefinen entwickelt und auch für die Charakterisierung von amorphen, olefinbasierten Elastomeren als wertvoll erwiesen. Die LAC trennt Makromoleküle basierend auf deren selektiver Adsorption auf einer grafitischen Oberfläche bei einer spezifischen Temperatur und Zusammensetzung der mobilen Phase. Die selektive Adsorption kann entweder isotherm (durch Variation der Zusammensetzung der mobilen Phase, sogenannte Lösungsmittelgradientenwechselwirkungs-chromatografie (*solvent gradient interactive chromatography*, SGIC) oder isokratisch (durch Variation der Temperatur, sogenannte Wechselwirkungschromatografie mit thermischem Gradienten (*thermal gradient interactive chromatography*, TGIC) erreicht werden.

Mehrere Forschergruppen haben sich mit der Suche nach Lösungsmitteln für die LAC von Polyolefinen beschäftigt. Dennoch gibt es keine umfassenden Erkenntnisse zum Einfluss der chemischen Struktur der adsorptions- und desorptionsfördernden Lösungsmittel auf das chromatografische Verhalten von Polyolefinen. Hinzu kommt, dass die LAC von EPDM-Terpolymeren nach wie vor ein weitgehend unerforschtes Gebiet ist. Im zweiten Teil dieser Arbeit wirddaher ein rationaler Ansatz für die Auswahl von Lösungsmitteln für die Adsorptionschromatografie von EPDM-Terpolymeren erarbeitet. Zunächst wird eine Reihe von Benzolderivaten als mobile Phase für die Trennung von EPDM-Terpolymeren auf PGC verwendet. Zwischen der molekularen Struktur der aromatischen Lösungsmittel und ihrem Einfluss auf die Retention von EPDM auf der grafitischen Oberfläche werden Zusammenhänge hergestellt. Abschließend wird eine Methode entwickelt, um die Lösungsmittelauswahl für die Flüssigchromatografie von EPDM effizienter zu gestalten.

Zwischen den Grenzfällen SEC und LAC heben sich entropische Effekte und enthalpische Wechselwirkungen an einem bestimmten Punkt gegenseitig auf. Dies bezeichnet man als Flüssigchromatografie bei kritischen Bedingungen (*liquid chromatography at critical conditions*, LCCC) und Makromoleküle, die identische Wiederholungseinheiten enthalten, eluieren unabhängig von ihrer Molmasse, sodass eine Trennung nach anderen molekularen Parametern erreicht werden kann.

Verschiedene Forschergruppen haben sich mit dem Einsatz von LCCC zur Analyse von Blockcopolymeren durch Verwendung von CC für eines der beiden Homopolymere beschäftigt. Jedoch gibt es keine Studien, die einen ganzheitlichen Ansatz für die Identifizierung von CC für statistische Copolymere darlegen. Im dritten Teil dieser Arbeit werden CC für statistische Ethylen-Propylen-Copolymere (EP-Copolymere) unterschiedlicher chemischer Zusammensetzung erarbeitet. Dazu werden geeignete Lösungsmittelkandidaten unter Verwendung eines kürzlich veröffentlichten Ansatzes, der Struktur-Retentions-Beziehungen und Hansen-Löslichkeitsparameter verwendet, ausgewählt. Da die CCD von EPDM-Terpolymeren weiterhin ein weitgehend unerforschtes Gebiet ist, ist davon auszugehen, dass die ermittelten CC ein hilfreiches Werkzeug für die Diengehalt-basierte Trennung und Charakterisierung von EPDM-Terpolymeren darstellen

Die Beziehung zwischen der MMD und den anderen molekularen Heterogenitäten von Polymeren (z.B. CCD x MMD) kann durch die Kopplung von HPLC und SEC untersucht werden. Dieses Konzept, das auch als zweidimensionale Flüssigchromatografie (*two-*

dimensional liquid chromatography, 2D-LC) bekannt ist, wurde zur Charakterisierung von Polymeren entwickelt und in anderen Arbeiten ausführlich vorgestellt.

In den meisten Fällen wurden 2D-LC-Ergebnisse als Kontourplots dargestellt und qualitativ verglichen. Das relative Volumen von Bereichen in verschiedenen Kontourplots wurde verglichen, um quantitative Informationen zur Zusammensetzung von Proben zu erhalten. Dieses Vorgehen liefert jedoch weder quantitative Informationen zu Anteilen, die in beiden Proben vorhanden sind (also Spezies die eine identische Molmasse wie auch chemische Zusammensetzung aufweisen), noch zu Bereichen, die nur in einer der beiden verglichenen Proben vorhanden sind (unterschiedliche oder einzigartige Anteile). Im Falle von 2D-LC-NMR wurden ebenfalls Informationen zu den molekularen Heterogenitäten in verschiedenen Polymeren in Form von Kontourplots erhalten.

Im letzten Kapitel dieser Arbeit werden EPDM-Copolymere mit unterschiedlicher durchschnittlicher chemischer Zusammensetzung unter Verwendung von HT 2D-LC/IR analysiert und es wird eine Methode zur Quantifizierung der identischen und einzigartigen Anteile in den Proben beschrieben werden. Die Kontourplots welche diesen EPDM-Copolymeren entsprechenden werden erstellt und die Matrizes die diesen Kontourplots entsprechen werden zur Quantifizierung eingesetzt.

2 Ethylene Propylene Diene (EPDM) terpolymers

Ethylene-propylene-diene (EPDM) terpolymer is the largest by volume and commercially most important non-tire elastomer. This can be attributed to the increasing demand due its superior application properties [1-3].

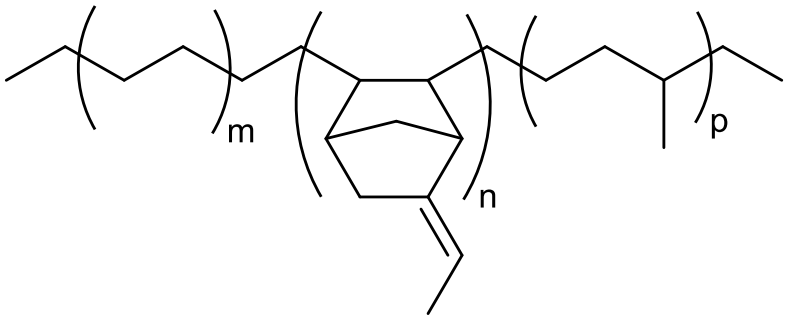

Fig. 2.1 Chemical structure of EPDM terpolymer. In the picture, the non-conjugated diene is 5-ethylidene-2-norbornene (ENB) [164].

It is well-known that ethylene-propylene copolymers (EPM) generally require the incorporation of a certain amount of a non-conjugated diene as third monomer (EPDM) which provides pendant unsaturation to the polymer chain. The unsaturation enables sulfur vulcanization of the rubber and the fully saturated EPM main chain is retained. This explains the excellent heat and ozone resistance and thus, excellent outdoor performance that is characteristic for EPDM rubber [3-5].

EPDM is exclusively produced via catalytic coordinative insertion polymerization [6, 7]. The most typically employed dienes are 5-ethylidene-2-norbornene (ENB), dicyclopentadiene (DCPD), and vinyl norbornene (VNB). The incorporated dienes provide a double bond to allow post-polymerization curing (e.g. with sulphur, peroxides, phenolic resins), and the order of commercial relevance is ENB > DCPD > VNB. ENB is the most widely used diene as it provides the highest efficiency of sulfur vulcanization at best commercial compromise from a commercial point of view [8]; VNB provides outstanding peroxide curing efficiency, [9, 10] while DCPD has the lowest cost of all non-conjugated dienes applicable for EPDM production and shows a peroxide curing efficiency, marginally greater than that of ENB [10]. The chemical structures of the most common dienes are shown in **Fig. 2.2**.

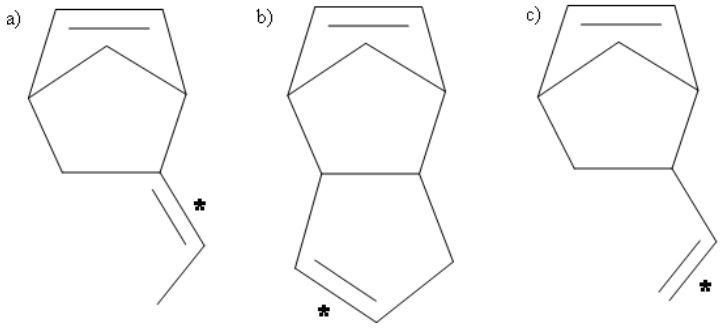

Fig. 2.2 Chemical structures of a) ENB b) DCPD c) VNB; the asterisk denotes the double bond which remains unaltered during terpolymerization with ethylene and propylene [164].

The tremendous versatility of EPDM properties can be credited to wide range of products that can be obtained via varying the ethylene content, diene content, molar mass (MM) and degree of branching, and the underlying distributions. All of these can be fine-tuned to meet the end use application [1-5, 11].

The selectivity of the employed catalysts plays a crucial role in determining the chain microstructure and therefore intimately influences the application performance of the EPDM produced [12, 13]. Polyolefin catalyst technology has seen tremendous development in the past 60 years, starting with Ziegler Natta (ZN) to metallocene and now the most recent post-metallocene catalysts leading to an ever-larger variety of EPDM copolymers [10, 14-16]. In general, EPDM produced by ZN exhibits a broad distribution with regard to molar mass and chemical composition [17], while single-site catalysts yield narrow CCD and MMD [18].

The metallocene catalyst systems allow an efficient incorporation of the dienes with ethylene and propylene into the polymer chain [3], thus widening the possibilities of designing EPDM rubber with customized end use properties. Conventional EPDMs are largely limited to ethylene contents between approximately 40 and 80 % by weight. Propylene conversion limits its incorporation in the polymer chain to a maximum value of about 40 wt. %. The incorporation of ethylene is limited by the final polymer crystallinity as it influences the polymer solubility during polymerization [3, 10]. On the other hand, metallocene catalysis allows better propylene conversions, so elastomeric propylene based EPDMs are attainable. Ethylene is converted with longer sequences, which translate to higher crystallinity than conventional ZN catalysts based EPDMs at comparable ethylene content. In rubber applications, the content of ethylene is generally above 40 wt. % in weight, to retain sufficient physical properties, especially at elevated temperature. EPDMs with ethylene content above 80 % do not possess enough elastomeric properties [3, 10].

Metallocene catalysts allow polymerization to take place at elevated temperatures compared to conventional processes [3]. Less catalyst is used and higher concentrations of polymer in the reactor solution can be achieved so that the solvent elimination process is more energy efficient. A key characteristic of the metallocene catalysts [3, 18] is their ability to design EPDMs with a very uniform molecular architecture. The molar mass distribution is generally narrower, which offer an effective ENB incorporation for better cross-linking with sulfur, resulting in faster cure rate and higher cured product [3].

3 Characterization of molecular heterogeneity present in synthetic polymers

3.1 Molecular Heterogeneity in Polymers

Polymers may exhibit different types of molecular heterogeneities which are interdependent of each other. Each macromolecule is built up of repeating units, and the number of monomer units forming a polymer chain is called degree of polymerization (DP). The length of macromolecules in each sample may vary, resulting in a molar mass distribution (MMD). Average molar masses can be calculated from the MMD with the most common ones being the weight average molar mass (M_w) and the number average molar mass (M_n). Each polymer chain (except cyclic and branched structures) comprises of two end groups. Macromolecules can differ in their architecture i.e. linear, cyclic or branched (star or comb like). In copolymers, the composition of the individual polymer chain may vary from one to another as well as their composition along the chain, resulting in an inter- and intramolecular chemical composition distribution (CCD). Segregation of monomer sequences along the polymer chain is defined as the degree of blockiness of the copolymer. The different types of molecular heterogeneities in a polymer sample are shown **Fig. 3.1** [19].

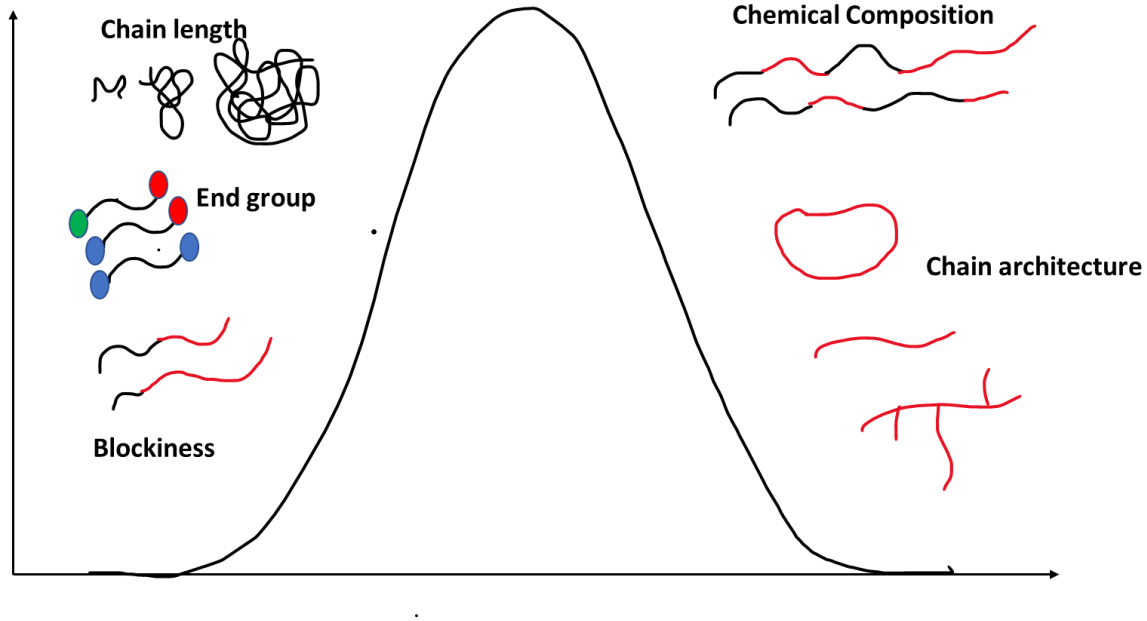

Fig. 3.1: Schematic representation of the different molecular heterogeneities occurring in polymers [27].

Measuring these heterogeneities is crucial in developing structure-property relationships and to understand the polymerization mechanism and kinetics. Additionally, the molecular heterogeneities are useful to develop processing - property relationships and to enhance the end-use properties of polyolefins. Fractionation techniques are used to separate

macromolecules according to molar mass, chemical composition, long chain branching or microstructure [20]. Thus, comprehensive characterization of the material molecular metrics establishes a link between polymer properties and polymerization conditions [21]. In the fast few decades, there has been an increased interest in polyolefin synthesis with well-defined structure and tailored properties. Consequently, this has resulted in a strong demand for methods which allow an in-depth characterization of macromolecular microstructure and at the same time can applied in routine lab environments.

3.2 Chromatographic techniques for the characterization of polymers

High performance liquid chromatography (HPLC) is a powerful tool for in-depth polymer characterization [22-26]. Over the last few decades, HPLC has served as a principal characterization tool to analyze complex copolymers, which exhibit various types of molecular heterogeneities. Depending on the separation mechanism, three modes of chromatographic may be distinguished (**Fig. 3.2).**

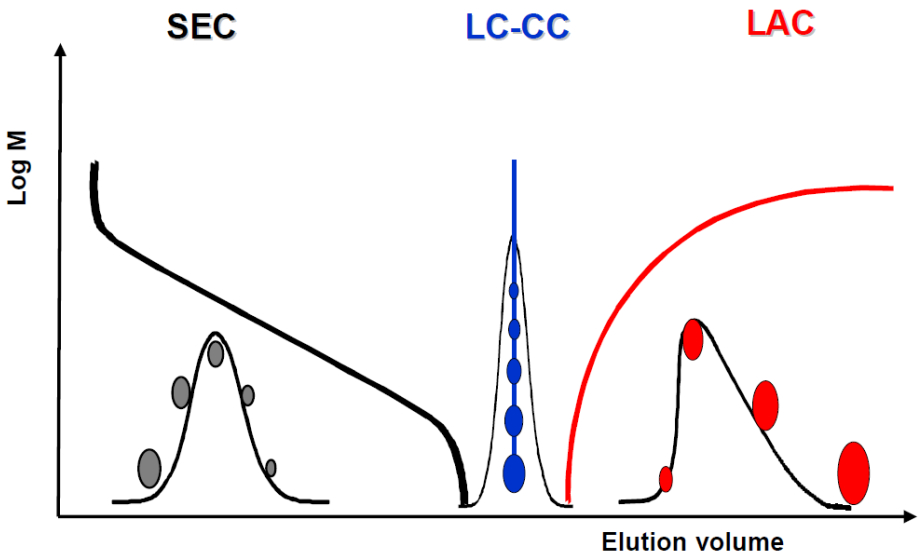

Fig. 3.2 Chromatographic behavior with respect to polymer molar mass in the three chromatographic modes [27].

In the size exclusion chromatography (SEC) mode, macromolecules are separated with regard to their size in solution (hydrodynamic volume). The elution volume generally decreases with an increase in molar mass. The separation in SEC mode is driven by entropy [28]. SEC of polyolefins and polyolefin elastomers is carried out at temperatures between 130 and 160 °C, which are required for their dissolution. In liquid adsorption chromatography (LAC), the separation is modulated by enthalpic interactions between the analyte and the stationary phase,

and the elution volume usually increases with the molar mass of the macromolecules until a critical molar mass is reached [29]. Chromatographic conditions inside the column are such that the macromolecules interact with the stationary phase and subsequently elute solely according to their chemical composition if the molar mass exceeds the critical threshold [29].

In liquid chromatography at critical conditions (LCCC), the enthalpic and entropic interactions balance each other, and the macromolecules of a given homopolymer elute at the same time irrespective of their molar mass. The critical conditions were first identified by Belenky and Tennikov [30-32]. The critical conditions for a given homopolymer or monomer unit of a block copolymer vary with temperature and mobile phase [30]. LCCC is of immense practical significance because it allows to realize separations that are not achievable with other modes of chromatography. For example, LCCC has been extensively applied for the separation of block copolymers by using critical conditions (CC) for a particular block, while the other block elutes in SEC mode [33-37].

In a chromatographic experiment, the polymer sample is dissolved in a solvent. The solution is then injected into a column. The separation in a chromatographic process is related to the selective distribution of the analyte between the mobile phase and stationary phase [38]. The separation process in liquid chromatography can be described by **equation 3.1**:

$$\Delta G = \Delta H - T\Delta S = -RT \ln K_d \qquad (3.1)$$

R is the universal gas constant, T is the absolute temperature, ΔH and ΔS are the changes in interaction enthalpy and conformational entropy, respectively, and $K_d$is the distribution coefficient, which corresponds to the ratio of the analyte concentration in the stationary phase and mobile phase.

K_d is related thermodynamically to the free energy difference ΔG of the molecules in the two phases [39]. This difference in free energy comprises of enthalpic (ΔH) and entropic (ΔS) contributions [40]. Experimentally, K_d is determined from the following **equation 3.2**:

$$K_d = \frac{C_{SP}}{C_{MP}} \qquad (3.2)$$

C_{SP} and C_{MP} are the concentrations of the analyte in the stationary phase and mobile phase, respectively. When studying small molecules, the entropic term does not play an important role compared to the enthalpic term. However, for macromolecules the entropic term is crucial since polymer molecules are able to undergo large changes in conformation when they are in the dissolved state in solution or adsorbed on the stationary phase [28].

3.2.1 Size exclusion chromatography (SEC)

SEC is the most prolific characterization technique to separate macromolecules according to their molar mass. In an SEC experiment, the separation is accomplished exclusively with respect to the hydrodynamic volume of the macromolecules, and ΔH, ideally, is negligible. In other words, there is no interaction between the stationary phase and the polymer molecules [22, 41]. The distribution coefficient is given by **equation 3.3**:

$$K_d = K_{SEC} = \exp\left(\frac{\Delta S}{R}\right) \tag{3.3}$$

Macromolecules which enter a pore are restricted with respect to the number of possible conformations. resulting in a decrease of their conformational entropy. As the conformational entropy decreases ($\Delta S < 0$), the distribution coefficient, $K_{SEC,}$ is < 1 in an ideal SEC experiment. The larger the hydrodynamic volume of the macromolecule, the greater the decrease in its conformational entropy. Consequently, macromolecules with the largest hydrodynamic size in the solution elute in the beginning, and elution occurs in the order of decreasing hydrodynamic volume [22, 41].

The mobile phase should dissolve completely the polymer and prevent interactions between the stationary phase and the macromolecules. These attributes are typically satisfied by a thermodynamically good solvent. As a result, separation is only a function of entropic effects [63]. As SEC separates according to hydrodynamic volume, macromolecules having the same hydrodynamic volume but differing in their chemical composition cannot be distinguished by SEC alone. For an accurate analysis of such polymers, hyphenating SEC with spectroscopic techniques like FTIR [42, 43] or NMR [44, 45] facilitates in determining the average chemical compositions along the molar mass axis.

3.2.2 Liquid Adsorption Chromatography (LAC)

LAC has been widely employed to separate polymers soluble at ambient temperatures according to their chemical composition [24, 39, 40]. The separation is driven by enthalpic interactions between the macromolecules and the stationary phase. In LAC, conformational changes are assumed to be zero ($\Delta S = 0$) because the pores of the stationary phase are large enough to accommodate all macromolecules. The enthalpic contribution (ΔH) is due to attractive interactions of the molecules with the stationary phase. Macromolecules with higher molar mass are adsorbed stronger on the stationary phase and elute later than macromolecules having lower molar mass [39, 40]. This is because higher molar mass molecules contain more

monomeric units that lead to stronger interactions with the stationary phase and hence retain longer on the column surface.

The distribution coefficient in adsorptive mode is given by **equation 3.4**:

$$K_d = K_{LAC} = \exp \frac{(-\Delta H)}{RT} \quad (3.4)$$

As ΔH is negative, the values of the distribution coefficient K_{LAC} are > 1. To accomplish enthalpic interactions between the macromolecules and the stationary phase, typically a thermodynamically poor i.e., adsorption-promoting solvent is used as the mobile phase. There is a general correlation between elution strength and the thermodynamic quality of a solvent, but this is not always true. By adding a thermodynamically good (desorption-promoting) solvent, the enthalpic interactions between the macromolecules and the stationary phase are diminished. Consequently, the macromolecules elute in an inverse correlation with respect to their molar mass i.e., small molecules elute first and large ones elute later, provided that we are considering only chemically homogeneous molecules. Thus, the molar mass dependency in LAC is opposite to that in SEC. The strength of interaction between the analyte molecules and the stationary phase can be either controlled by the eluent composition (i.e., solvent gradient) and/or the temperature [27].

3.2.3 LAC of polyolefins

The chromatographic separation of semi-crystalline polyolefins necessitated the use of higher temperature in order to dissolve the polymer and keep it in solution. This created a technology gap in characterizing polyolefins and led to the development of high-temperature LAC (HT-LAC). An HT-LAC method for separation of polyolefins according to their chemical composition was not reported until lately due to the absence of a stationary phase that could reversibly adsorb polyolefins from solution at conditions needed for a chromatographic separation.

In 2003, in the nascent stages of method development, Macko et al. showed the irreversible retention of linear PE and isotactic PP from dilute solution on zeolites as a stationary phase. However, the adsorbed polymer could not be desorbed from the zeolite and thus this approach was deemed infeasible for characterizing the CCD of polyolefins [46-49]. Subsequently, in 2005 Heinz et al. separated HDPE and iPP blends by using silica-gel as the stationary phase and applying a TCB → ethylene glycol monobutyl ether (EGMBE) gradient as the mobile phase. Separation was achieved by a mechanism of precipitation/dissolution (EGMBE is a solvent for iPP and does not dissolve PE). However, the separation was considerably influenced

by the molar mass of the polymer, which outweighs the effect of chemical composition [50-52].

The breakthrough was achieved with the use of porous graphitic carbon (PGC) as the stationary phase for polyolefin separation in 2009 [53-57]. The development of PGC for liquid chromatography, commercially available as Hypercarb^{TM}, is credited to Knox et al. PGC comprises of porous spherical particles with a surface that is crystalline and devoid of micro-pores [58].

LAC can be conducted in two ways based, depending on the type of gradient that governs the separation. When the latter is controlled by varying the mobile phase composition, and keeping the temperature constant, the LAC method is called solvent gradient interactive chromatography (SGIC). On the other hand, if the separation is controlled by varying the temperature of the stationary phase at isocratic mobile phase composition, the method is referred to as thermal gradient interactive chromatography (TGIC).

3.2.4 Liquid chromatography at critical condition (LCCC)

Liquid chromatography at critical conditions (LCCC) is the third mode of chromatography which exists at the transition between SEC and LAC. LCCC is achieved for a given combination of polymer/stationary phase/mobile phase at a specific temperature when the entropic contribution completely equals the enthalpic one i.e., $\Delta G = 0$. In LCCC the macromolecules with identical repeating units elute independent of their molar mass and their elution behavior is determined by slight changes in mobile phase composition or temperature. LCCC has been applied for:

1. Separation of block copolymers [34, 59-65]
2. Determining the molar mass distribution of constituent blocks in di- and tri-block copolymers [66, 67]
3. Separation of end-functionalized polymers based on the type of functional group [68, 69]
4. Separation of polymers based on their architecture (for example, linear from star-shaped, or linear from rings) [70-73]

3.2.5 Two-dimensional Liquid Chromatography

As the size of a macromolecule in solution depends on different molecular parameters such as molar mass, chemical composition and chain architecture, selective separations of macromolecules with regard to these metrics provide crucial structure-property information.

on d. MMD and CCD are the two fundamental molecular parameters which are of interest in industrial polyolefins, as they predominantly influence the end use properties of the final products. Even though these can be studied independently by HPLC and SEC, the relationship between MMD and CCD can only be retrieved by coupling the two chromatography modes (2D-LC). This procedure was first applied for the analytical characterization of synthetic polymers by Balke [74] in 1982 and subsequently developed by Pasch [75, 76] and Kilz [77, 78].

Two-dimensional chromatography consists of off-line [79-82] or on-line [83, 84] collection of eluent fractions from the first chromatographic separation (D1) followed by re-injection of the individual fractions into the second chromatographic system (D2). However, the off-line approach runs into the challenging problem of obtaining a sufficient number of analyte fractions to describe the elution profile of the D1 chromatographic separation. This drawback is overcome by on-line coupling, giving rise to comprehensive two-dimensional liquid chromatography [85]. Therefore, on-line automated 2D-LC has gained popularity in recent times. **Fig. 3.3** shows the scheme of an on-line two-dimensional liquid chromatographic system.

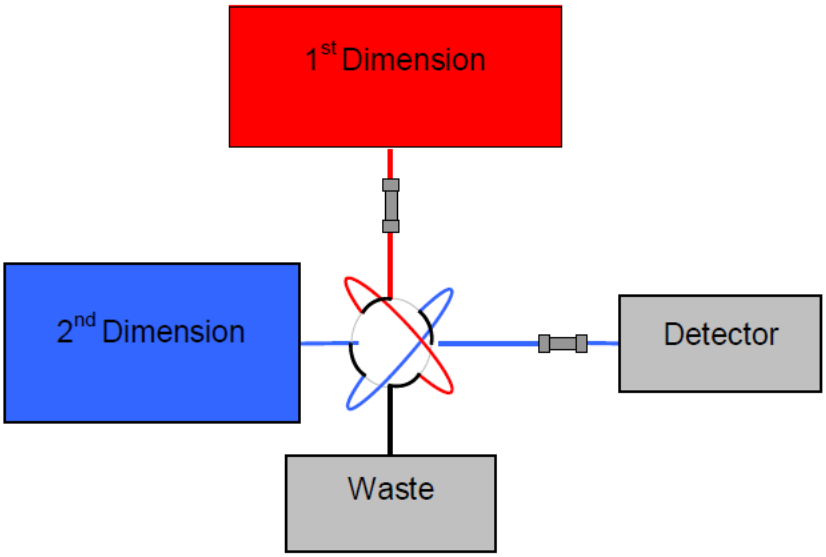

Fig. 3.3 Schematic representation of a 2D-LC system, in red the first-dimension route (D1), in blue the second-dimension route (D2) [27].

The coupling between the two dimensions is achieved via a switching valve equipped with two loops. As one of them collects the eluent from the D1 column, the sample having been collected in the other loop is injected into the D2 column. The separation in the D2 column has

to be completed within the time frame defined by the ratio of the volume collected in sample loop divided by the flow rate of D1 [86]. To represent a continuous distribution, a large number of fractions from the D1 separation, each with a small volume, is required. High speed in the D2 separation is thus mandatory to analyze the sample in a reasonable time.

Using HPLC as D1 and SEC as D2 (HPLC x SEC) has been widely performed [87-89], whereas studies on 2D LC by SEC x HPLC were seldom reported [90]. The acceptance of the former arrangement is because the speed of SEC separation can be easily increased. Parameters such as column length, flow rate, and temperature were investigated to achieve better resolution at high operation speed [91,92]. An important benefit is that multiple detectors can be used in the HPLC x SEC configuration, but not in the SEC x HPLC case. However, such separations were realized at high temperatures only recently for functionalized semicrystalline polyolefins [93], ethylene/1-olefin copolymers [94], and polyolefin blends [95, 96]. Polymer samples go through two fractionation stages in 2D-LC, ultimately yielding very diluted solutions of the analyte fractions. Highly sensitive detectors are thus essential for quantitative analysis.

3.3 Nuclear magnetic resonance (NMR) spectroscopy

NMR spectroscopy is a powerful technique for the analysis of chemical structure and has broad applications in the field of organic chemistry, biochemistry and medical sciences to name a few. The principle of NMR is based on the quantized interaction of the magnetic dipole moment of a nucleus with an external magnetic field. In the absence of an external magnetic field, the nuclei are aligned such that the magnetic dipoles are randomly oriented. However, when an external magnetic field is applied, the dipoles orient in different quantized energy states based on an energy difference, ΔE, governed by:

$$\Delta E = \left(\frac{h\gamma}{2\pi}\right) B_0 \tag{3.5}$$

Where, γ = *gyromagnetic ratio*

h = *Planck's constant*,

B_0 = the strength of the external magnetic field.

The energy states in the presence and absence of an external magnetic field for ^1H are shown in **Fig. 3.4**.

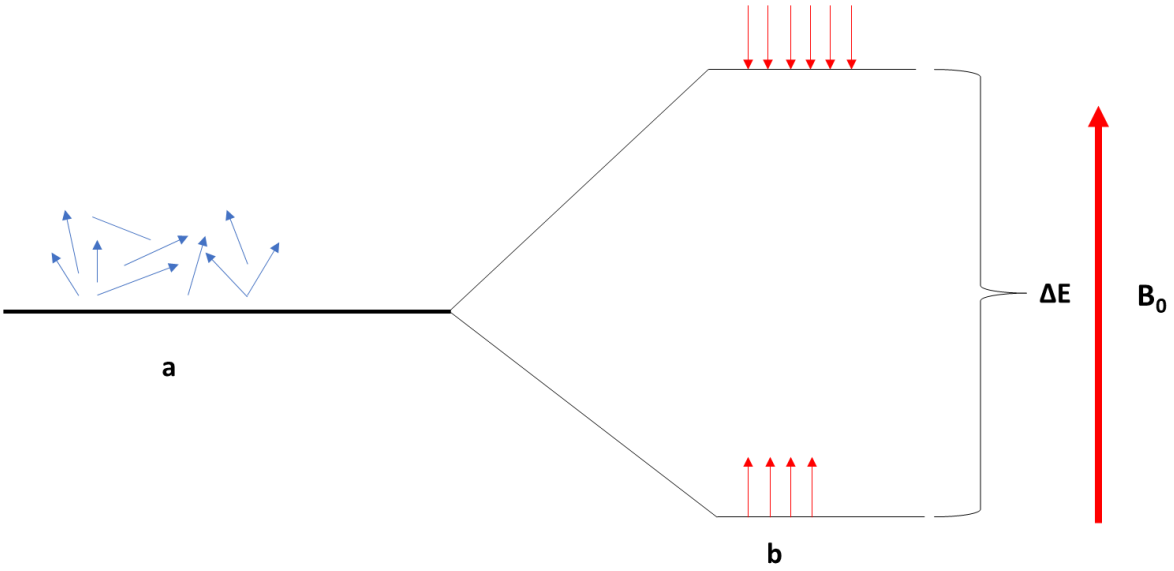

Fig. 3.4 Representation of spins of ^{1}H atoms under (a) no magnetic field and (b) external magnetic field B.

The applied magnetic field not only interacts with the nucleus but also with the electrons spinning around the nucleus. The spinning electrons induce a secondary small magnetic field which modulates the effective magnetic field experienced by the nuclei. Due to the chemical nature of a molecule, the electron cloud is distributed unevenly and the magnetic field experienced by a specific nucleus depends on its electronic environment. This provides important information about the molecular structure of the sample being analyzed. Examples of nuclei studied in NMR are ^{1}H, ^{13}C, ^{15}N, ^{19}F, ^{31}P, etc. Among these, ^{1}H and ^{13}C are the most ubiquitous and hence most commonly investigated in NMR spectroscopy.

3.3.1 NMR of polyolefins

For polyolefins, NMR spectroscopy serves as an excellent characterization tool for structure elucidation. A variety of structural information may be obtained from an NMR-spectrum by studying the *chemical shift* (ppm) which signifies the ΔE relative to the reference proton (e.g., ^{1}H in **Fig. 3.4**). A reference is normally chosen, e.g., tetramethylsilane (TMS), whose chemical shift is assigned 0.00 ppm, and the different resonances are arranged according to the recommendation from IUPAC δ chemical shift scale [97]. The shielding effect from the neighboring electrons also affects the chemical shift. The same nucleus may exhibit different shifts due to the presence of differences in the electron cloud in its surrounding and this contributes to gaining crucial information about the composition and microstructure of polyolefins. Thus, the factors that influence the chemical shift in an NMR experiment is the magnetic field created by the other nuclei and the neighboring electrons in the molecule.

NMR spectroscopy of polyolefins typically necessitates high temperatures for their dissolution and thus solvents with a high boiling point which are chemically stable at such elevated temperatures. Furthermore, for quantitative analysis of polyolefins, experimental parameters of the NMR-spectrometer like probe tuning and relaxation delay need to be optimized [98].

^{1}H and ^{13}C are the commonly applied nuclei for NMR spectroscopy of polyolefins. ^{1}H NMR has significantly higher sensitivity compared to ^{13}C NMR and is frequently applied for determining the chemical composition e.g., functional groups [99], end-groups [100], unsaturation [101, 102 etc., that are present in too small quantities to be detected by ^{13}C NMR. ^{1}H NMR finds application as a tool for quantification as it doesn't require additional calibration. The area under the curve of each ^{1}H NMR signal is proportional to the number of equivalent protons generating the signal. Hence, by integrating the area under each curve the relative number of protons that constitute each curve can be calculated.

^{13}C NMR is the preferred technique for investigating the microstructure of polyolefins. The larger spectral width (~ 20 times) of ^{13}C NMR compared to ^{1}H NMR enables the elucidation of the polyolefin microstructure. ^{13}C NMR has been successfully applied to determine microstructural information such as tacticity [103], mode of insertion [104] and comonomer sequence distribution [105]. ^{13}C NMR has also been applied to quantify SCB [106] and LCB content [197-109] in PE.

3.4 Raman Spectroscopy

Raman spectroscopy is sensitive to structural changes of carbon materials [110-114]. Several researchers utilized Raman spectroscopy to characterize different carbon materials and focused on the origin of the D and G bands [115-119]. The Raman spectrum of graphite exhibits three prominent bands, namely the G-band (graphite band), the D-band (disorder band), and the 2D band (overtone of the D-band) [110-113, 115]. The G-band is the primary Raman active mode in graphite, and it provides a good representation of the sp^2-bonded carbon that is present in the planar sheet configurations of graphite. The G-band originates from the tangential vibrations of the carbon atoms, and these in-plane vibrations are Raman active [113, 121, 122]. The D-band, also known as the disorder or defect mode, originates from edge configurations in graphite where the planar sheet configuration is disrupted [113, 121, 122]. The 2D-band is an overtone of the D-band, but its intensity does not necessarily track with that of the D-band. Yet, the 2D-band is generally more sensitive to the changes in the environment of planar sheet configuration than the D-band [110, 113].

The G-band, which appears for the graphitic structures, is characteristic of the C-C vibrations

[115, 123]. In case of interactions between an analyte and graphite in a solution this G-band can shift [110-113, 115, 121, 122, 124, 125]. Hodkiewicz et al. [113] reported a G-band shift to higher wavenumber when comparing the spectrum of graphene with that of graphite. The interaction between the basal planes of graphite is largely dominated by long-range van der Waals forces, which originate from the correlated motions of electrons in different planes [113]. Thus, Raman spectroscopy can for example be utilized to gain more insight into the interaction between graphite and hydrocarbons like polyethylene (PE) in an organic solvent at temperatures above the crystallization temperature of PE.

3.5 Carbon sorbents for HT-HPLC of polyolefins

A number of carbon sorbents are commercially available, and a few varieties of carbon are industrially produced[ref]. Carbon sorbents are widely used in filtration processes, and it is state of the art in pulp, paper, and petroleum industries to eliminate environmentally hazardous chemicals from wastewater by utilizing graphitized carbon black (GCB) or porous graphitic carbon [126]. GCB filters can be employed to capture detrimental chemicals from drinking water [127, 128]. Ever since the pioneering work of Kiselev et al. [129, 130], carbon sorbents have been regularly applied in gas and liquid chromatography. However, in several cases the sorbent material had poor mechanical stability, a low surface area available for interactions, lack of energetically homogeneous surface, and non-uniform pore structure, which limited its applications in liquid chromatography (LC). The first attempt to prepare a carbonaceous sorbent appropriate for LC was carried out by Guiochon and co-workers [131]. To meet the requirements of LC, various procedures for the preparation of carbon sorbents were recommended [132-141] and their adsorption properties were investigated[142-146].

Carbon supports are generally more retentive for polar compounds and are often more selective for the separation of isomers and homologs than bonded phases. Additionally, they exhibit better chemical stability over a wider range of pH and temperature than the bonded phases [147-149].

3.5.1 Hypercarb™

Hypercarb™ is a porous graphitic carbon that was first applied in HPLC and gas chromatography (GC) by Gilbert and Knox [134, 58]. It is commercially produced by:

1. A highly porous silica material is used as a template for the carbon-based material and impregnated with a phenol-formaldehyde mixture.
2. This mixture is polymerized to produce a phenol-formaldehyde resin.

3. This material is then carbonized by heating to approximately 1000 °C in nitrogen to yield solid particles consisting of a silica backbone with carbon filled pores.
4. The silica backbone is then removed by dissolution in 5 M sodium hydroxide solution.

By heating the material above 2000 °C, a complete rearrangement of the carbon structure occurs transforming the material from a microporous amorphous structure to a crystalline one with a planar surface. The resulting material was called "porous graphitized carbon" (PGC). It is now marketed under the trade name Hypercarb^{TM}.

Table 3.1 Physical attributes of a typical Hypercarb^{TM} column

Property	**Absolute values**	**To meet specific requirements**
Particle shape	Spherical, fully porous	No micropores
Specific surface area	120 m^2/g	Retention linearity and loading capacity
Median pore diameter	250 Å	Mass transfer for wide range of analyte‘s shapes and sizes
Pore volume	0.7 m^3/g	
Mean particle diameters	3, 5, 5 µm	Packing bed uniformity
Porosity	75 %	Mass transfer within particles
% C	100 %	Chemical stability
Mechanical strength	> 400 bar	Operational particle stability; pressure gradients in packing process

Particles of PGC are spherical and fully porous. The surface of PGC is crystalline and does not contain micropores. The internal surface of PGC comprises flat sheets of hexagonally arranged carbon atoms comparable to a very large polynuclear aromatic hydrocarbon molecule [150]. **Fig. 3.5** shows a schematic representation of graphite on which n-decane is adsorbed with its carbon chain parallel to the plane of graphite surface.

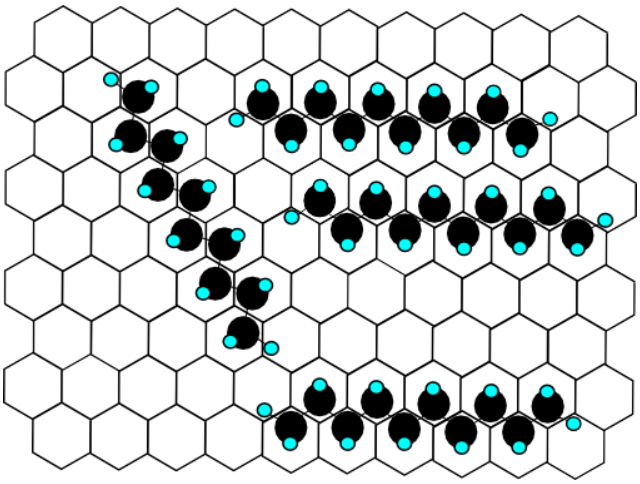

Fig. 3.5 Schematic representation of adsorption of n-decane on graphite. Reprinted (adapted) with permission from [151]. Copyright 2001 American Chemical Society.

Ideally, there are no functional groups on the surface as the aromatic carbon atoms have fully satisfied valencies within the graphitic sheets. The individual sheets of carbon atoms are held together by London dispersion interactions (i.e., instantaneous dipole-induced dipole interactions between the carbon atoms in adjacent sheets).

PGC behaves primarily as a strong reversed-phase stationary phase. However, due to its flat and highly crystalline surface and aromatic nature, the mechanism of interaction is very different from that of the conventional silica-based reversed phases [150]. The aromatic electron system of the graphite can interact with non-polar analytes due to dispersive interactions as well as with polar ones through dipole-induced dipole type interactions. Increasing the hydrophobicity of an analyte by adding methylene groups increase the retention. Analytes having lone pairs or π-electrons can also interact with the PGC surface via electron transfer [150, 152]. Hence, the nature of the interactions between the analytes and the carbon is rather complex. The strength of interaction depends on both the molecular area of an analyte in contact with the graphite surface and on the nature and type of functional groups at the point of interaction with the flat graphite surface. Higher the planarity of the analyte, higher the retention it has on the flat, crystalline PGC surface due to its closer alignment with the graphite surface. This leads to a greater number of points of interactions. However, flatness of the surface reduces the retention of highly structured and rigid molecules. This is because, these molecules can interact the graphite surface only through the aligned functional groups present in their structure compared with planar molecules having the same molecular mass. This is illustrated in **Fig. 3.6**.

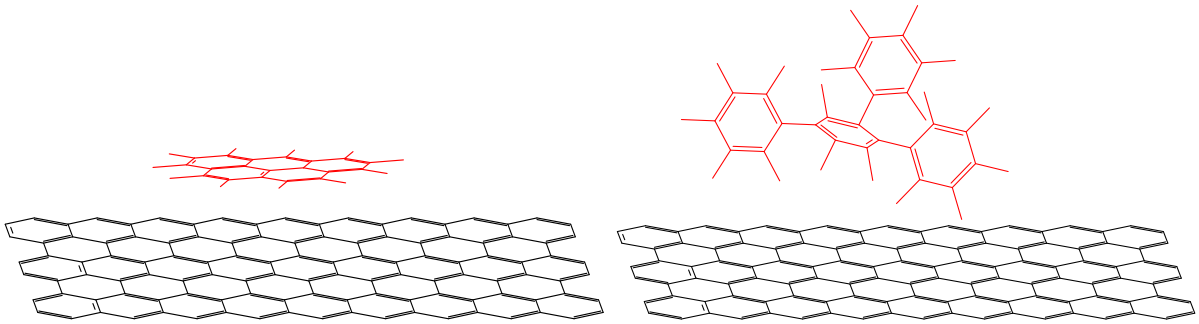

Fig. 3.6 Effect of the solute shape on the strength of the interaction with the graphite surface: a) Good alignment of a planar molecule to the flat graphite surface; b) Poor alignment of non-planar molecule to the flat graphite surface [153].

PGC has proven to be unique in chromatographic separation. Several studies have indicated that PGC is superior to silica-based reversed phases because it shows enhanced selectivity towards certain structural features in molecules such as alkyl chains or isomeric structures [142, 145]. These studies reveal that the flat rigid surface structure provides good discrimination, especially in the case of geometric isomers and some diastereomers. Tanaka et al. [142] observed that when changing from alkanes to their corresponding alkanols, the retention was substantially reduced on octadecylsilane (ODS). However, on PGC the retention was larger for the alkanols. This feature of PGC is attributed to the flat graphite surface, which allows for stronger dispersive interactions with those molecules which can better align themselves to the atomically flat surface.

Coquart and Hennion highlighted the polar retention effect in their study of the trace-level determination of polar phenolic compounds in aqueous samples [154]. Their results showed that by increasing the hydroxyl substitution on the benzene ring, the retention was decreased substantially, often leading to the analytes being unretained on ODS. Conversely, increasing the number of hydroxyl functionalities on the aromatic ring increased the retention significantly on PGC. Wan and co-workers studied the retention of various structural isomers of substituted benzenes on PGC and C18-silica and confirmed the superior steric selectivity of PGC [155]. Forgács and co-workers carried out extensive studies on the retention of various classes of compounds such as phenol, aniline and derivatives of barbituric acid by PGC [156-160] and found that more polar or hydrophilic analytes are retained stronger and eluted later. The retention behavior of polyethoxylated alcohols on PGC and C18-silica was studied by Chaimbault et al. [152]. It was comprehensively shown that the retention on PGC increased with both, the length of the hydrocarbon chain (of the alcohol) and the number of ethylene oxide units. PGC showed a stronger retention for equivalent compounds than C18 silica. Hennion et

al. [161] analyzed the solute polarity and concluded that the retention factor increases with the number of polar substituents on the aromatic ring. Jackson and Carr showed that any polar functional group attached to the benzene ring induces an increase in retention, regardless of its electron-donor or electron-acceptor properties [162]. This behavior was explained by the polarizability of the carbon surface due to the overlapping of the hybridized orbitals, allowing dipole type and electron lone pair donor-acceptor interactions.

4 Results and Discussion

4.1 Characterization of EPDM terpolymers using high-temperature size exclusion chromatography coupled with ultraviolet-evaporative light scattering dual detection

4.1.1 Abstract

The distribution of the pendant double bond along the MMD affects the end use of ethylene-propylene-diene (EPDM) terpolymers. However, a comprehensive analysis of this molecular metric has hitherto been hampered by the lack of suitable detection methods. In the first step, the potential of an ultraviolet detector (UV) detector suitable for hyphenation with high temperature SEC of EPDM terpolymers containing 5-ethylidene-2-norbornene (ENB), dicyclopentadiene (DCPD), and vinyl norbornene (VNB) as diene was investigated. Therefore, the influence of the diene structure and experimental parameters such as mobile phase, analyte concentration, and temperature on the spectroscopic response was probed.

In the next step, a method was developed to evaluate the content of ENB along the molar mass axis. Towards this goal, an evaporative light scattering detector (ELSD) was employed to monitor the analyte concentration, in combination with a UV detector, to quantify the ENB content along the MMD.

4.1.2 Polymer samples

EPDM samples were prepared and characterized by ARLANXEO Netherlands B.V. The average chemical composition was measured by FTIR in accordance with ASTM D3900 for ethylene and propylene and D6047 for ENB and DCPD, VNB. The molar mass parameters (from HT-SEC) are summarized in **Table 4.1**. The chemical structure of the different dienes is shown in **Fig. 4.1**.

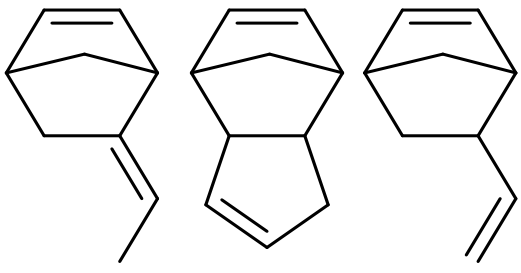

a) **b)** **c)**

Fig. 4.1 Chemical structure of a) ENB; b) DCPD and c) VNB.

Table 4.1 Chemical composition, weight average molar mass (M_w) and dispersity (Đ**)** of EPDM samples.

Sample #	Diene [wt. %]	C_2 [wt. %]	M_w [kg/mol]	Đ
1	0.3	69.1	947	2.3
2	0.6	68.9	932	2.5
3	1.1	68.1	1032	2.2
4	1.7	68.6	1148	2.3
5	2.0	67.9	1048	2.3
6	2.5	68.1	1180	2.2
7	3.4	67.4	973	2.6
8	4.0	67.3	1220	2.2
9	0	49.2	332	2.6
10	4.8	47.9	453	2.6
11	7.1	50.6	503	2.7
12	9.8	48.2	354	2.7
13	14.5	47.8	395	2.6
14	3.0	50.0	341	2.5
15	4.5	58.0	334	2.2

Samples # 1-13: ENB, sample #14: VNB and sample #15: DCPD.

4.1.3 UV Absorption characteristics of double bond in EPDM and effect of diene structure

EPDM samples were examined by SEC-full spectrum IR to estimate the unsaturation content along the molar mass axis. However, the C=C stretching vibration at 1689 cm^{-1} could not be detected even after adjusting the experimental parameters or by increasing the analyte concentration [163].

This lead us to investigate the potential of HT SEC-UV. In **Fig. 4.2**, the contour plot of the UV absorbance for sample # 10 is shown.

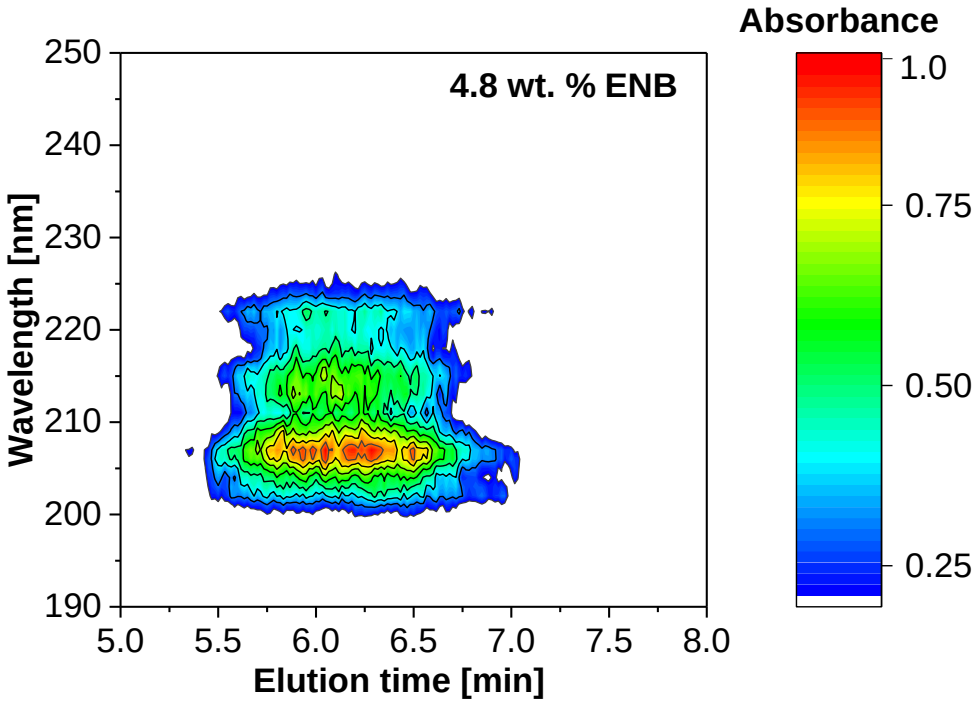

Fig. 4.2 Color coded contour plot of the UV absorbance of EPDM sample #10 in decalin; concentration: 2 g/ L; temperature: 140 °C; stationary phase: SDV [164].

In general, it has been established in several research studies that isolated double bonds in polymers have insufficient UV absorbance in solvents typically used in HT-SEC, owing to their low absorption coefficient [165-167]. In addition to this, limitations of spectrophotometer optics have hampered their detection and quantification [165]. In contrast, our result demonstrated that the absorption of the isolated double bond in EPDM is strong enough to be detected in the wavelength region between 200 and 230 nm. The absorbance with a maximum at 209 nm decreased substantially with an increase in wavelength. No measurable UV response was detected in the wavelength region > 250 nm, thus implying the presence of a discrete transition of a non-conjugated unsaturation.

Fig. 4.3 shows the elugrams of EPDM containing various dienes and neat decalin at the wavelength of their respective maximum absorbance**.**

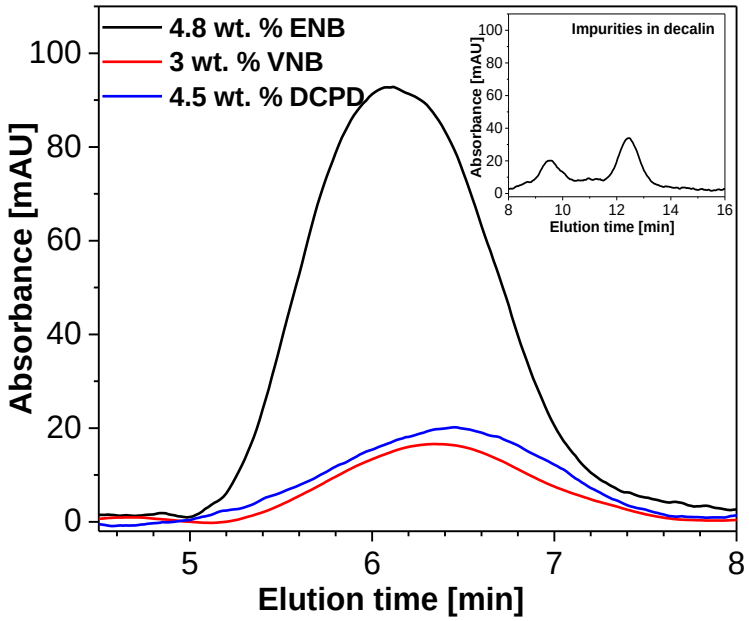

Fig. 4.3 Elugrams of EPDM with different types of diene in decalin; concentration: 2 g/L; temperature: 140 °C; stationary phase: SDV; sample #10 was monitored at 209 nm and sample #14 and #15 at 207 nm [164].

The UV absorbance of sample # 10 was 92 mAU, whereas EPDM containing VNB or DCPD exhibited a substantially weaker UV-absorption compared to EPDM with ENB.

According to the Beer-Lambert law, the absorbance of a molecular species is proportional to its molar absorption coefficient at a specific optical path length and concentration. The molar absorptivity of double bonds is an intrinsic property influenced by numerous factors such as substituents, ring strain, and the proximity of ionic groups neighboring the absorbing species [166, 167]. For instance, in cyclohexene, alkyl substitution leads to a minor shift in wavelength maximum, but a substantial increase in absorbance. It is worth considering the comparison between ß-pinene and α-pinene with regard to the double bond strain and its effect on the UV absorbance. The higher molar absorbance coefficient of the ß-pinene double bond (embedded in the cyclic ring) compared to the one in α-pinene (pendant) results from the higher double bond strain in the former [166]. Likewise, it is hypothesized that the double bond in α position to the bridge ring in ENB is more strained than the double bond in VNB and DCPD ring thus causing higher absorbance for $EPDM_{ENB}$. Subsequently, a bathochromic displacement in $EPDM_{ENB}$ at 209 nm compared to $EPDM_{VNB}$ and $EPDM_{DCPD}$ at 207 nm can be explained by its less stable ground state due to ring strain [167].

The two peaks at elution times of 9.5 and 12.5 min in **Fig. 4** represent the differences in impurities (in decalin) between what was injected and what is running through the column.

Impurities in decalin are dominated by the byproducts of hydrogenation of naphthalene, which is used as starting material for commercial decalin production [168]. Alternatively, impurities can also be attributed to the oxidation products resulting from the chemical reaction of dissolved oxygen with highly reactive tertiary hydrogens to form peroxides. Subsequently, the peroxides decompose to impurities [169]. A study demonstrated that purging decalin with nitrogen or argon significantly reduced the UV absorbance at 193 nm [169]. However, this method is not successful in eliminating impurities that absorb in the 200-230 nm range. A blank run was carried out to establish that the source of the peaks at 9.5 and 12.5 min is from the impurities in decalin.

The absorbance of EPDM at peak maximum is plotted in **Fig. 4.4**.

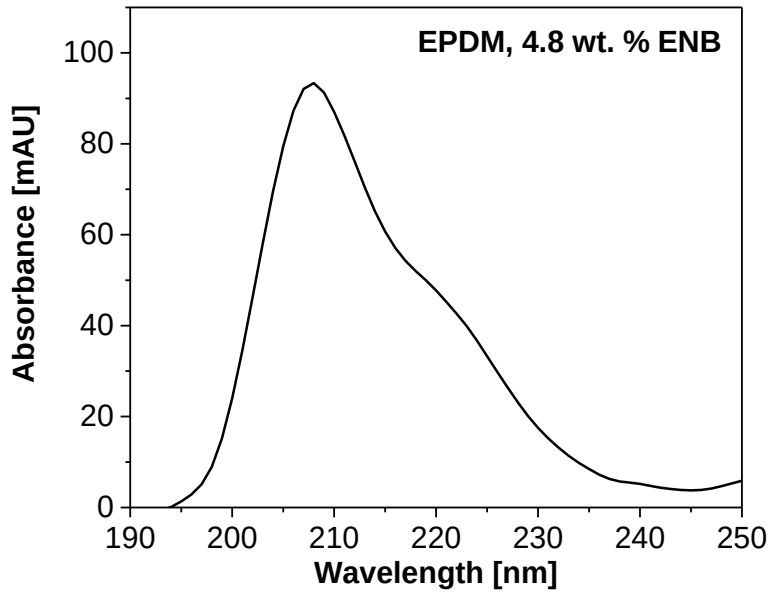

Fig. 4.4 UV spectrum of sample #10 at peak maximum (elution time of 6.2 min); concentration: 2 g/ L; temperature: 140 °C; stationary phase: SDV [164].

It was observed that the absorbance decreases considerably with increasing wavelength after peaking 209 nm. Zhou et al. measured the UV response of a model $EPDM_{ENB}$ in chloroform at room temperature and observed the absorbance maximum at 250 nm [170]. However, the maximum of the UV absorbance of EPDM in decalin was detected at 209 nm with no variation in wavelength of the maximum within the temperature range 80-140 °C. This difference in peak absorbance can be attributed to the effect of solvent polarity [171]. Decalin is relatively less polar than chloroform. In unsaturated compounds, the $\pi - \pi^*$ transitions are of the lowest energy and the transition energy depends on the solvent polarity [171]. The excited states are more polar than the ground state, and dipole–dipole interactions with solvent molecules lower the energy of the excited state more than the ground state. Therefore, a polar solvent decreases the

transition energy which can be correlated to the bathochromic shift of the wavelength for $EPDM_{ENB}$ in decalin compared to that in chloroform.

A low molar attenuation coefficient is an intrinsic feature of isolated double bonds like in EPDM thus making it difficult to identify and quantify [164-167. Thus, our observation indicates the capability of high-temperature SEC-UV for analyzing isolated double bonds.

Fig. 4.5 shows the UV absorbance (at 209 nm, absorbance maximum) as a function of ENB content.

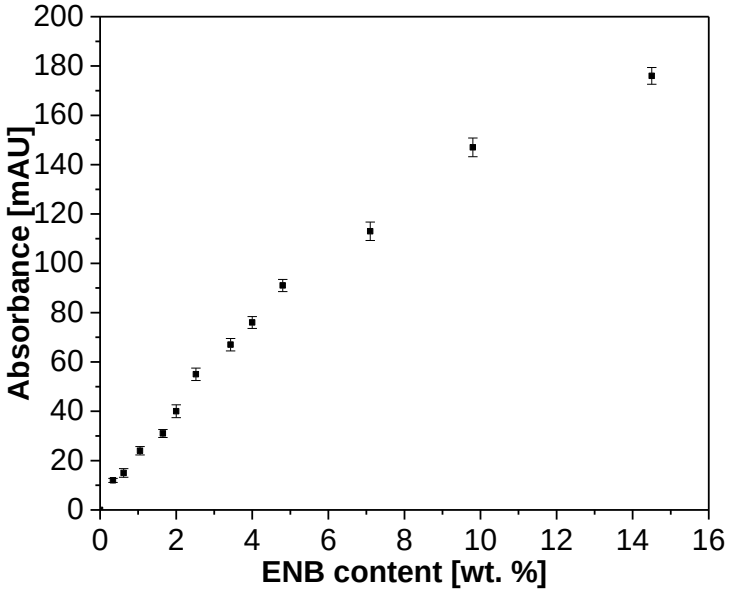

Fig. 4.5 Absorbance of EPDM with varying content of ENB in decalin at 209 nm; concentration: 2.0 g/L; temperature: 140 °C; stationary phase: SDV [164].

The absorbance was quantifiable at very low levels of unsaturation implying high sensitivity of the detector. A linear relationship between the absorbance and ENB content was observed. However, the intensity started to saturate and thus deviate from linearity at higher ENB content.

Beer-Lambert law states that there is a direct correlation between the absorbance (A) of a molecule and its concentration (c). This relationship is characteristically linear but may under specific conditions be non-linear. Deviations can be a result of scattering [172] or possibly due to association, dissociation, or interaction of the analyte with solvent to yield a chemical species with different absorption characteristics [173].

4.1.4 Concentration effect on UV absorbance of EPDM

To probe the linear range of detection, the UV response of EPDM containing different dienes was measured by varying the polymer concentration (**Fig. 4.6**).

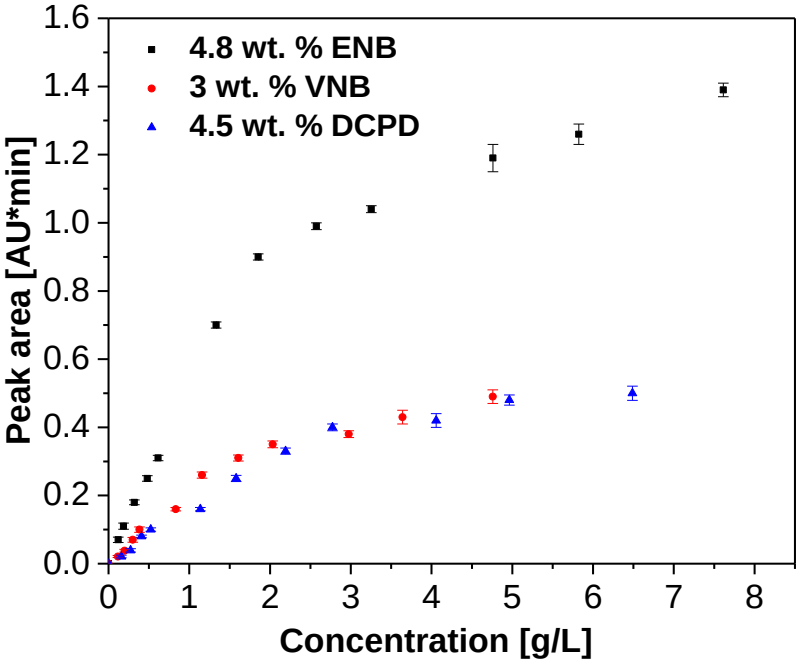

Fig. 4.6 Absorbance vs. concentration for sample #10, #14 and #15 with different dienes in decalin; temperature: 140 °C; stationary phase: SDV [164].

The absorbance of $EPDM_{ENB}$ was substantially higher than that of $EPDM_{VNB}$ and $EPDM_{DCPD}$. This observation is in line with results of **Fig. 4.3**. All the three curves in **Fig. 4.6** showed saturation in the absorbance with increasing EPDM concentration. Tolbin et al. conducted a study to precisely quantify the threshold concentration of a dye molecule indicative for non-linearity in Beer–Lambert law [174]. According to the study, divergence from the linear correlation can be attributed to factors such as shift in absorption wavelength and change in the refractive index (η) of a solution at high concentration.

Besides deviation from linearity, high polymer concentration may lead to decrease in chromatographic resolution due to column overloading. The latter results from high viscosity of the polymer solution at high concentration [175, 176]. This makes it important to establish a critical concentration beyond which there is a loss in resolution. The effect of concentration on elution behavior is shown in **Fig. 4.7**.

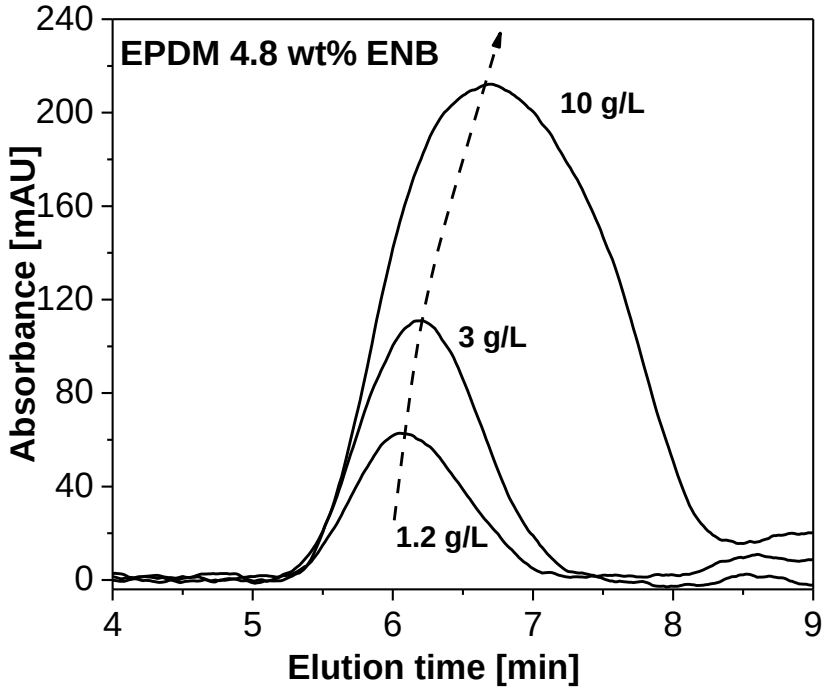

Fig. 4.7 Effect of concentration on elution profile for EPDM in decalin; temperature: 140 °C; wavelength: 209 nm; stationary phase: SDV [164].

It was observed that with increasing analyte concentration, the peak shifted to higher elution volume and became broader. The elugrams moved to higher elution volume at 3 g/L and severe overloading was observed at 10 g/L. The concentration at which the peak moved to higher elution volume is a function of the polymer's molar mass. These characteristic features such as peak skewing, broadening and elution delay can be ascribed to viscous fingering [177].

4.1.5 Effect of temperature, stationary phase, and mobile phase on UV absorbance

Factors influenced by temperature are the refractive index of the mobile phase [178] and interactions between the analyte and the stationary phase [179]. The UV absorbance for cyclopentadiene in iso-octane i.e., a non-aromatic molecule in a non-polar solvent involving van der Waals intermolecular interactions revealed a 0.03 %/°C decrease in absorbance. The effect of temperature on the UV absorbance can be important to consider in the case of aromatic molecules in a polar solvent [180]. Nonetheless, to investigate the effect of temperature on the absorbance of EPDM, samples #9 to #13 were tested at different temperatures.

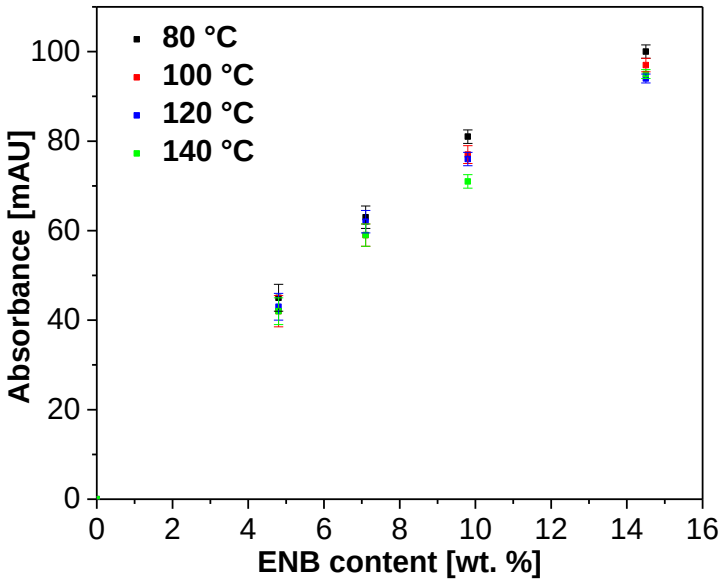

Fig. 4.8 Effect of temperature on the UV absorbance of sample #9, #10, #11, #12 and #13 in decalin; concentration: 1 g/L; stationary phase: SDV [164].

It was noticed that temperature had an insignificant effect on the UV absorbance of EPDM. The minor 0.03 %/°C decrease in absorbance was within the standard deviation. In addition, no shift in wavelength with temperature was observed.

Decalin is produced by hydrogenation of naphthalene and contains UV absorbing byproducts. Furthermore, with every batch the quantity of impurities might vary. Linear or cyclic alkanes are potential alternative solvents for EPDM due their similar Hansen Solubility Parameters and exhibit low absorbance in the wavelength region 200-250 nm. However, these solvents are not compatible with SDV and consequently, there is a need for an alternative stationary phase. Therefore, it becomes essential to probe the potential of a silica column as an alternative to SDV.

Fig 4.9 shows the UV-response of EPDM in silica gel/decalin.

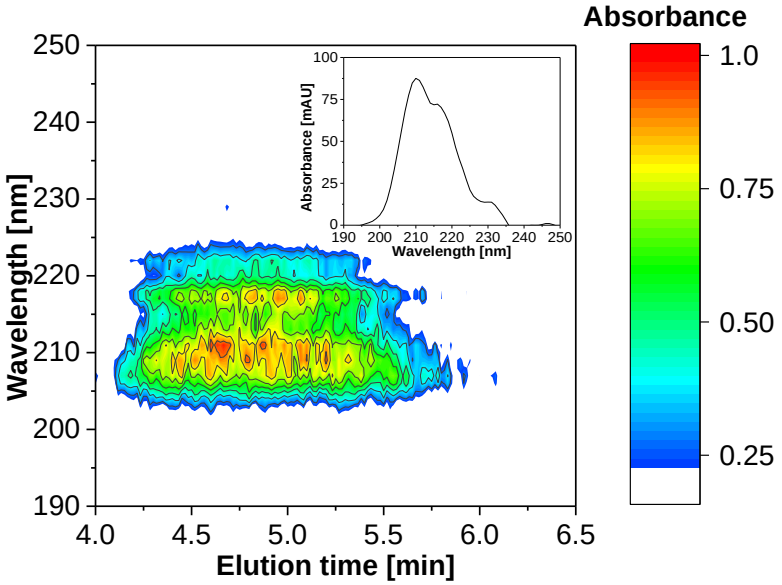

Fig. 4.9 Color coded contour plot of the UV absorbance of sample #10 in decalin; concentration: 2 g/L; temperature: 140 °C; stationary phase: silica gel [164].

The UV absorbance in the elution time range of 4.2-6 min was attributed to the ENB diene. The absorbance of EPDM separated using a silica gel column exhibited similar features like same wavelength range of absorption and a maximum at 209 nm when compared to the absorbance characteristics using an SDV column. A comparison of the UV absorbance at 209 nm for a series of EPDM samples separated using SDV vs. silica gel stationary phaseis presented in **Fig 4.10.** The stationary phase was replaced by a capillary to rule out the possibility of adsorption of the polymer on the stationary phase.

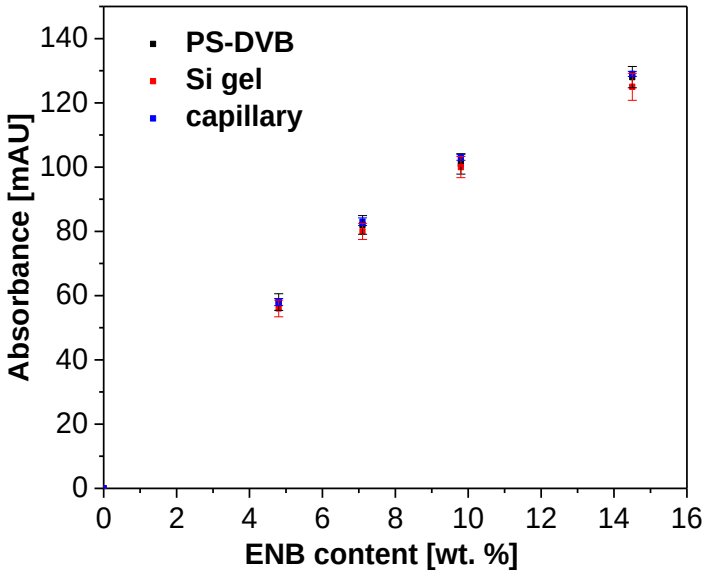

Fig. 4.10 Comparison of the UV absorbance of EPDM separated in SDV vs. silica gel column at 209 nm; concentration: 1.5 g/L; mobile phase: decalin [164].

The UV response was similar for all three systems. This provided a proof that there was no issue with the analyte recovery and both the stationary phases can be used for quantitative analysis.

Sample #10 was injected at concentrations ranging from 0.05 to 10 g/L and the UV response at 209 nm is shown in **Fig. 4.11.**

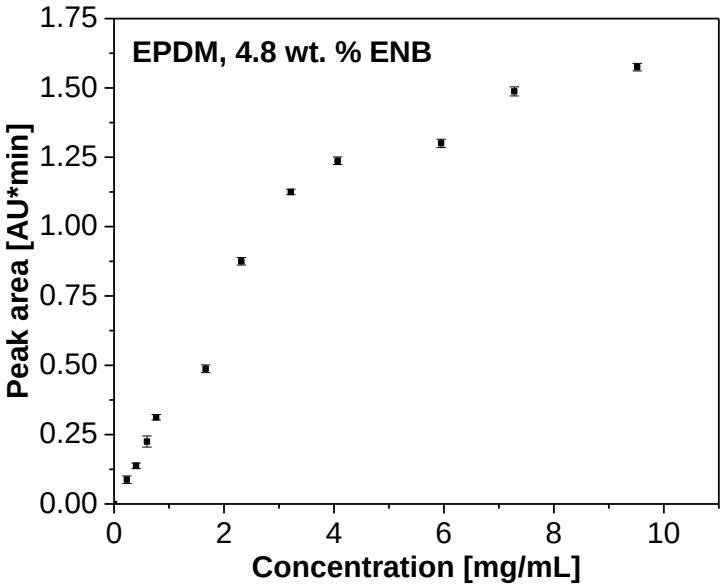

Fig. 4.11 Absorbance vs. concentration for sample #10 in decalin; temperature: 140 °C; stationary phase: silica gel [164].

It was observed that the base-line quality of the SDV column was marginally better compared to that of silica gel. This could be attributed to the high pressure encountered in the silica gel column causing an increased resistance to flow. Subsequently, this might have led to higher pressure fluctuation and thus manifest as poor S/N for inherently low absorbance.

The important characteristics that define a suitable mobile phase are that is should be a thermodynamically good solvent, UV-transparent, compatible with the stationary phase and should have high boiling point and no interactions with the stationary phase. Thus far, decalin has been the solvent of choice. It has minor UV-absorbing impurities and these can vary batch-wise. Based on the UV absorbance spectra of pure solvents and taking into consideration the specified physical attributes, cyclohexane was chosen as a possible alternative to decalin.

Fig. 4.12 shows the UV absorbance of EPDM in the system silica gel/cyclohexane.

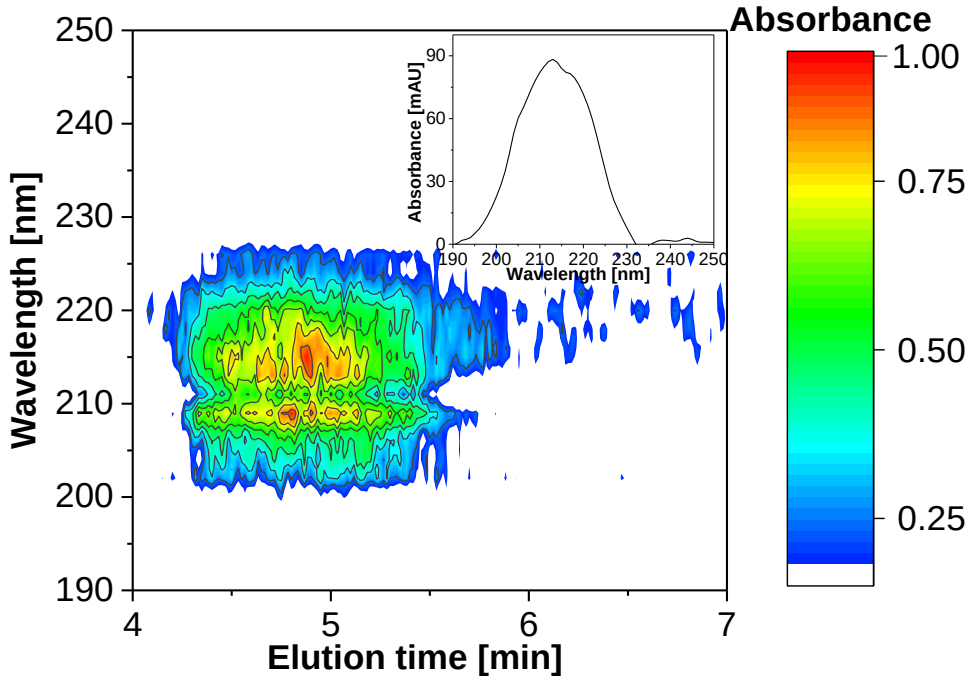

Fig. 4.12 Color coded contour plot of the UV absorbance of sample #10 in cyclohexane; concentration: 2 g/ L; temperature 70 °C; stationary phase: silica gel [164].

The absorbance maximum in cyclohexane was at 213 nm, slightly different from that in decalin (209 nm). This was credited to the impact of polarity on the absorbance characteristics of the analyte. These results indicate that cyclohexane is a suitable alternative to decalin as mobile phase in HT SEC-UV separation of EPDM terpolymers.

4.1.6 Limit of blank (LoB), the limit of detection (LoD) and limit of quantification (LoQ)

In further investigations, the limit of blank (LoB), the limit of detection (LoD) and the limit of quantification (LoQ) were determined. LoB is defined as the highest apparent analyte concentration expected to be found when replicates of a sample containing no analyte are tested [181-183]. Although the sample analyzed to define LoB does not contain any analyte, a blank sample can produce an analytical signal that may otherwise be consistent with an analyte of low concentration. The LoB was estimated by measuring replicates of a blank sample (n=20) and calculating the mean value and standard deviation (SD) by **equations 4.1** and **4.2** [183]:

$$LoB = mean_{blank} + 1.645 \times SD_{blank} \quad (4.1)$$

$$LoB\ [mAU] = 2.08\ mAU + 1.645 \times 0.354 = 2.66\ mAU \quad (4.2)$$

Similarly, the LoD was determined by using both the measured LoB and replicates of a sample containing a low concentration of analyte [0.1 g/L]. The median and SD of the low concentration sample was then calculated according to **equations 4.3** and **4.4** [183]:

$$LoD = LoB + 1.645 \times SD_{low\ concentration\ sample}) \quad (4.3)$$

$$LoD\ [mAU] = 2.66 + 1.645 \times 0.95 = 4.22\ mAU \quad (4.4)$$

A Gaussian distribution of the low concentration sample was observed, and 95 % of the values exceeded the defined LoB, and 5 % of the low concentration sample generated values below the LoB and thus erroneously appeared to contain no analyte.

The LoD was converted from absorbance [mAU] to concentration [g/L] via the calibration line by **equations 4.5** to **4.7**. A linear response was found throughout the tested range as this was within the range of the Beer-Lambert law ($r^2 = 0.998$):

$$Absorbance = 1.89 + 38.9 \times concentration \quad (4.5)$$

$$4.22\ mAU = 1.89 + 38.9 \times LoD\ [g/L] \quad (4.6)$$

$$LoD\ [g/L] = 0.059\ g/L \quad (4.7)$$

LoQ is defined as the lowest concentration at which the analyte can not only be reliably detected but at which some predefined goals for bias and imprecision are met. The LoQ may be taken as equivalent to LoD or it could be at a much higher concentration [183]. Based on a similar set of equations, the LoD for the decalin/silica gel system was 0.09 g/L and the LoQ was defined as a concentration ≥ 0.09 g/L.

Table 4.2 Limit of detection and limit of quantification of $EPDM_{ENB,\ 4.8\ \%}$ for different chromatographic systems.

System	LoB [g/L]	LoD [g/L]	LoQ [g/L]
Decalin/PS-DVB, 140 °C	0.02	0.06	≥0.06
Decalin/silica, 140 °C	0.03	0.09	≥0.09
Cyclohexane/silica, 70 °C	0.03	0.09	≥0.09

4.1.7 Distribution of ENB along the MMD using UV-ELSD dual detection

To profile the ENB content along the MMD, an ELSD was hyphenated with the UV detector. The UV response is indicative of unsaturation in the analyte, and the ELSD signal corresponds to the total sample concentration. Thus, the UV/ELSD ratio signifies the ENB content along the MMD. The response characteristics of ELSD has been investigated by several research groups [184-186] and the consensus is best described by the exponential **equation 4.8**:

$$ELSD\ response\ (peak\ area) = a \times m^b \quad (4.8)$$

with a and b being empirical constants and m representing the eluent mass (equivalent to its concentration).

For quantitative analysis, the exponent b might be approximated as 1 if the right conditions are found, but exponential (b > 1) as well as sigmoidal relationships have generally been reported [50]. For instance, in solvent gradient interactive chromatography a non-linear relation is inevitable and distorts elution curves to a certain extent. However, the overall effect is insignificant as analyte concentration tends to vary strongest at the peak edges. As a result, peaks from an ELSD are typically narrower compared to other detectors but are similar in shape. Similarly, when hyphenated to SEC, narrow peaks still exist because the material at the edges of a peak is present in minute concentration and a non-linear response might mean small amounts of material are underestimated.

Boborodea et al. observed an improvement in the ELSD response under isocratic conditions [187]. This was attributed to the advanced nebulizer technology that resulted in a controlled droplet size and distribution, lower operation temperature, decrease in sample loss for high boiling solvents. To study the response of an ELSD, sample #10 was injected at different concentration **Fig. 4.13**.

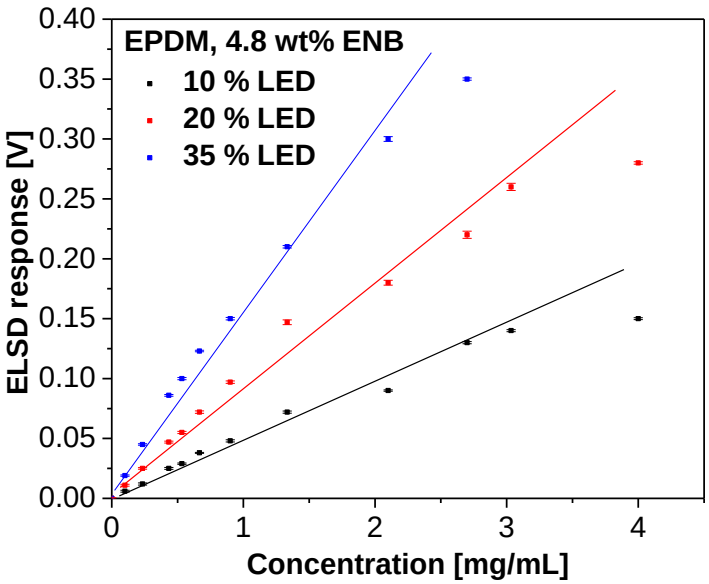

Fig. 4.13 Calibration of ELSD at three different percentages of LED power; mobile phase: decalin; temperature: 140 °C; stationary phase: SDV [164].

At a concentration > 3 g/L, the ELSD operating at 35 % LED power was saturated and thus further quantification was not possible. To gain access to a wide range of concentration, the LED power was decreased. As observed, a linear correlation between the signal intensity and concentration was obtained with low scattering for all the LED powers.

To profile the ENB content along the molar mass, the elution volume axis was calibrated using PS standards. A calibration of the UV/ELSD ratio with different $EPDM_{ENB}$ samples of known chemical composition was carried out to quantify the ENB along the molar mass axis (**Fig. 4.14**).

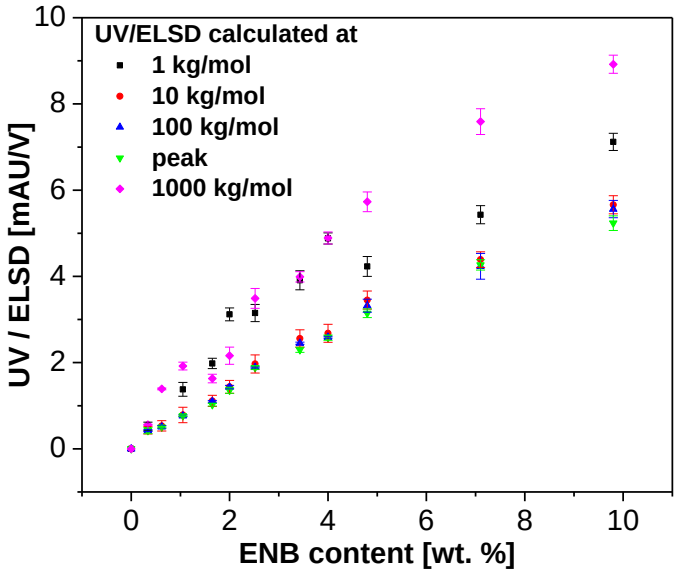

Fig. 4.14 Calibration of UV/ELSD using EPDM of known composition; LED power: 35 %. Mobile phase: decalin; temperature: 140 °C; stationary phase: SDV [164].

The UV/ELSD ratio was calculated at different positions along the molar mass axis. This was done to identify the molar mass at which the calibration deviates. Theoretically, the UV/ELSD ratio should be constant along the molar mass axis as the EPDM samples were synthesized using single site catalyst. However, the ratio diverged from the value at peak maximum. In a typical molar mass distribution elugram, it is always difficult to determine the values at the two edges i.e., front and tail. The molar mass 1 and 3000 kg/mol lie at the edges of peaks where the concentration of material is minute. The ELSD, due to its nonlinear response, would generate narrower peaks than the UV detector and may lead to an overestimate at the edges of peaks as shown in **Fig. 4.14**. Thus, a molar mass dependency of the UV/ELSD ratio was evident and it is essential to take that into account for monitoring the ENB content along the molar mass.

The ENB content along the MMD for sample #10 is shown in **Fig. 4.15a**. Based on the findings of **Fig 4.14**, the UV/ELSD ratio at peak maximum was employed to determine the ENB content.

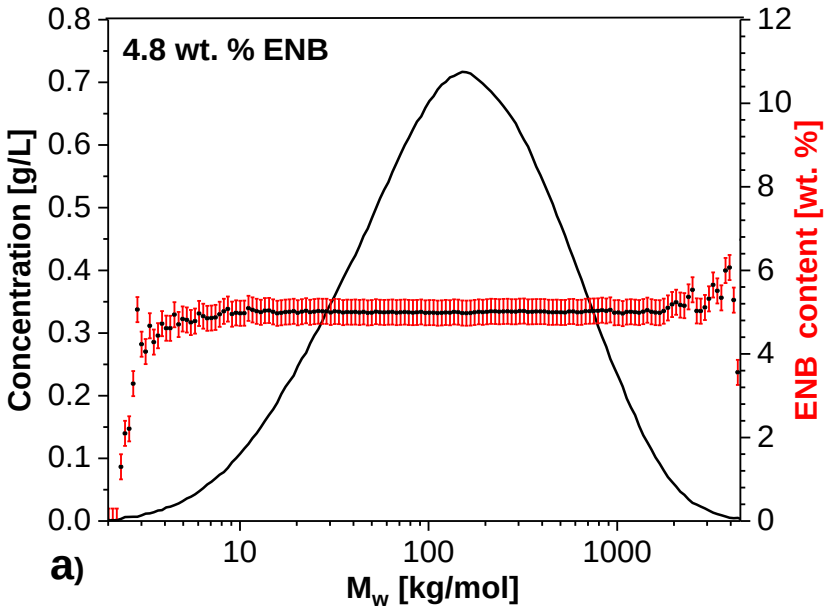
4.8 wt. % ENB
Concentration [g/L]
ENB content [wt. %]
M$_w$ [kg/mol]
a)

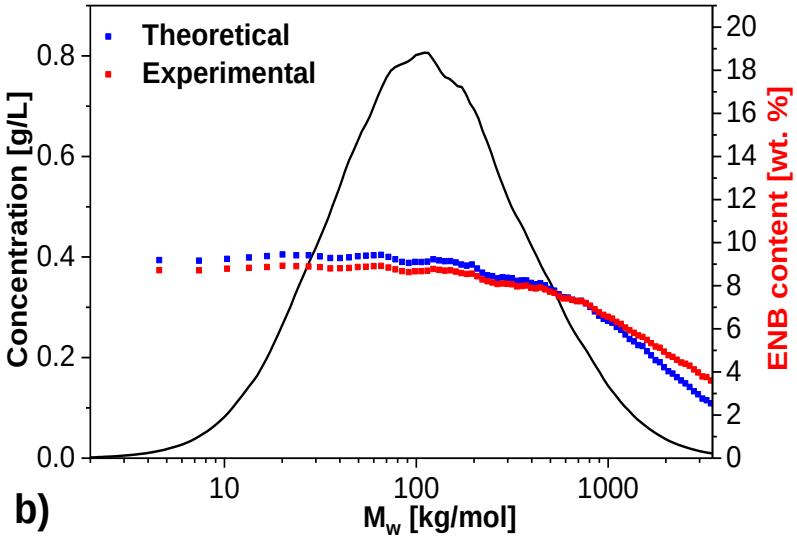
Theoretical
Experimental
Concentration [g/L]
ENB content [wt. %]
M$_w$ [kg/mol]
b)

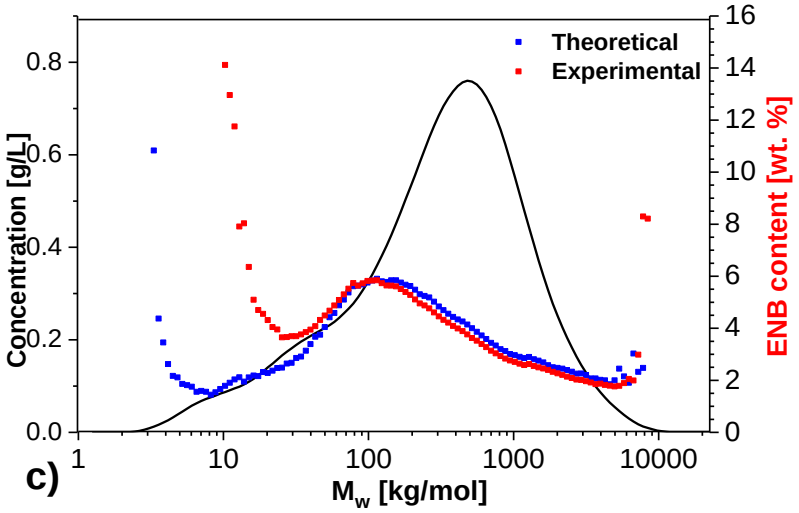
Theoretical
Experimental
Concentration [g/L]
ENB content [wt. %]
M$_w$ [kg/mol]
c)

Fig. 4.15 Distribution of ENB along molar mass axis obtained with HT SEC-UV-ELSD: **a)** sample #10, **b)** blend of sample #11 and #12 (1:1, w/w), c) blend of samples # 1 and # 12 (1:1, w/w); mobile phase: decalin; concentration: 2 g/L; temperature: 140 °C; stationary phase: SDV [164].

The ENB content did not vary with the molar mass, which is in line with the expectation as the polymer synthesis was done using a single-site catalyst in a continuous stirred-tank reactor. Five measurements were used for estimating the ENB content in **Fig. 4.15a**. The experimental ENB content along the MMD was 5.1 wt. % with a standard deviation of 0.12, considering that the actual value is 4.8 wt. % ENB.

To verify the applicability of the UV/ELSD ratio in a heterogeneous system, a blend of sample #11 and #12 (1:1, w/w) was studied (**Fig. 4.15b**). The expected ENB content along the molar mass was calculated by combining the individual elugrams of the individual EPDM samples. As observed, the experimentally determined ENB distribution was in good agreement with the expected value. Sample #12 (higher ENB) has a lower molar mass than sample #11. The result in **Fig. 4.15b** is consistent with expectation i.e., the ENB content decreased as molar mass increased. In other words, a blend of these two EPDM samples would produce an ENB content that varied along the MMD in the manner as in **Fig. 4.15b**. A similar outcome was obtained for a blend of sample #1 and sample #12. The experimental distribution diverged significantly at the edges of the curve probably due to the molar mass dependency of the UV/ELSD ratio.

4.2 Solvent selection for liquid adsorption chromatography of EPDM terpolymers by combining Structure Retention Relationships and Hansen Solubility Parameters

4.2.1 Abstract

Liquid Adsorption Chromatography (LAC) of polyolefins has seen a remarkable growth since its inception but studies focusing on the polyolefin elastomer ethylene-propylene-diene terpolymer (EPDM) are rare. In this work, LAC of EPDM terpolymers was carried out using porous graphitic carbon (Hypercarb^{TM}) as stationary phase and investigating benzene derivates as components of the mobile phase. Structure-retention relationships (SRRs) were elaborated for several substituted aromatic solvents which were classified as either adsorption (adsorli) or desorption (desorli) promoting.

Subsequently, by combining the SRRs with a simplified form of the Hansen Solubility Parameters (HSPs), a predictive tool for solvent selection in LAC of EPDM was created. Using this approach, for the first time new non-chlorinated desorlis were identified, instead of the widely used chlorinated aromatic desorlis 1,2,4-trichlorobenzene (1,2,4-TCB) and 1,2-dichlorobenzene (ODCB).

4.2.2 Polymer samples

EPDM samples were prepared and characterized by ARLANXEO Netherlands B.V. The average values of their chemical composition, as measured by FTIR, and their molar masses (from SEC) are summarized in **Table 4.3**. HSP of solvents can be found in literature [188]. Similarly, the HSPs and R_0 of the polymer correspond to a commercial EPDM (Keltan 8550C) of high molar mass and medium degree of branching [189].

Table 4.3. Chemical composition of EPDM, weight average molar mass and dispersity.

2-ethylidene-5-norbornene (ENB) [wt. %]	**Ethylene (E) [wt. %]**	**Propylene (P) [wt. %]**	**E/P**	**M_w [kg/mol]**	**Đ = M_w/M_n**
0	51.8	48.2	1.07	520	2.4
4.8	47.9	46.9	1.02	353	2.6
7.1	50.6	42.3	1.19	503	2.7
9.8	48.2	42.0	1.15	394	2.7
14.5	47.8	37.7	1.26	395	2.6

4.2.3 Solvent Gradient Interactive Chromatography (SGIC)

Typically, SGIC of polyolefins is carried out by applying a solvent gradient (adsorli→desorli) wherein the analyte is adsorbed onto the stationary phase using an adsorli and subsequently eluted using a desorli. An overlay of chromatograms of EPDM samples in different solvent gradients is shown in **Fig. 4.16a and 4.16b.**

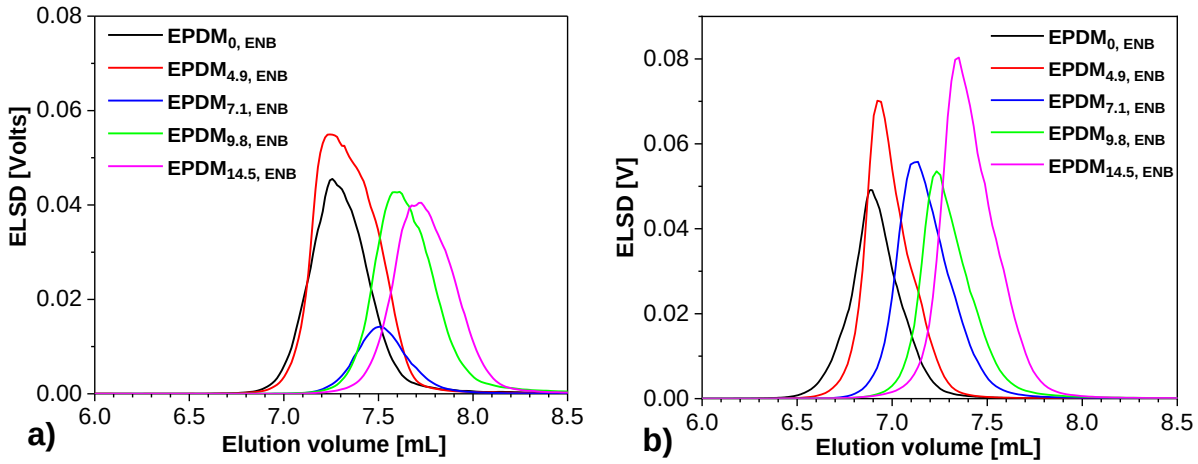

Fig. 4.16a Overlay of chromatograms of EPDM terpolymers. a) Mobile phase: toluene →1,2,4-TCB and b) xylene (mixture of isomers)→1,2,4-TCB [215].

The elution volume of samples increased with increasing ENB content for both the solvent gradients. In an investigation, Chitta et al. observed that EPDM with higher ENB content adsorbed strongly on the porous graphitic carbon in a 1-decanol→1,2,4-TCB solvent gradient [190, 191]. **Fig. 4.16** demonstrates that the elution volume (V_e) of EPDM samples using xylene as adsorli is lower compared to toluene. This indicates that the samples adsorb poorly when xylene is employed in comparison to toluene.

Different adsorlis like 1,3,5-TMB, EB and DEB (**Fig. 4.17a**) and monoalkyl substituted benzene derivatives (**Fig. 4.17b**) were screened to investigate the effect of the chemical structure of adsorlis on the elution behavior.

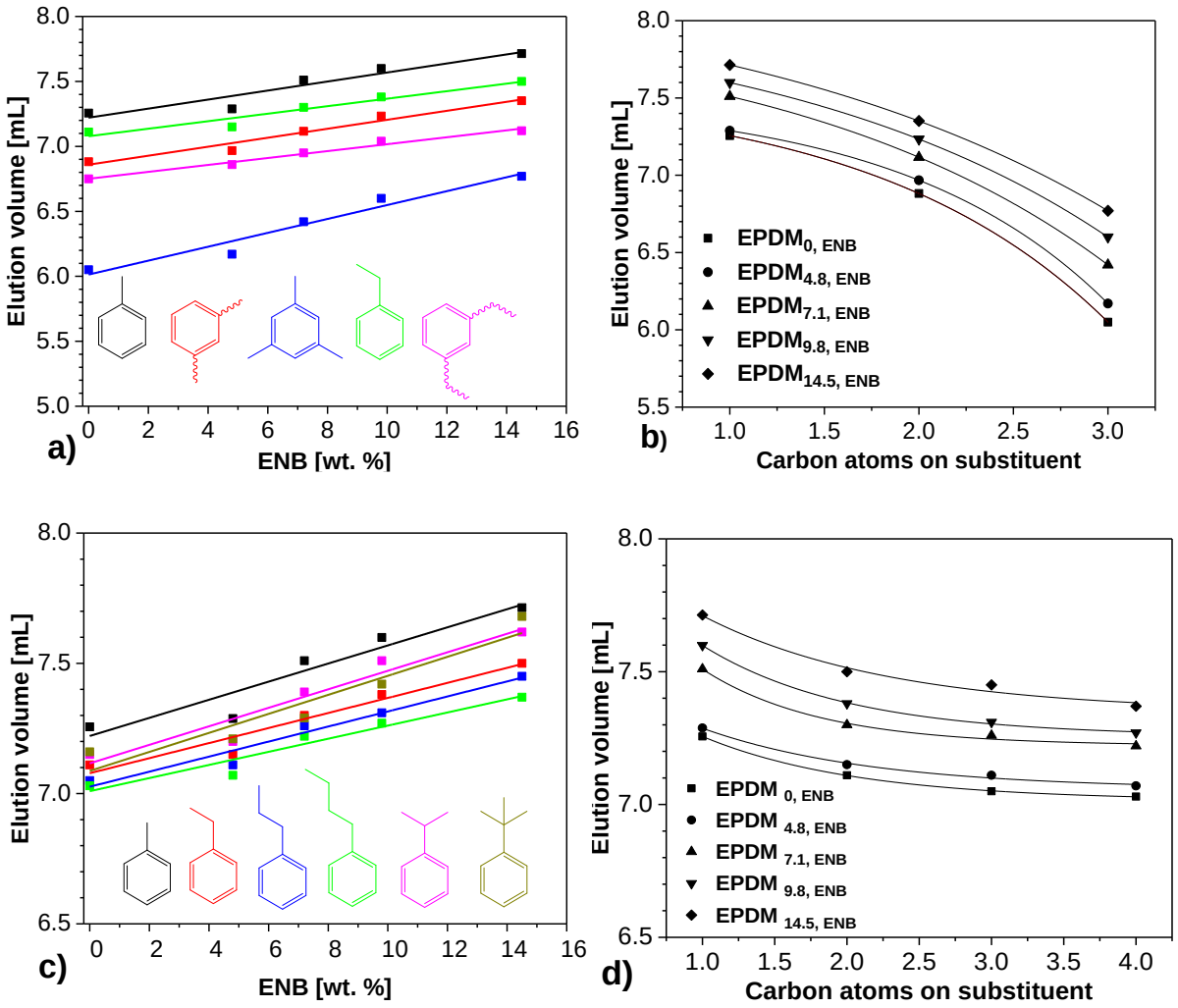

Fig. 4.17 a, c) Relationship between the elution volume and average ENB content of the EPDM terpolymers and b, d) dependence between the elution volume and number of carbon atoms in the substituents of linear alkylbenzene adsorli. Solvent gradient: adsorli→1,2,4-TCB [215].

As shown in **Fig. 4.17a**, the elution volumes of EPDM were lowest for 1,3,5-TMB→1,2,4-TCB i.e., 1,3,5-TMB is apparently the weakest adsorli when compared to toluene and xylene. A pattern can be established where the adsorption promoting capability of the adsorli decreases by increasing the number of methyl groups on its aromatic ring (**Fig. 4.17b**). The mechanism of LAC separation can be qualitatively described as polymer and solvent molecules competing for adsorption on the sorbent surface. Accordingly, a weak adsorli (1,3,5-TMB) is characterized by a stronger interaction with the PGC surface than a strong one (toluene). A similar trend of decreasing V_e is observed from EB→1,2,4-TCB to DEB→1,2,4-TCB (**Fig. 4.17a**). Thus, it is implied that alkyl substitution on the aromatic ring of the adsorli decreases the retention of polymer chains on the sorbent surface. Therefore, it can be concluded that the strength of interactive forces between the stationary phase and adsorli is important controlling the elution behavior of EPDM terpolymers.

In **Fig. 4.17c,** the elution volumes slightly decreased with the alkyl chain length on the ring: toluene > ethylbenzene > n-propylbenzene > n-butylbenzene. As plotted in **Fig. 4.17d**, ΔV_e between two successive adsorlis (e.g., toluene and EB) decreased with increase in the length of alkyl chain. This is indicative of possible saturation in the adsorption promoting strength of linear alkylbenzene adsorlis. Branched alkyl substituents had a marginally positive effect on the adsorption promoting capability as evidenced by the higher V_e for isopropylbenzene (IB) or tert-butylbenzene (TB) compared to n-propylbenzene.

It can be hypothesized that the number of alkyl substituents (mono, di and tri) on an aromatic adsorli significantly influences its adsorption promoting capability (**Fig. 4.17a**). However, differences in the alkyl substituent structure did not have any considerable effect on their adsorption strength (**Fig. 4.17c**).

Physical parameters such as polarity, polarizability, and the 3D conformation are known to modulate the adsorption or desorption-promoting capabilities. A study by Monrabal et al. concluded that solvent polarity played a secondary role in polymer interaction, but greatly influenced its adsorption [192]. A plot of the dipole moments of the adsorlis and average elution volume of EPDM samples (V_{avg}) in respective solvent gradients (keeping the desorli constant) is shown in **Fig. 4.18**. V_{avg} was calculated by averaging the elution volume at the peak maximum of all EPDM samples.

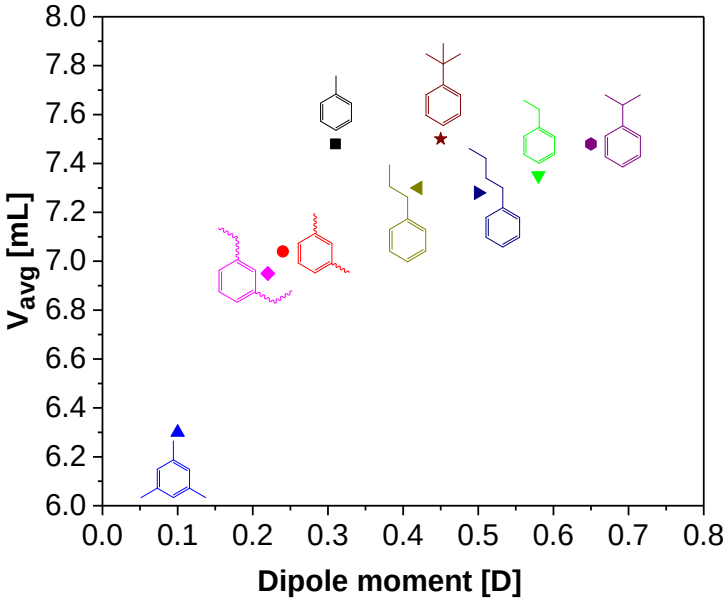

Fig. 4.18 Relation between the V_{avg} of EPDM terpolymers and the polarity of adsorli. Mobile phase: adsorli→1,2,4-TCB [215].

EPDM is non-polar and hence the adsorli with the least polarity is chemically most compatible with the polymer and this should result in lower elution volume for the particular adsorli. The polarity of the adsorlis is in the following order: toluene > xylene > 1,3,5-TMB and the trend in **Fig 4.17b** agrees with this hypothesis. However, the V_{avg} did not correlate with the dipole moment of other linear alkylbenzenes (toluene, EB, PB, BB). In other words, V_{avg} of EPDM is similar for solvent gradients with these adsorlis whereas their polarities are different. This suggests that the elution of polymers might be associated with the polarity of the adsorli but cannot be generalized.

4.2.4 Effect of desorption promoting solvents on adsorption behavior of EPDM

LAC of polyolefins has consistently employed ODCB and 1,2,4-TCB as desorption promoting solvents [193, 194]. The elution behavior of EPDM was probed by using chlorine-substituted aromatic solvents as desorli to investigate the effect of chemical structure on EPDM adsorption. By employing xylene→chlorobenzene, no elution was observed which implied very weak desorption capability of chlorobenzene. F**ig. 4.19** illustrates the elution of EPDM terpolymers using xylene→ODCB.

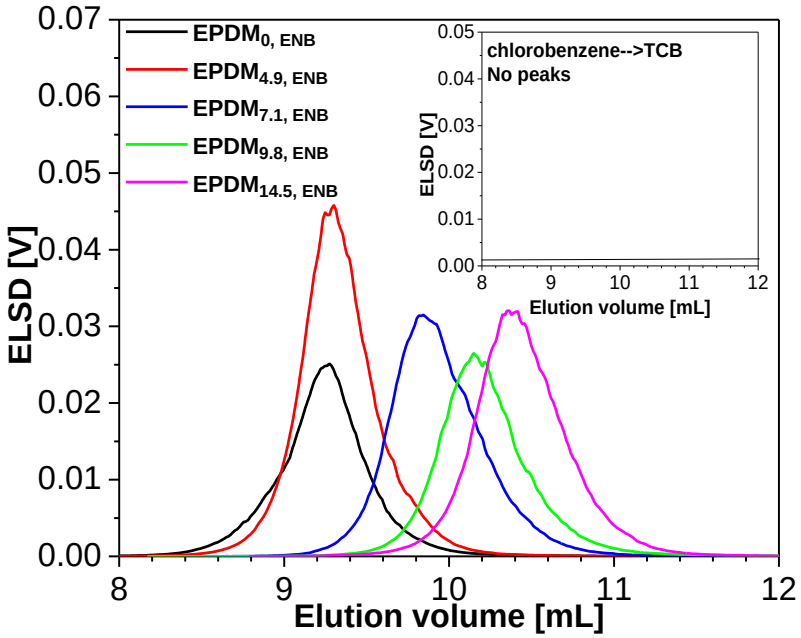

Fig. 4.19 Overlay of chromatograms of EPDM terpolymers. Mobile phase: xylene→ODCB [215].

The samples eluted at higher elution volume compared to xylene→1,2,4-TCB (**Fig. 4.16b**). This implies that ODCB is a weaker desorli compared to 1,2,4-TCB. In a study by Arndt et al., the elution strength was correlated to the distance between the peaks obtained for two samples

of ethylene/1-octene copolymers of a given composition [195]. Considering greater distance between the peaks of two EPDM samples by using xylene→ODCB than by xylene→1,2,4-TCB, it was concluded that better separation was achieved using the former gradient.

To further investigate the effect of functional groups on aromatic desorlis on the elution of EPDM, different chlorinated solvents like 1,3-dichlorobenzene (MDCB), 1-chloronaphthalene (1-CN), 2-chlorotoluene (2-CT) and 4-chlorotoluene (4-CT) were tested as desorli. **Fig. 4.20** shows the dependence between the V_e and the average ENB content of the EPDM terpolymers for different desorlis.

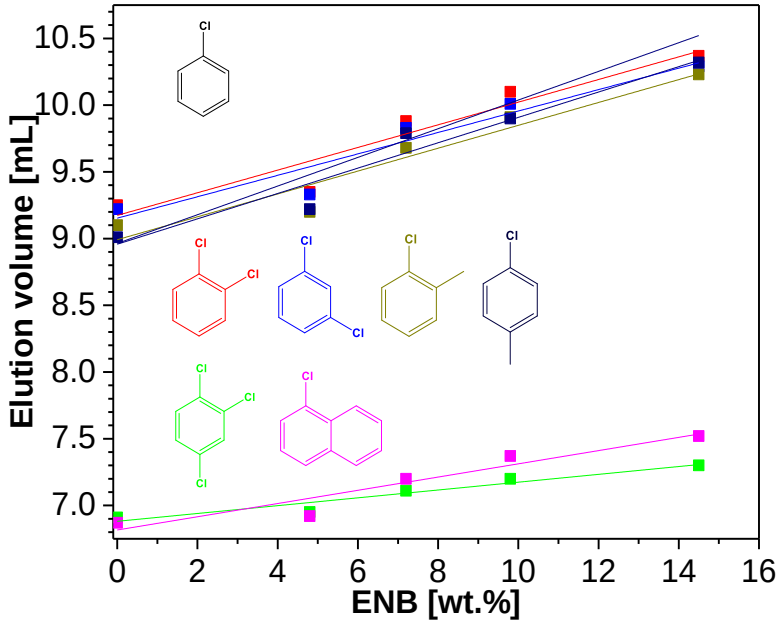

Fig. 4.20 Dependence between the elution volume and the average ENB content of the EPDM terpolymers. Mobile phase: xylene→desorli. Notice: No elution of EPDM after using chlorobenzene as desorli [215].

In the first place, the addition of a methyl (2-CT and 4-CT), chlorine (ODCB, MDCB, 1,2,4-TCB) or a benzene functional group (1-CN) to chlorobenzene increased the desorption promoting ability as evidenced by elution of the polymer. Furthermore, based on the elution volume of EPDM, it is evident that 1-CN and 1,2,4-TCB have the highest desorption strength and that there is no discernible difference in the elution volumes when structural isomers ODCB and MDCB are used. Thus, the desorption strength is as follows: 1,2,4-TCB ~ 1-CN > ODCB ~ MDCB ~ 2-CT ~ 4-CT >>> CB. An important point to note is that the desorlis are clustered in three groups (non-desorbing, mildly-desorbing and strongly-desorbing). It can be concluded that the desorption strength increases with an increase in the number of chlorine atoms on the aromatic desorli.

So far, the effect of functionality on the adsorption/desorption strength of solvents has been studied. Accordingly, the effect of these structural changes on the separation and resolution of EPDM terpolymers was explored. The lines shown in **Fig. 4.17** and **4.20** are described with the following **equation 4.9**:

$$V_e = mX + c \tag{4.9}$$

V_e is the elution volume of an EPDM sample, X is the ENB content [wt. %]

The chromatographic resolution (R) was calculated by **equation 4.10** [196, 197:

$$R = \frac{2\,[V_1 - V_2]}{1.7\,[w(1) + w(2)]} \tag{4.10}$$

where V_1 and V_2 correspond to the elution volume and w(1) and w(2) are equal to the peak width at half height for $EPDM_1$ and $EPDM_2$, respectively. An R value of 1.5 indicates that the two peaks are baseline resolved, with smaller values indicating poorer resolution. $EPDM_{4.8,\ ENB}$ and $EPDM_{14.5,\ ENB}$ were used to calculate the resolution and the results are summarized below.

Table 4.4 Slope and resolution for different solvent gradients.

Solvent gradient adsorli/desorli	**Slope × 100**	**Coefficient of Determination (R^2)**	**Resolution (R)**
toluene→1,2,4-TCB	3.8	0.909	0.68
xylene→1,2,4-TCB	3.2	0.964	0.88
1,3,5-TMB→1,2,4-TCB	4.8	0.954	1.03
EB→1,2,4-TCB	3.2	0.942	0.91
DEB→1,2,4-TCB	3.4	0.982	0.95
PB→1,2,4-TCB	3.1	0.958	0.72
BB→1,2,4-TCB	3.2	0.936	0.85
IB→1,2,4-TCB	3.5	0.929	0.73
TB→1,2,4-TCB	3.6	0.906	0.78
xylene→ODCB	8.6	0.915	1.25
xylene→MDCB	8.1	0.923	1.26
xylene→1,2,4-TCB	3.2	0.932	0.88
xylene→1-CN	4.9	0.916	0.74
xylene→2-CT	8.6	0.908	1.32
xylene→4-CT	9.5	0.943	1.29

The addition of a methyl group has a significant influence on the retention going from toluene to 1,3,5-TMB (**Fig. 4.17a**). However, the effect on separation (slope in **Table 4.4**) is negligible, even though resolution improves. Similarly, the separation with n-alkylbenzenes as adsorli is almost similar and is practically the same when the alkyl substituent is branched (PB vs. IB and BB vs. TB). Furthermore, the improvement in resolution by varying the adsorli is not substantial. It is thus established that the changes in the functionality of the aromatic adsorlis play a minor role in improving the separation and resolution.

The addition of a chlorine functionality translates to a significant impact on the desorption promoting capability as follows: CB << ODCB/MDCB < 1,2,4-TCB (**Fig. 4.20**). Additionally, the effect on separation and resolution is considerable (**Table 4.4)**. 1,2,4-TCB weakly separates EPDM (least slope and resolution) in comparison to ODCB or MDCB. A comparison of the solvent gradients suggests that the largest increase in separation is achieved when 4-CT is the desorli and the maximum resolution is attained with 2-CT. It is therefore concluded that varying the desorli has a larger effect on separation and resolution in comparison to changing the adsorli.

4.2.5 Retention characteristics of aromatic derivatives (Adsorlis and Desorlis)

From the previous findings, it is undeniable that the strength of interaction between the adsorli or desorli and the stationary phase is a primary factor influencing the elution volume, separation and resolution of EPDM terpolymers. Consequently, the initial objective is to develop correlations between the molecular structure of benzene derivatives and their retention on the sorbent surface. Furthermore, the goal is to estimate the relative strength of solvent-stationary phase interactions and ultimately obtain a possible correlation with the elution pattern of EPDM terpolymers (**Fig. 4.17a, 4.17c and 4.20**).

The retention characteristics of the benzene derivatives were measured by injecting them in methanol. The results are shown in **Fig 4.21** for the adsorlis.

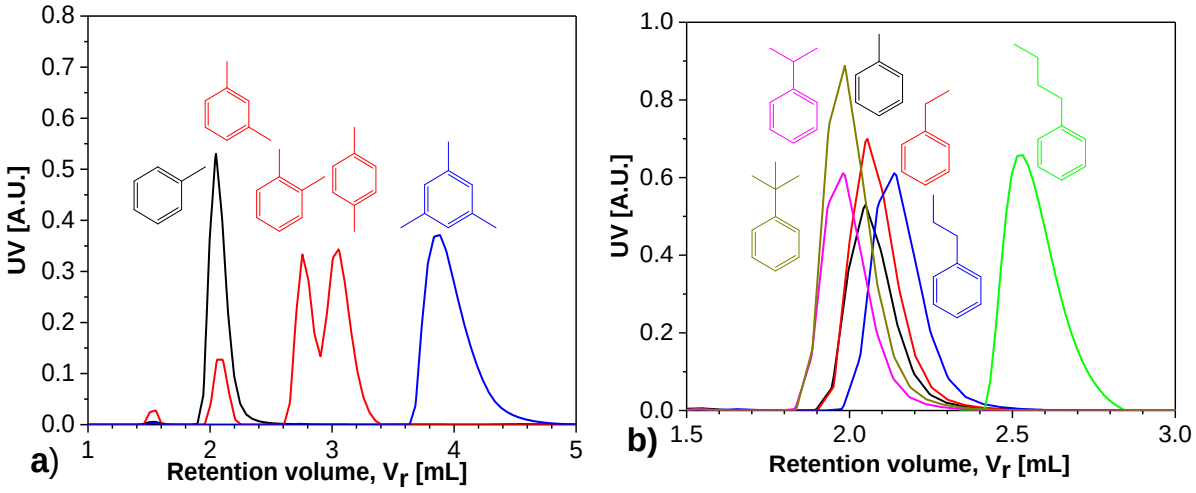

Fig. 4.21 Effect of structural changes on the isocratic elution of a) mono, di and tri methylbenzenes, b) monoalkyl benzene derivatives [215].

The retention volume (V_r) increases significantly with an increase in the number of alkyl substituents (electron donating groups, EDG) on the aromatic ring (**Fig. 4.21a**). Similar observations were previously made (**Fig. 4.17a**) i.e., a decrease in V_e of EPDM with an increase in the number of alkyl groups (**Fig. 4.17a and 4.17b**). It is noticed that the experiment is sensitive to differentiate between the structural isomers of xylene (ortho, meta and para). As noticed in **Fig. 4.21b**, the retention increased rapidly with the length of linear alkyl substituent (toluene to n-butylbenzene) whereas in **Fig. 4.17c and 4.17d,** the effect on EPDM elution possibly saturated.

To understand how substitution on the benzene ring influences the retention, the PGC surface can be considered analogous to a graphene sheet. The presence of an EDG increases the π-electron density on the benzene ring as compared to benzene which leads to strong π–π repulsion between the π-electrons of the aromatic derivative and those of the PGC. This should hinder its adsorption on PGC [198, 199] and yet on the contrary, increased adsorption was observed (**Fig 4.21a**). Several investigations have modeled the adsorption of aromatic compounds on a graphene sheet using density-functional theory [200-202]. These studies concluded that a primary reason for increased adsorption of the benzene derivative in comparison to benzene is the interaction between the substituent itself and graphene. For example, the C–H bond of -CH_3 interacts with the delocalized π-electrons of graphene and may form C–H···π interactions which are modulated by several factors. This reasoning suggests a positive contribution to the total interaction between the adsorli and PGC and hence it is inferred that the increased retention volume is a consequence (**Fig. 4.21a)**.

Branched alkyl substituents decrease the retention on PGC as indicated in **Fig. 4.21b**. Zhou et al. proposed that the direction and the number of hydrogen (H) atoms on the substituent regulate the electron transfer from graphene. For instance, although the number of H atoms is equal in PB vs IB and BB vs TB, the conformation of the molecule (direction of the C-H bonds) may not be ideal for interaction with the atomically flat graphene surface. Thus, the retention decreases marginally for the branched alkyl benzene derivatives [201].

V_r is an important parameter that signifies the relative strength of interaction between the benzene derivative and the sorbent surface. It is converted to a retention factor (log k) i.e., relative retention compared to benzene by **equation 4.11:**

$$log_{10}\, k = log_{10}\, \frac{V_r - V_{r,benzene}}{V_{r,benzene}} \qquad (4.11)$$

Based on previous observations, V_r < 3 mL (log k < -0.18), except 1,3,5-TMB (**Fig. 4.21a)** for solvents tested as adsorli for EPDM (c.f. **Fig. 4.17**).

To better understand the effect of molecular structure of the benzene derivatives on retention, a series of aromatic hydrocarbons with different substitution patterns was injected in methanol. **Fig. 4.22** shows the relation between the retention factor and the number of carbon atoms on the substituent.

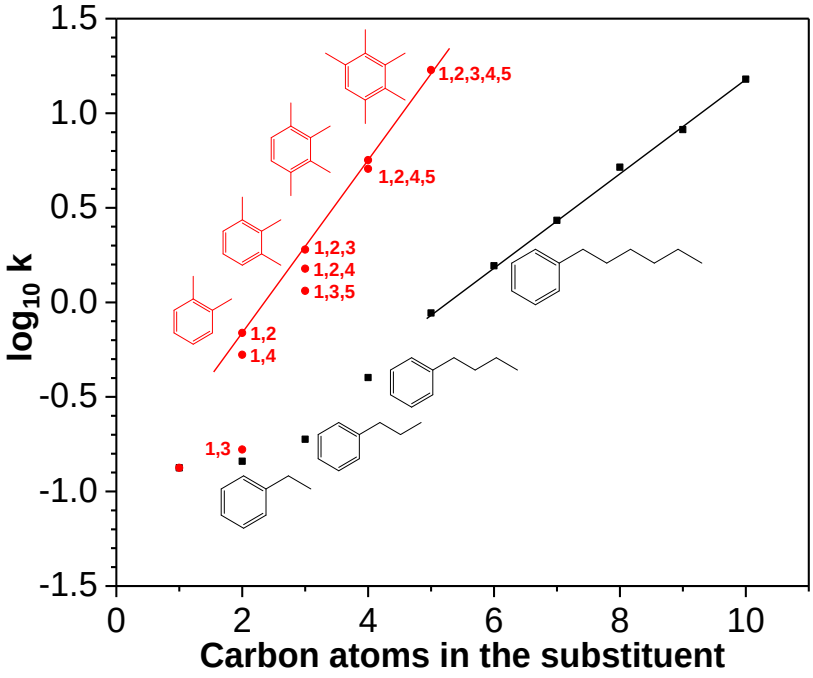

Fig. 4.22 Dependence between log k and number of carbon atoms in the substituent [215].

Log k of linear alkylbenzenes increases almost in a linear fashion with the increase in the number of carbon atoms after four carbon atoms. In the case of ortho-substituted benzene

derivatives, the dependence is linear, and the slope is steeper compared to linear counterparts which is indicative of stronger adsorption for the former.

The retention characteristics of chlorinated benzene derivatives and aromatics with different mono-substituents are shown in **Fig. 4.23a and 4.23b**, respectively**.**

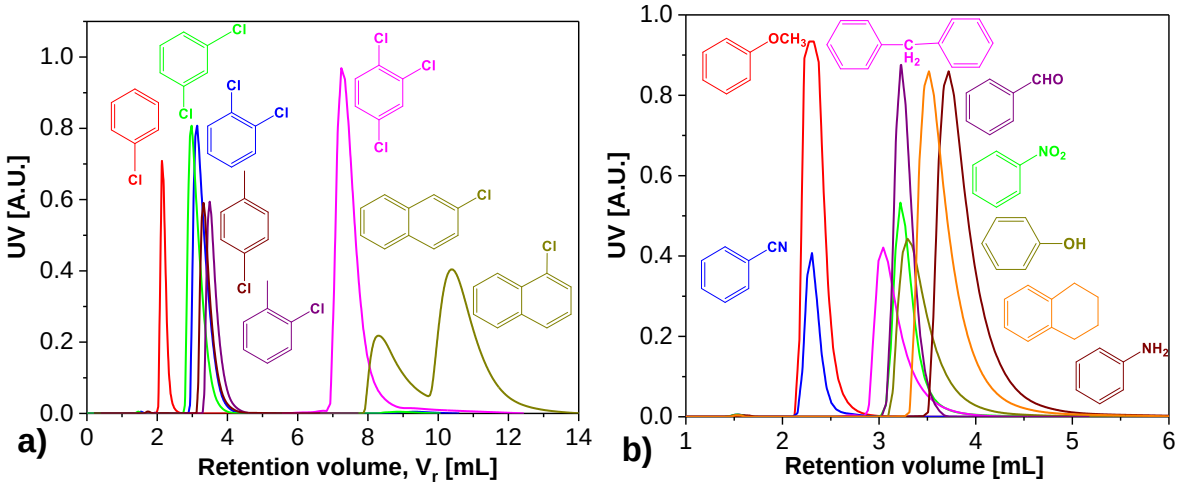

Fig. 4.23 Effect of structural changes on the isocratic elution of a) chlorinated benzenes and b) monosubstituted benzene derivatives [215].

As seen in **Fig 4.23a**, the retention volume increases with an increase in the number of chlorine atoms (EWG). This is because an EWG decreases the π-electron density on the benzene ring and hence reduces the π–π repulsion [198, 199], thereby strengthening the interaction with the graphene surface**.** Moreover, addition of a benzene ring increases the retention drastically, CB vs. chloronaphthalene.

It is observed that the retention volume (V_r) for benzene derivatives employed as desorlis is > 3 mL (log k > -0.18) (**Fig. 4.23**) whereas for adsorlis, log < -0.18 (**Fig. 4.21**). Therefore, it may be postulated that a benzene derivative with log k > -0.18 can be a potential candidate for desorli. Chlorobenzene was found to have log k = -0.56 and hence can be classified as an adsorli which agrees with its inability to desorb EPDM (**Fig. 4.19**). This classification seems to be valid for almost all the benzene derivates tested as either adsorli or desorli. However, for 1,3,5-TMB, log k = 0.06 and thus can be classified as a desorli according to our hypothesis. However, in practice it is an adsorli (**Fig. 4.17a**), which indicates that factors other than strength of interaction influence the LAC mechanism.

Several candidates in **Fig. 4.22** (e.g., n-hexylbenzene, 1,2,4-trimethylbenzene) and **Fig. 4.23b** (e.g., tetralin and benzaldehyde) can be classified as desorli if their log k value is considered.

Similarly, log k being < -0.18 for anisole and benzonitrile suggests they can be employed as adsorli.

Now that the solvent and stationary phase interactions have been calibrated using benzene as a reference, their correlation with the elution of EPDM will be analyzed. The dependence between retention factor and V_{avg} of EPDMs (**Fig. 4.17a, 4.17c** and **4.20**) is plotted in **Fig. 4.24**. V_{avg} is calculated by averaging the elution volume at peak maximum of all EPDM samples.

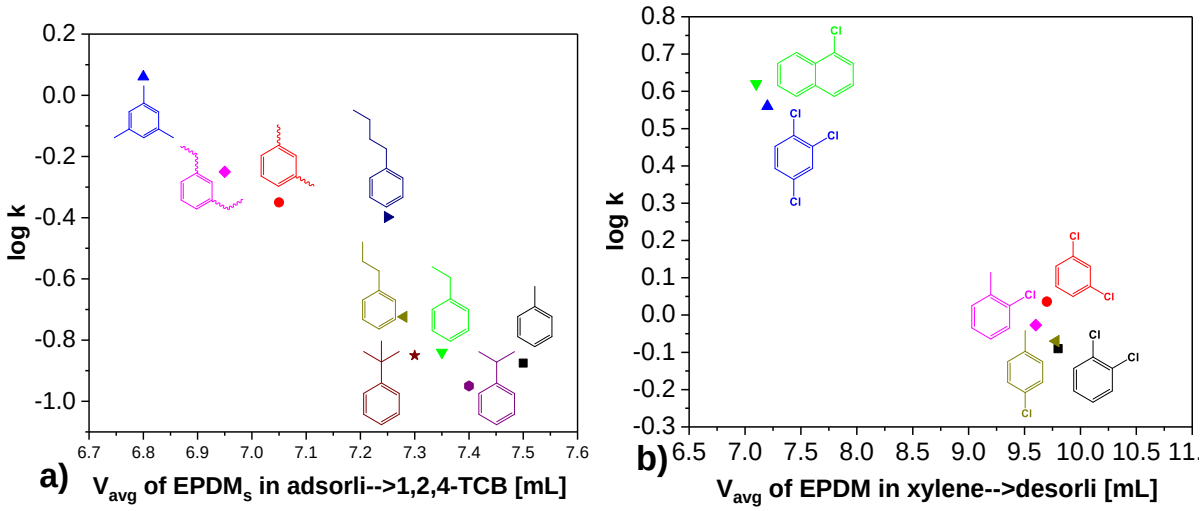

Fig 4.24 a) Dependence between log k of adsorlis and V_{avg} of EPDM in different solvent gradients; b) Dependence between log k of desorlis and V_{avg} of EPDM in different solvent gradients [215].

As **Fig. 4.24** demonstrates, an inverse proportionality exists between the retention factor of solvents and the elution volume of EPDM. In the adsorli→1,2,4-TCB gradient, log k represents the strength of interaction between the adsorption promoting solvent and PGC. Lower k-values imply weaker interaction. V_{avg} reflects the interaction strength between EPDM and PGC wherein higher values of $V_{avg,}$ suggest stronger adsorptive interactions. Stronger adsorlis (weak interaction or lower log k) increase the adsorption of the analyte on the stationary phase and therefore V_{avg} is higher. When evaluating xylene→desorli gradients, a higher log k (1,2,4-TCB and 1-CN) implies stronger interaction with PGC and consequently, interactions between EPDM and PGC are lowered resulting in lower V_{avg}.

4.2.6 Raman spectroscopy to estimate interactions between solvent and graphite

The relative strength of interactions between the stationary phase and solvent molecules was determined by a complementary technique to support our previous hypothesis on SRR. The Raman spectrum of graphite exhibits three distinct bands, namely the G-band, the D-band, and its over-tone, the 2D-band [203, 204]. The G-band (graphite band) arises from the tangential

vibrations of the carbon atoms and represents the sp^2-bonded carbon present in the planar sheet configurations of graphite [205-207]. Interactions involving the solvent molecules and graphite translate to a distinctive shift in the G-band which can be used to quantify the intermolecular forces. The Raman spectrum of neat Hypercarb^{TM} was recorded to determine the position of the characteristic graphite bands (**Fig.4.25a**). The shift of the G-band upon combination with the benzene derivatives and its relationship with the retention factor is shown **in Fig. 4.25b**.

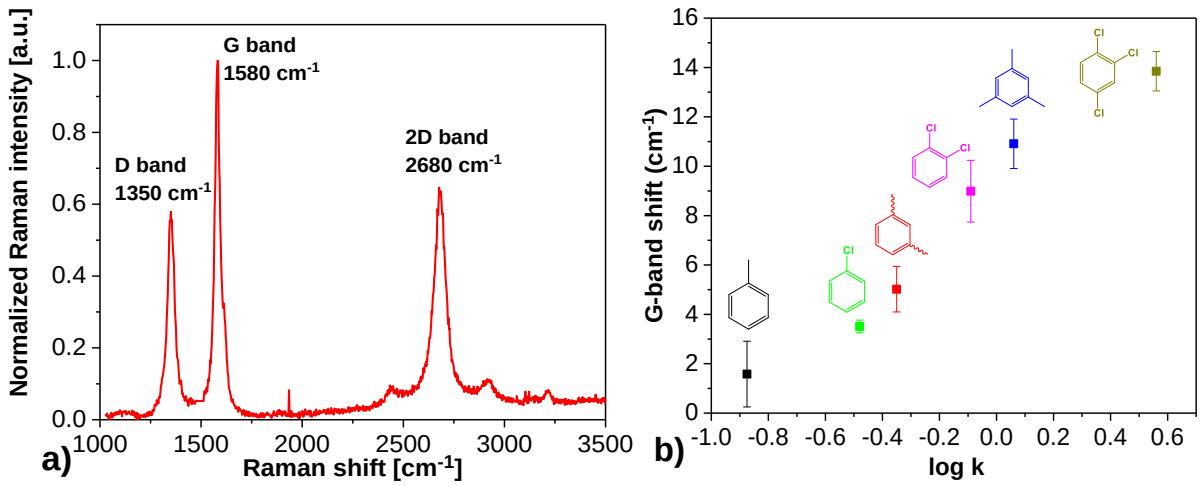

Fig. 4.25a) Raman spectrum of neat Hypercarb ^{TM} with characteristic bands and **b)** Dependence between the mean G-band shift and log k and the mean G-band shift [215].

In accordance with the mean G-band shift, the interactions of the benzene derivatives with PGC can be described as follows: 1,2,4-TCB > TMB > ODCB > xylene > chlorobenzene > toluene. These results corroborate with our previous observations (**Fig. 4.21a and 4.23a**). According to **Fig. 4.25b**, a proportional correlation of the G-band shift and log k with an almost linear dependence is observed. A higher shift in the G-band suggests stronger interaction of the solvent with PGC and it can thus be used as a desorli.

4.2.7 SRR and HSP plot

Hansen solubility parameters (HSPs) are defined by three different types of intermolecular interactions: dispersive interactions (non-polar interactions, δ_D), polar interactions (δ_P), and hydrogen bonding (δH) [188, 208, 209]. A solvent is represented in a three-dimensional space with the coordinates δ_D, δ_P and δ_H. In a similar way, the polymer is represented as a volume increment in that 3D space. A solvent can dissolve a polymer, if its solubility parameter point lies inside the volume corresponding to the solubility parameter of polymer [188]. The volume corresponding to the solubility parameter of a polymer is described by a radius R0 from the center with δ_D poly, δ_P poly and δ_H poly. Hansen proposed the relative energy difference (RED), a parameter that is related to the interactions between the solute and solvent. He defined it as

the ratio between the radius of interaction (Ra), **equation 4.12**, and the experimental sphere radius for the polymer (R0), shown in **equation 4.13**: [44, 48]

$$R_a = \sqrt{\left(\delta_D^{polymer} - \delta_D^{solvent}\right)^2 + \left(\delta_P^{polymer} - \delta_P^{solvent}\right)^2 + \left(\delta_H^{polymer} - \delta_H^{solvent}\right)^2} \quad (4.12)$$

$$\text{RED} = \frac{R_a}{R_o} \quad (4.13)$$

RED < 1 indicates high affinity between the solvent and polymer i.e., good solvent

RED > 1 implies low affinity between the solvent and polymer i.e., poor solvent.

The SRRs developed earlier do not consider the solubility of the polymer. Polymer-solvent interactions are evaluated by applying the solubility parameters. By combining the solvent-stationary phase (log k) and solvent-polymer interactions (RED, **equation 4.12 and 4.13**), a guide to solvent selection in LAC is shown.

Fig 4.26 displays a plot of the two parameters, and the results are grouped into different categories [44].

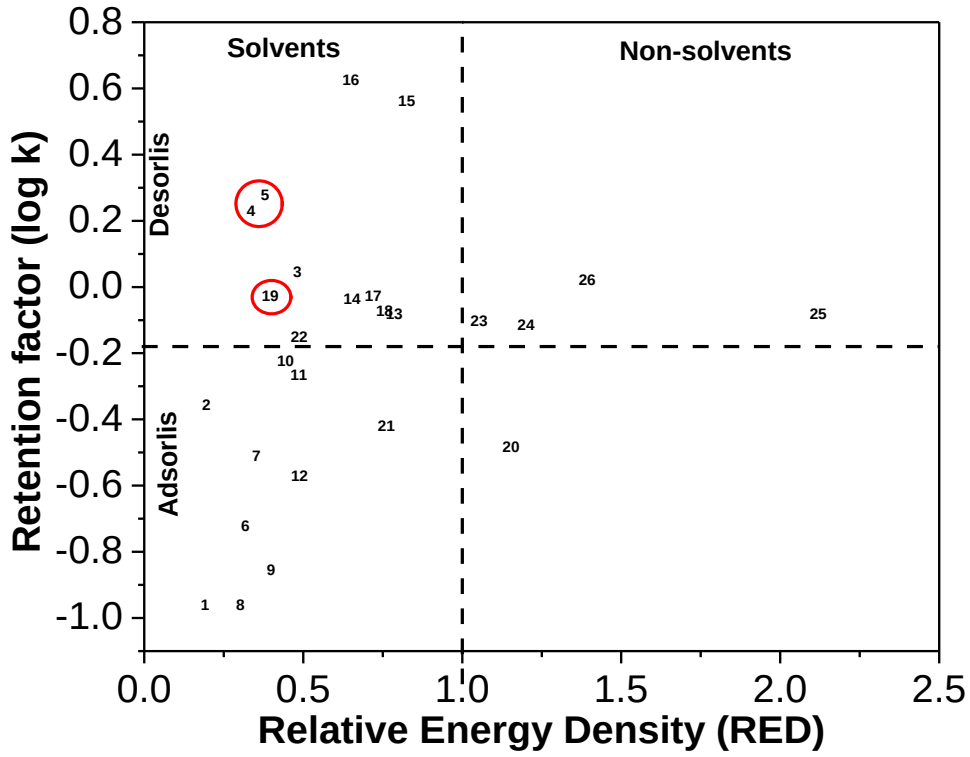

Fig. 4.26 Plot of Retention Factor (log k) vs Relative Energy Density (RED). The Hansen solubility parameters and log k values of solvents 1-26 are given in **Table 4.5** [215].

Table 4.5: List of solvents, three components of Hansen Solubility Parameters (HSP), RED and log k. All values of HSP are in unit of $MPa^{1/2}$.

Solvent number in Fig. 12	Solvent name	Dispersion (δ_D)	Polarity (δ_P)	Hydrogen Bonding (δ_H)	RED	log k
1	Toluene	18	1.4	2	0.191179	-0.95861
2	Xylene	17.6	1	3	0.194661	-0.35655
3	1,3,5-Trimethylbenzene	18	0	0.6	0.481867	0.045323
4	1,2,4-Trimethylbenzene	18	1	1	0.335966	0.230449
5	1,2,3-Trimethylbenzene	17.8	0.4	1	0.38	0.28
6	Ethylbenzene	17.8	0.6	1.4	0.317881	-0.72125
7	Propylbenzene	17.4	0.1	0.1	0.351982	-0.50864
8	isopropylbenzene	18.1	1.2	1.2	0.302724	-0.95861
9	tert-butylbenzene	17.8	1	1	0.398195	-0.85387
10	Diethyl benzene	17.6	1.2	0.8	0.444138	-0.22185
11	1,3,5-Triethylbenzene	17.8	0	0.5	0.486584	-0.2647
12	Chlorobenzene	19	4.3	2	0.488789	-0.56864
13	ortho-dichlorobenzene	19.2	6.3	3.3	0.78586	-0.08092
14	meta-Dichlorobenzene	19.7	5.6	2.7	0.653068	-0.03621
15	1,2,4-Trichlorobenzene	20.2	6.0	3.2	0.825553	0.563481
16	1-Chloronaphthalene	19.9	4.9	2.5	0.649768	0.625312
17	2-Chlorotoluene	19.6	6.5	2.2	0.71982	-0.02687
18	4-Chlorotoluene	19.1	6.2	2.6	0.7557	-0.07058
19	Tetralin	19.6	2.0	2.9	0.396504	-0.02687
20	Benzonitrile	17.4	9.0	3.3	1.15373	-0.48149
21	Anisole	17.8	4.1	6.7	0.761546	-0.42022
22	Diphenylmethane	19.5	1	1	0.487688	-0.14874
23	Benzaldehyde	19.4	7.4	5.3	1.053398	-0.10237

24	Nitrobenzene	20	8.6	4.1	1.200757	-0.11351
25	Phenol	18	5.9	14.9	2.119387	-0.08092
26	Aniline	19.4	5.1	10.2	1.393057	0.021189

A thermodynamically good solvent implies that the solvent and polymer have almost similar values in the three HSPs (RED < 1). In accordance with our hypothesis, a solvent can be classified as desorli or adsorli if the retention factor is as follows: log k > -0.18 and < -0.18, respectively. Thus, it is postulated that it is possible to use the SRR-HSP plot for streamlining solvent selection. As an example, benzaldehyde has log k = -0.09 which makes it a potentially weak desorli, but RED = 1.05 and hence it is a non-solvent for EPDM. This was experimentally verified by testing the solubility of EPDM in benzaldehyde. Furthermore, tetralin (#19): log k = -0.02, RED = 0.39 and 1,2,4-TMB (#4): log k = 0.18, RED = 0.33 and 1,2,3-TMB (#5): log k = 0.28, RED = 0.38 are prospective desorlis. Linear alkylbenzenes higher than n-hexylbenzene also fulfill the desorli criteria. Likewise, anisole (log k = -0.42, RED = 0.38) can be employed as a potential adsorli. The experimental results are shown in **Fig. 4.27**.

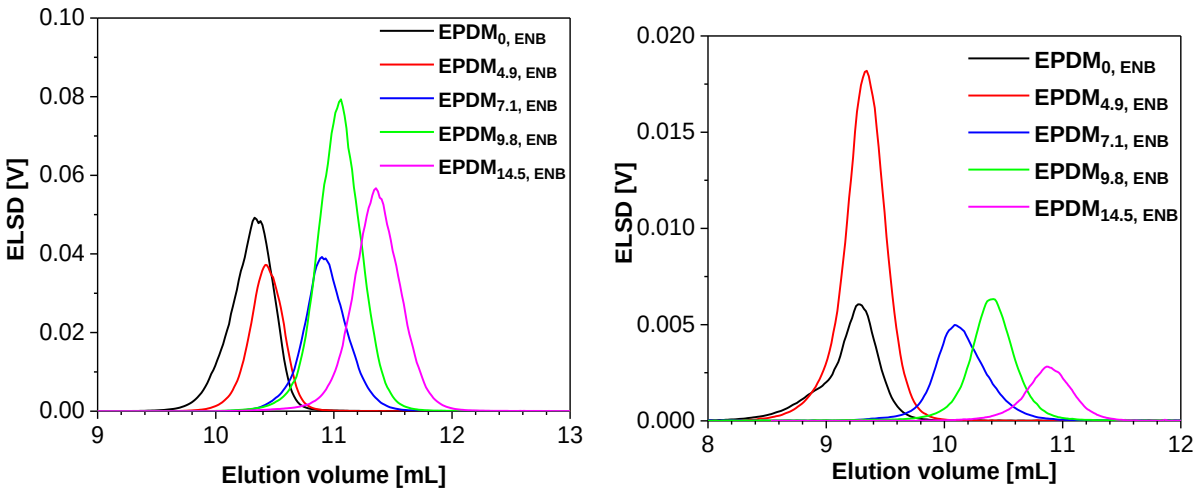

Fig. 4.27 Overlay of chromatograms of EPDM terpolymers. 3a) Mobile phase: xylene → tetralin; b) xylene → 1,2,4-TMB [215].

The elution volumes suggest that tetralin and 1,2,4-TMB can be categorized as weak desorlis as they elute in the same range as in the xylene→ODCB gradient (**Fig. 4.19**). Therefore, the approach of using SRRs-HSPs plot gives a correct prediction to identify new adsorlis and desorlis for EPDM. **Fig. 4.27** also shows better separation and resolution (**Fig. 4.27a**, R = 1.47, **Fig. 4.27b**, R = 1.49), compared to the chlorinated desorlis, i.e., 1,2,4-TCB and ODCB (**Table 4.4**).

Furthermore, xylene→n-hexylbenzene until xylene→nonylbenzene gradients lead to no elution of EPDM terpolymers. This indicates that though the strength of interactions between solvent-sorbent is a major factor influencing the adsorption/desorption, additional solvent selection criteria need to be taken into account. We now postulate the desorption mechanism and consider the characteristics required in a solvent to function as a desorli. A schematic representation of the effect of structural changes in the desorli on its desorption-promoting capability is shown in **Fig. 4.28**.

Besides being thermodynamically good solvents, the desorli molecules displace adsorbed macromolecules and undergo preferential stronger interactions with PGC as compared to the polymer molecules. These characteristics of desorli were established in log k vs. RED plot.

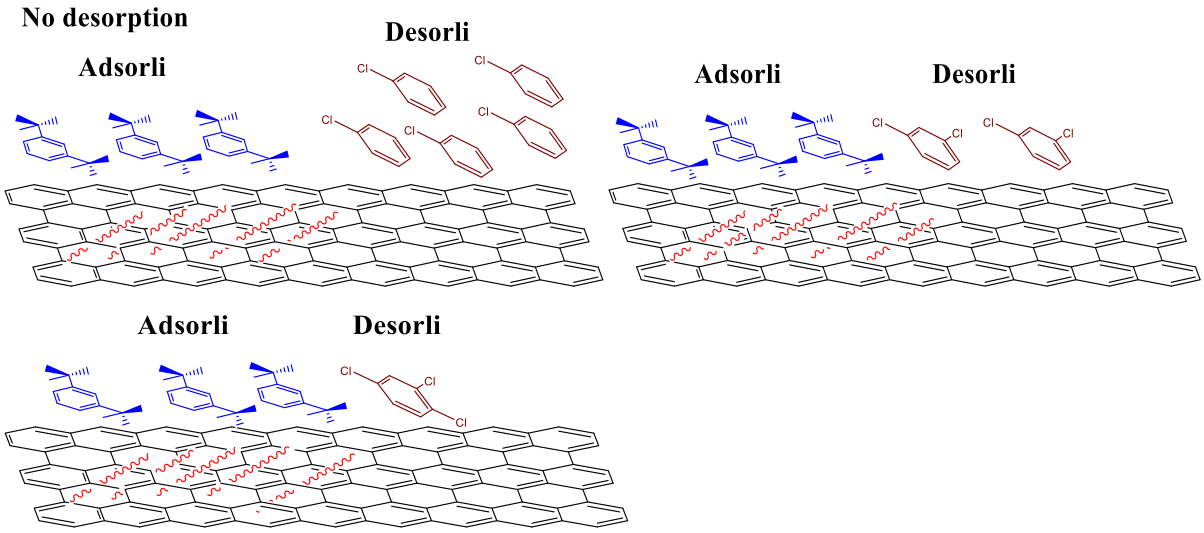

Fig. 4.28 Schematic illustrating the effect of successive chlorine substitution on the benzene ring of a desorli on its desorption strength [215].

Typical chlorinated desorlis, like 1,2,4-TCB, possess an aromatic ring marginally polarized due to the EWG and has a planar shape as a result of sp^2 hybridization. Consequently, the macromolecules are desorbed from the PGC and elute from the column. The newly discovered desorlis fulfill all these attributes. For instance, the benzene ring in 1,2,4-TMB is polarized by the three methyl groups and although the carbon atoms are sp^3 hybridized, the molecule can be considered sufficiently planar to desorb EPDM chains.

Nevertheless, the SRR-HSP plot does not consider the polarization of the aromatic ring by the substituent groups and the planarity of the molecule needed to desorb polymer chains. It is speculated that for linear alkylbenzenes the polarization induced by the alkyl chain is insufficient, and that the alkyl chain is not in the same plane as the benzene ring. Hence, even though these solvents have strong interactions with PGC, they cannot desorb the polymer.

Polyethylene adsorbs from thermodynamically poor solvents [210], but adsorption from n-decane, which is a thermodynamically good solvent, is interesting [211]. This may be explained by taking into consideration the increase in adsorption enthalpy with the increase in the molar mass of homologues of linear alkanes [212]. The conformational entropy of a chain decreases upon adsorption and this reduction is higher for a higher molar mass member of a homologous series. Therefore, n-decane adsorbed on the graphite surface is displaced by PE macromolecules because the latter being a higher molar mass homologue of the n-alkane series. An analogous effect may justify why higher homologues of n-alkylbenzenes act as adsorlis for EPDM, although there is no direct evidence yet.

4.3 Critical conditions for liquid chromatography of statistical polyolefins: Evaluation of diene distribution in EPDM terpolymers

4.3.1 Abstract

Liquid chromatography at critical conditions (LCCC) is of interest as it can unravel molecular information on macromolecular structures not possible by other analytical techniques. However, such conditions have never been experimentally determined for statistical olefin copolymers, which belong to one of the commercially most relevant categories of polymeric materials. Consequently, critical conditions (CC) for statistical ethylene propylene (EP) copolymers were identified by two methods.

In the first approach, the composition of the binary mobile phase was varied while keeping the temperature constant. In the second method, the adsorption-desorption temperature was modulated without varying the mobile phase composition. Solvents for both methods were identified by using a novel route by creating the structure retention relationships and the Hansen Solubility Parameters plot. For the first time, the heterogeneity of an ethylene propylene diene terpolymer sample with regard to the pendant double bond of the diene was determined. This novel chromatographic approach was validated by offline hyphenation of LCCC with NMR spectroscopy. This work gave the first experimental evidence for the existence of CC for statistical olefin copolymers, as postulated by Brun.

4.3.2 Polymer samples

EPDM and EP samples were prepared by ARLANXEO Netherlands B.V. The average values of their chemical composition and their molar masses (kg/mol) are summarized in **Tables 4.6-4.8**. The samples in **Table 4.7** were produced in a batch polymerization reactor using advanced single-site catalysts. The polymer samples listed in **Table 4.6** and **4.8** were prepared in a continuously stirred tank reactor (CSTR) also employing an advanced single-site catalyst.

It is assumed that the samples possess similar intramolecular structures in terms of sequence distribution statistics (i.e., randomness) and tacticity because the same metallocene catalysts were used in their preparation. According to the theory of Brun, a statistical copolymer (of a given chemical composition) with random monomer distribution behaves like a hypothetical homopolymer with a single critical point of adsorption (CC) [213, 214]. The EP copolymers used in this investigation have random comonomer incorporation with narrow CCD.

Table 4.6 Ethylene-propylene copolymers - Similar E/P ratio and variation in average molar mass.

E (mol. %)	P (mol. %)	E/P	M_w (kg/mol)	Đ
52.6	47.4	1.1	585	2.1
52.7	47.3	1.1	495	2.1
52.8	47.2	1.1	730	2.1
52.9	47.1	1.1	320	2.1
53.8	46.2	1.1	230	2.1

Table 4.7 Ethylene-propylene copolymers - Variation in E/P ratio.

E	P	E/P	M_w	Đ
42.7	57.3	0.7	1405	2.1
52.6	47.4	1.1	2270	2.0
55.3	44.7	1.2	1160	1.9
58.3	41.7	1.4	405	2.2
60.1	39.9	1.5	2075	2.2
62.7	37.3	1.7	755	2.2

Table 4.8 EPDM samples with ENB, weight average molar mass, M_w, and dispersity, Đ.

ENB	E	P	E/P	M_w	Đ
0.8	62.2	37.0	1.7	530	2.2
1.1	60.2	38.7	1.6	515	2.1
1.4	59.7	38.9	1.5	353	2.6
2.1	62.9	35.0	1.8	503	2.7
2.9	61.4	35.7	1.7	394	2.7
4.4	62.7	32.9	1.9	395	2.6

The sample nomenclature for EP copolymers is as follows: $EP_{1.2}$, the number in the subscript denotes the E/P ratio. For EPDM terpolymers, $EPDM_{1.7,\ 2.9}$, the first number represents the E/P ratio and the second number is the ENB content.

4.3.3 Determination of CC of statistical EP copolymers by varying the binary mobile phase composition: Mixed eluent method

In the first approach, a mixture of two eluents differing in their elution strength was used as the isocratic mobile phase. As per the investigations in our previous study on solvent selection for LAC, solvents were classified as either adsorli (weak eluents) or desorli (strong eluents) based on their strength of interaction with the stationary phase, in this case PGC. Solvents with strong interaction with the sorbent surface (higher retention factor, log k) were recognized as desorli and those with weak interactions (lower log k) were identified as adsorli [215]. This study was extended to streamline solvent selection for identifying CC in EP copolymers using the mixed eluent method. Consequently, a structure retention relationship (SRRs) and Hansen Solubility Parameters (HSPs) plot was created for potential solvent candidates and an statistical EP copolymer (**Fig. 4.29**).

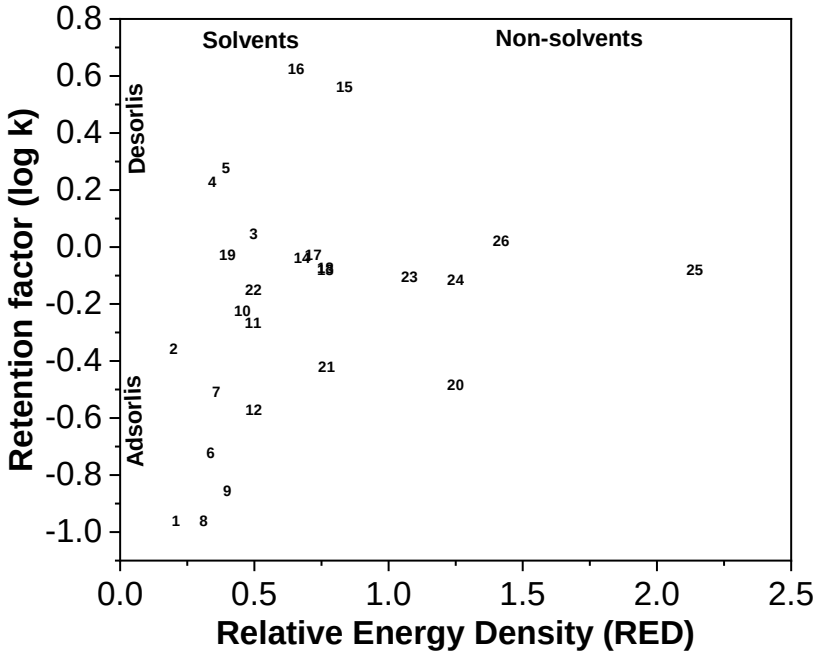

Fig. 4.29 Plot of retention factor (log k) versus RED. The HSPs and log k values of solvents 1-26 are given in **Table 4.5**. 1,3,5-TMB is #3 and 1,2,4-TMB is #4 [225].

As per our previous conclusions, solvents that satisfy the two criteria i.e., log k < log k_c and relative energy difference (RED < 1) can be classified as adsorli whereas those with log k > log k_c and RED < 1 are categorized as desorli. Solvent candidates which have RED > 1 are non-solvents. We define k_c as the critical value of the retention factor that distinguishes an adsorli from a desorli and is specific for a given polymer. The relative energy difference (RED) is characterized by the interactions between the solute and solvent [188]. The RED values for any given solvent-EP copolymer combination and log k for the solvents were calculated according

to the procedure described before [215]. HSPs of solvents and EP copolymer are available in literature [188].

1,3,5-TMB was chosen as the weak eluent which would promote the adsorption of $EP_{1.1}$ copolymers on the PGC surface, whereas 1,2,4-TCB was the strong eluent to enable desorption. To identify the CC, the volume ratio of weak to strong eluent was varied thereby modifying the elution strength of the isocratic mobile phase. By methodically varying the elution strength, the chromatographic behavior of $EP_{1.1}$ copolymer was measured in binary mixtures of 1,2,4-TCB and 1,3,5-TMB starting with 100 % strong eluent. Five statistical EP copolymers with similar chemical composition (E/P = 1.1, $EP_{1.1}$) and different M_w (**Table 4.6**) were injected at room temperature **(Fig. 4.30).**

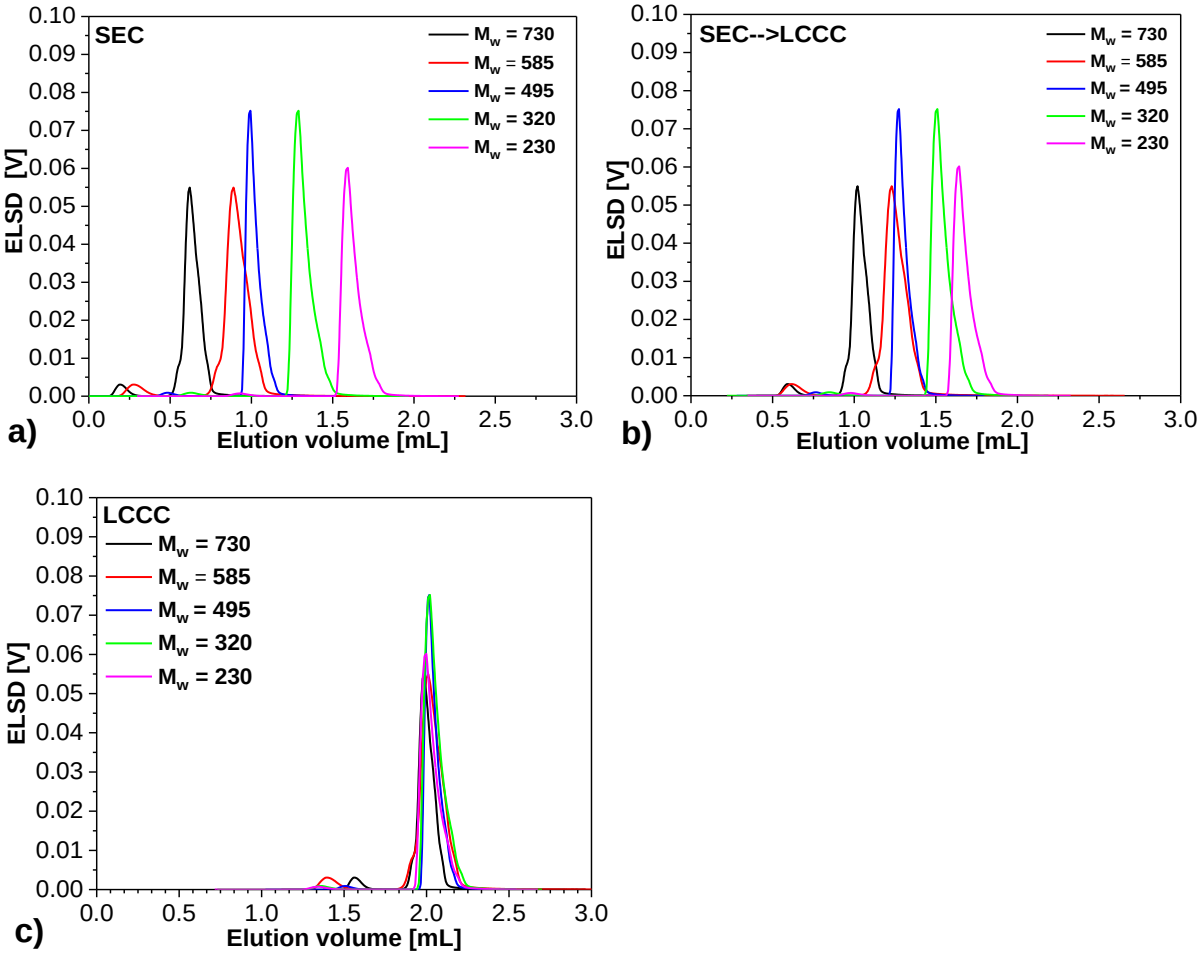

Fig. 4.30 Chromatograms for EP copolymers (all with E/P = 1.1) in a) 100 % 1,2,4-TCB; b) 1,2,4-TCB/1,3,5-TMB, 90/10 vol. %; c) 1,2,4-TCB/1,3,5-TMB, 26.5/73.5 vol. %. Column temperature: 70 °C [225].

$EP_{1.1}$ copolymers eluted in 1,2,4-TCB in a narrow range of elution volume (V_e) and the effect of molar mass on V_e implies size exclusion mode (**Fig. 4.30a**). The addition of a weak eluent, 1,3,5-TMB, to 1,2,4-TCB increased the V_e (**Fig. 4.30b**) due to enthalpic interactions of the

macromolecules with the stationary phase. Additionally, the hydrodynamic volume of macromolecules is dependent on the solvent (i.e., mobile phase composition) and hence influences the elution behavior of the polymer chains. Thus, at this adsorli/desorli ratio, the increase in elution volume is determined by the molar mass of the polymer.

When the amount of the weak eluent was increased further, all the copolymers eluted at the same V_e at a unique mobile phase composition. This was the critical solvent composition or CSC (1,2,4-TCB/1,3,5-TMB, 26.5/73.5 vol. %) of the solvent mixture for $EP_{1.1}$ at T_c = 70 °C (**Fig. 4.30c**). The statistical $EP_{1.1}$ copolymer chains can be described by Bernoulli statistics and therefore may be represented as hypothetical homopolymer chains with an effective monomer unit and hence a single CPA. The macromolecules are described as being 'invisible' to the chromatographic system under such conditions. [213, 214]. When the percentage of weak eluent is increased beyond the CSC, the equilibrium moves away from LCCC and the copolymers would elute in LAC mode.

An alternative method was used to verify the accuracy of the critical conditions determined from the above method. (**Fig. 4.31).**

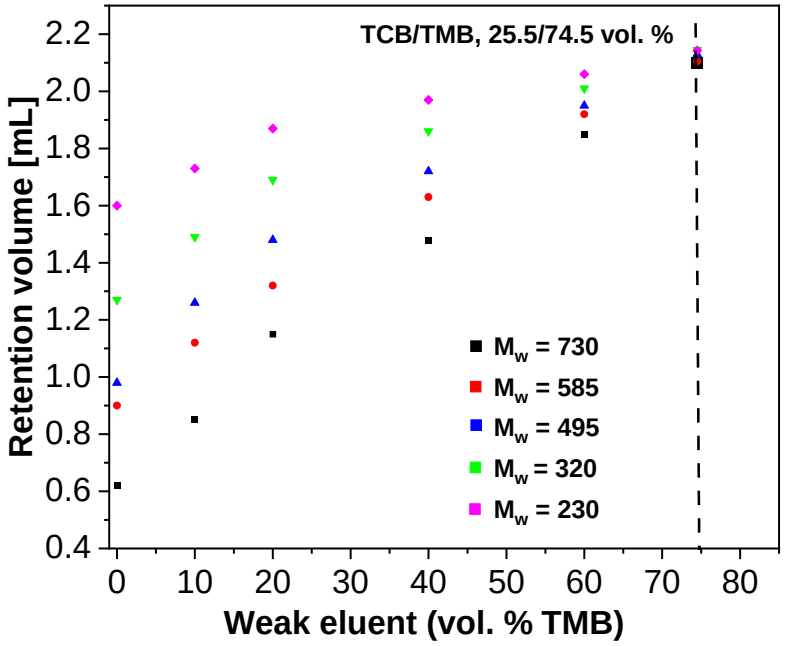

Fig. 4.31 Retention volume versus percentage of 1,3,5-TMB to determine the critical conditions of $EP_{52.6}$ copolymer series [225].

Based on the method developed by Cools et al. [216], the critical condition can be identified from the crossing point of curves plotted between the retention volume of the polymer samples and the percentage of non-solvent (**Fig. 31)**. $EP_{1.1}$ copolymers were injected in an isocratic

mobile phase 1,2,4-TCB/1,3,5-TMB of varying composition. The retention volumes at different volume ratios of weak/strong eluent converge at a particular mobile phase composition. Thus, 24.5/74.5 vol. % 1,2,4-TCB/1,3,5-TMB was identified as the critical condition for $EP_{1.1}$ copolymers which agrees well with the critical solvent composition obtained using the previous method SEC-LAC plots (**Fig. 4.30c**).

The CC for EP copolymers with different chemical compositions was evaluated using the mixed eluent method. **Fig. 4.32** shows a plot of 1,2,4-TCB vol. % vs. E/P ratio.

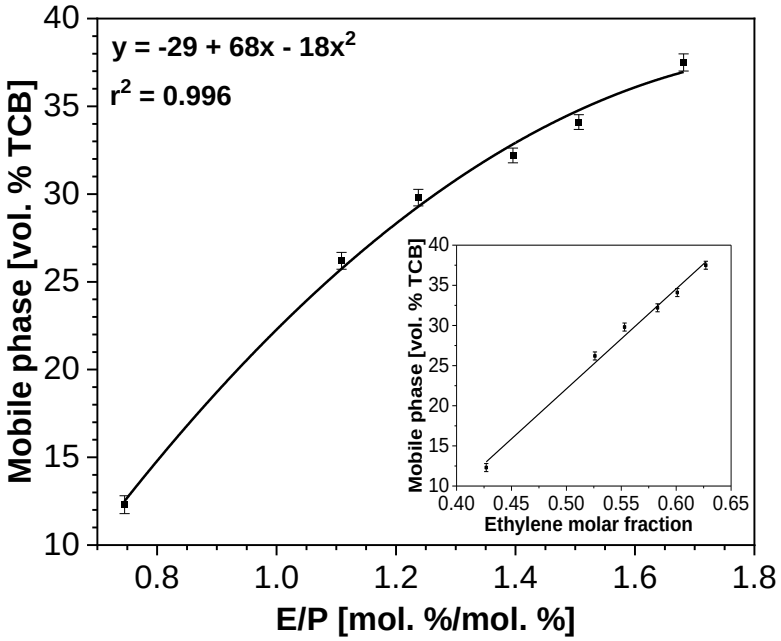

Fig. 4.32 Dependence between the critical condition (vol. % 1,2,4-TCB) and chemical composition (E/P ratio) of EP copolymers [225].

As observed, a higher amount of strong eluent (1,2,4-TCB) is required to reach CC for copolymers with a higher E/P ratio (**Fig. 4.32**). This is attributed to the higher amount of ethylene units in the polymer which promote strong interactions with the stationary phase. This curve can be used to identify the CC of statistical EP copolymers given their E/P ratio. Brun developed a theory predicting the existence of a critical adsorption point (CPA) for statistical copolymers [213] of a given chemical composition and sequence distribution. These measurements provide the first experimental evidence for the same.

There are several challenges coupled to the mixed eluent method. To begin with, achieving repeatability when determining CC can be difficult. This is because the retention of polymers is sensitive to the solvent composition, moisture content, and variation in impurities due to different solvent batches and grades [59, 217]. By measuring the CC for $EP_{1.1}$ (E = 52.6 mol. %) three times, a standard deviation (σ = 0.47 vol. % TCB) was evaluated which converts to an

uncertainty of 0.66 mol. % in measuring the ethylene content. Furthermore, individual components of the solvent mixture can adsorb in a different manner on the polymer chains and stationary phase. Finally, the preferential sorption may depend on the molar mass of the polymer chains. Thus, it is not simple to conclude that the macromolecules are chromatographically invisible [218, 219]. Therefore, developing a single-solvent critical condition method is important. The new approach can improve the repeatability of the mixed eluent method and possibly eliminate the preferential sorption of the solvents for the macromolecules.

4.3.4 Determination of CC of statistical EP copolymers by modulating adsorption-desorption temperature: Single eluent method

The adsorption-desorption temperature (T_{AD}) can also be employed as a thermodynamic parameter to adjust the chromatographic behavior by keeping the eluent composition constant or by using a single eluent (isocratic conditions). Consequently, it is possible to shift from the entropy-driven SEC mode attained by increasing the T_{AD} to the enthalpy dominated LAC-mode achieved by lowering T_{AD}.

In the mixed eluent method, a mixture of an adsorli ($\log k < \log k_c$) and a desorli ($\log k > \log k_c$) was employed. Therefore, while choosing a single eluent to replace the mixture of solvents, it is reasonable to assume that its elution strength should be between that of a desorli and an adsorli. On the one hand, the solvent should not promote polymer adsorption ($\log k < \log k_c$) to such an extent that the macromolecules might be adsorbed on the stationary phase too strongly to elute in a reasonable time. On the other hand, the eluent should not hinder the interactions excessively ($\log k > \log k_c$) so that the polymer chains elute within no time. Thus, a good place to begin for the single eluent system would be to select a solvent with $\log k \sim \log k_c$.

Thus, 2-chlorotoluene was selected as an eluent by using the log k vs RED plots developed for EP copolymers (**Fig. 4.29**). Subsequently, the column adsorption-desorption temperature was adjusted to establish CC for the $EP_{1.1}$ copolymers. A series of chromatograms is shown in **Fig. 4.33a and 4.33b** representing the SEC and LCCC, respectively. The calibration for EP copolymers with different chemical compositions is shown in **Fig. 4.33**.

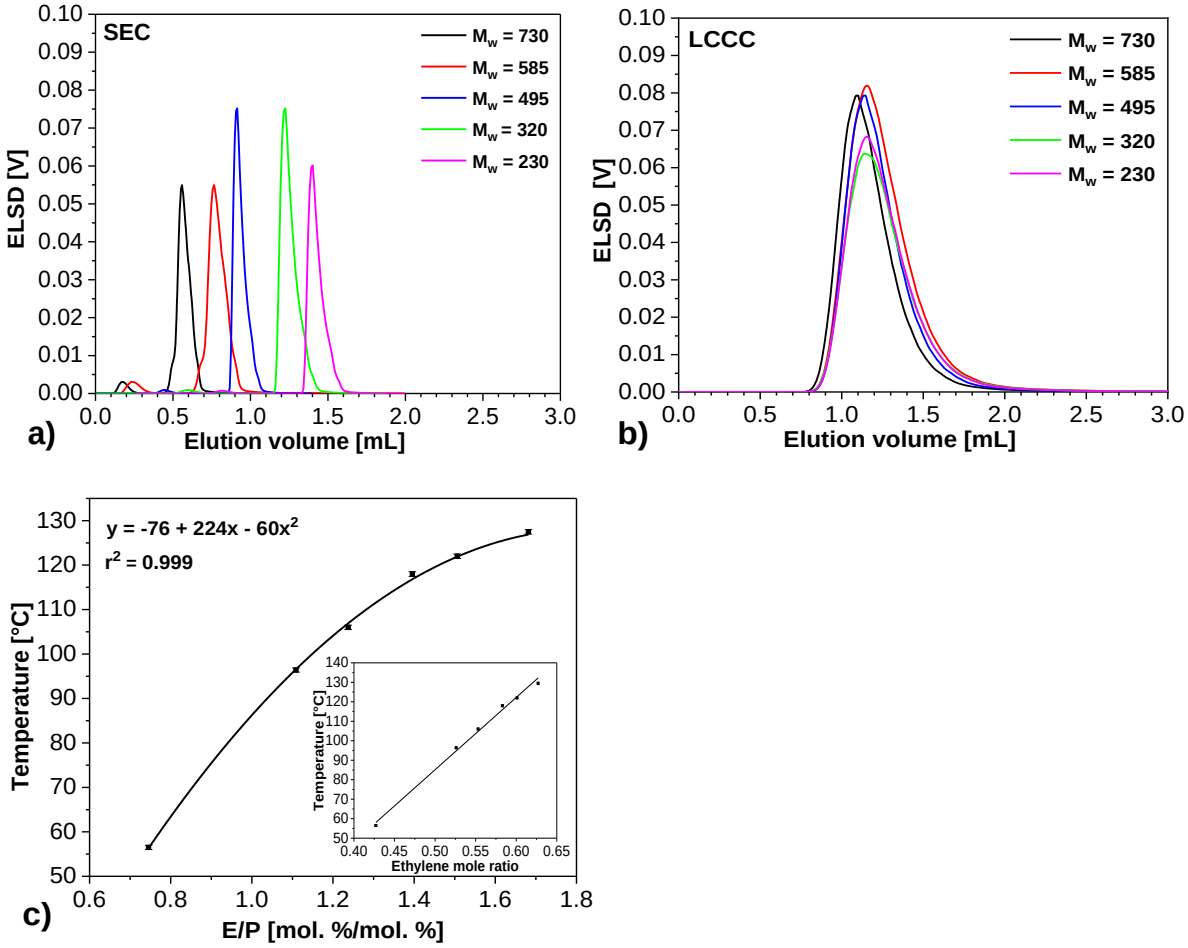

Fig. 4.33 Chromatogram for EP copolymers: a) SEC at T_{AD} = 140 °C; b) LCCC at T_{AD} = 96 °C; c) Dependence between the critical temperature and E/P ratio [225].

According to the elugrams in **Fig. 4.33a,** at T_{AD} = 140 °C, 2-chlorotoluene desorbs the $EP_{1.1}$ copolymers and separation is achieved according to their hydrodynamic volume. It can be stated that the solvation strength of 2-chlorotoluene allows to shift from SEC to LAC simply by lowering the T_{AD}. LAC conditions cannot be realized using 1,2,4-TCB or other desorlis due to their desorption-promoting strength ($\log k > \log k_c$). Similarly, SEC mode cannot be achieved with xylene or other adsorlis on account of their poor desorption promoting capability ($\log k < \log k_c$).

By delicately regulating the T_{AD}, CC for $EP_{1.1}$ copolymers was identified as 96 °C, evidenced by the same elution volume (**Fig. 4.33b**). Analogously, CC for EP copolymers with different chemical compositions were identified. To check the repeatability, three measurements of $EP_{1.1}$ (E = 52.6 mol. %) copolymer sample produced a standard deviation, σ = 0.42 % °C which converted to an uncertainty of 0.45 mol. % in measuring the ethylene content. Thus, it be asserted that compared to the mixed eluent approach, the use of a single eluent is better if achieving better repeatability is the foremost goal. The mixed eluent method, nevertheless,

offers flexibility with regards to selecting eluents. Different combination of adsorli/desorli mixture can be used to arrive at the CC.

Comparing the elution strength for the different solvent combinations can be a useful exercise. For reversed-phase systems, the Hildebrand solubility parameter is a useful parameter to estimate the eluent strength [220]. This is significant because the parameter can be used as a guiding tool possible to predict the critical solvent composition (CSC) for other solvent mixtures after determining the CSC for one combination. Nevertheless, this has not yet been established for the separation of polymers on a PGC stationary phase. Previously, retention factor of the eluent was identified as a measure of the elution strength [215]. Retention factor for the CSC using different eluent combinations is presented in **Table 4.9**. The experimental value of k was compared to the 1,3,5-TMB/1,2,4-TCB combination, 1.78. The retention factor was not used in its logarithmic form. Instead for calculation, k was used as this did not generate negative values. The desorli in all the mixtures is 1,2,4-TCB.

Table 4.9 Eluent strength for the CSC of different solvent combinations on the PGC column

Adsorli	vol. /vol.	Retention factor, k	% Error
Toluene	56.9	1.64	7.8
Xylene	62.7	1.69	5.0
Ethylbenzene	58.2	1.71	3.9
Propylbenzene	60.2	1.62	8.9

Thus, the retention factor can be used as a starting point in estimating the CSC for an adsorli/desorli combination instead of a trial-and-error approach.

One of the objectives to determine CC for EP copolymers is for separating EPDM terpolymers solely according to chemical composition. It is postulated that the calibration in **Fig. 4.33c** and **Fig. 4.32** may be used for separating EPDM terpolymers based on diene content. Accordingly, by applying CC in the right manner, the contribution of ethylene to the EPDM retention can be considered constant. Thus, solely the diene units would govern the separation instead of both ethylene and diene.

The equations governing EPDM retention are as follows.

$$\text{Retention}_{EPDM} = \text{Retention}_{E} + \text{Retention}_{ENB} \quad (4.14)$$

Retention_{E} is contribution of ethylene to the EPDM retention

Retention_{ENB} is the contribution of ENB to the EPDM retention

By applying CCs based on E/P ratio, it is hypothesized that the contribution of ethylene to the EPDM retention would be identical across EPDM samples of varying chemical composition.

Equations 4.15 and 4.16 demonstrate our hypothesis**.**

$$\text{Retention}_{E,1} = \text{Retention}_{E,2} = \ldots\ldots\ldots\ldots\ldots = \text{Retention}_{E,n} = \text{constant} \quad (4.15)$$

$$\text{Retention}_{EPDM} \; \alpha \; \text{Retention}_{ENB} \quad (4.16)$$

To apply CC to an EPDM sample with a specific chemical composition, the E/P ratio for both EP and EPDM polymer should be identical. Thus, the effective monomer units comprising of E and P will be identical in the EP and EPDM polymers.

4.3.5 Modified liquid adsorption chromatography

The EPDM samples synthesized using metallocene catalysts have similar ethylene/propylene (E/P) ratio. Thus, the retention arising from ethylene is almost identical between the EPDM samples and thus it can be assumed that the separation is exclusively a function of the ENB content. To check this hypothesis, EPDM samples with varying ENB content and almost similar E/P ratios were measured by SGIC using a 1,3,5-TMB →1,2,4-TCB gradient shown in **Fig. 4.34**.

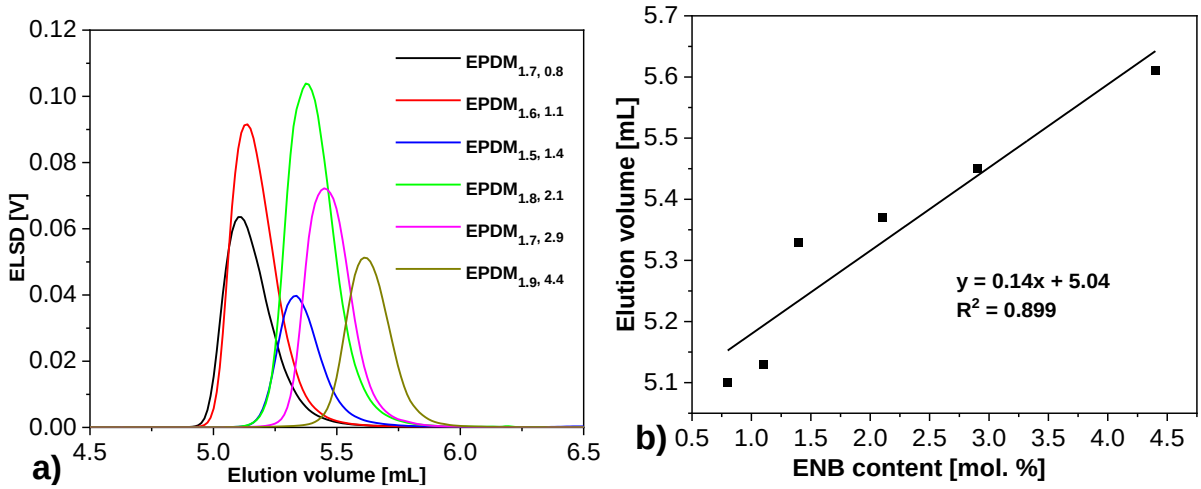

Fig. 4.34a Overlay of chromatograms and **b)** dependence between the elution volume and the average ENB content in mol % of the EPDM terpolymers. Mobile phase: 1,3,5-TMB→1,2,4-TCB. Temperature: 140 °C. Linear solvent gradient: 10 min [225].

As noticed in **Fig. 4.34a**, the samples seem to be separated according to the average ENB content, but the poor R^2 = 0.899 in **Fig. 4.34b** implies that the separation is influenced by another factor, possibly the contribution of ethylene to the retention or a different molar mass. However, the effect of molar mass on separation should be insignificant as it was concluded

that for samples having M_w > 14 kg/mol, the elution depends only on the chemical composition [195]. The EPDM samples in this investigation contain around 5 % material with M_w < 14 kg/mol and cannot explain the above phenomenon. Thus, it is not possible to determine the diene content and its distribution by the SGIC approach.

4.3.6 Separation of EPDM terpolymers by ENB content

Critical conditions obtained from the calibration in **Fig. 4.32** using the mixed eluent method were applied to the EPDM samples as shown in **Fig. 4.35**. Similarly, critical conditions (T_{AD}) from the calibration in **Fig. 4.33c** using the single eluent method were applied to the EPDM samples (**Fig. 4.36)**.

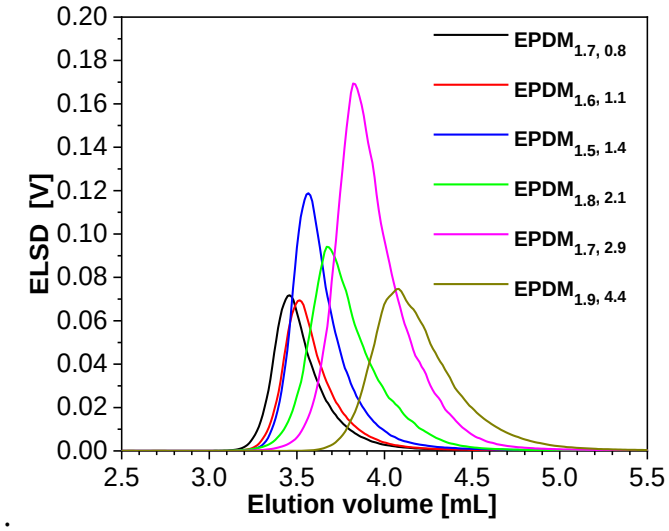

.

Fig. 4.35 Overlay of chromatograms of EPDM terpolymers by applying CC. Mobile phase: x vol. % 1,2,4-TCB (in 1,3,5-TMB). x is obtained from **Fig. 4.32** based on the E/P ratio. Column temperature: 70 °C [225].

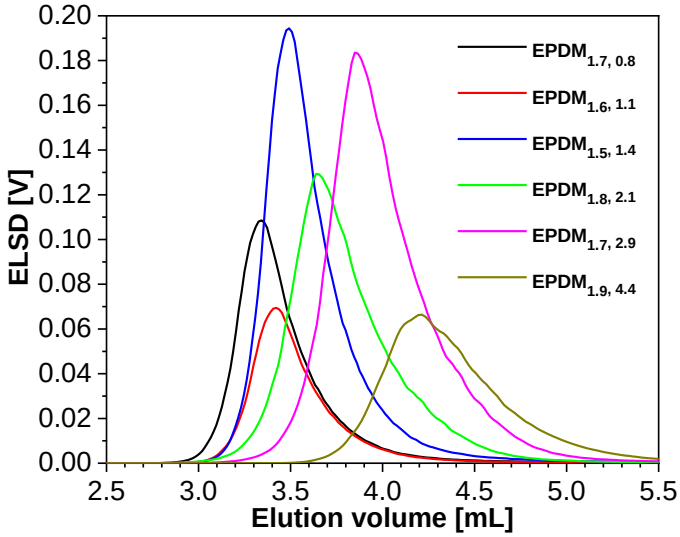

Fig. 4.36 Overlay of chromatograms of EPDM terpolymers by applying CC. Mobile phase: 2-chlorotoluene. Column temperature: T_{AD} (96 °C), obtained from **Fig. 4.33c** based on E/P ratio [225].

4.3.7 Comparison of diene distribution using different methods

The two methods were verified using offline hyphenation with ^{1}H-NMR. Therefore, EPDM$_{1.8, 2.1}$ was fractionated as described in the experimental part, into four fractions. The ENB content of each fraction was measured by ^{1}H-NMR [221] and plotted against its elution volume. The calibration obtained by hyphenating LCCC with ^{1}H-NMR is shown and compared to SGIC (**Fig. 4.34**), mixed eluent (**Fig. 4.35**), and single eluent (**Fig. 4.36**) procedures. The ^{1}H-NMR spectrum of the EPDM sample is shown in Fig. **4.37**.

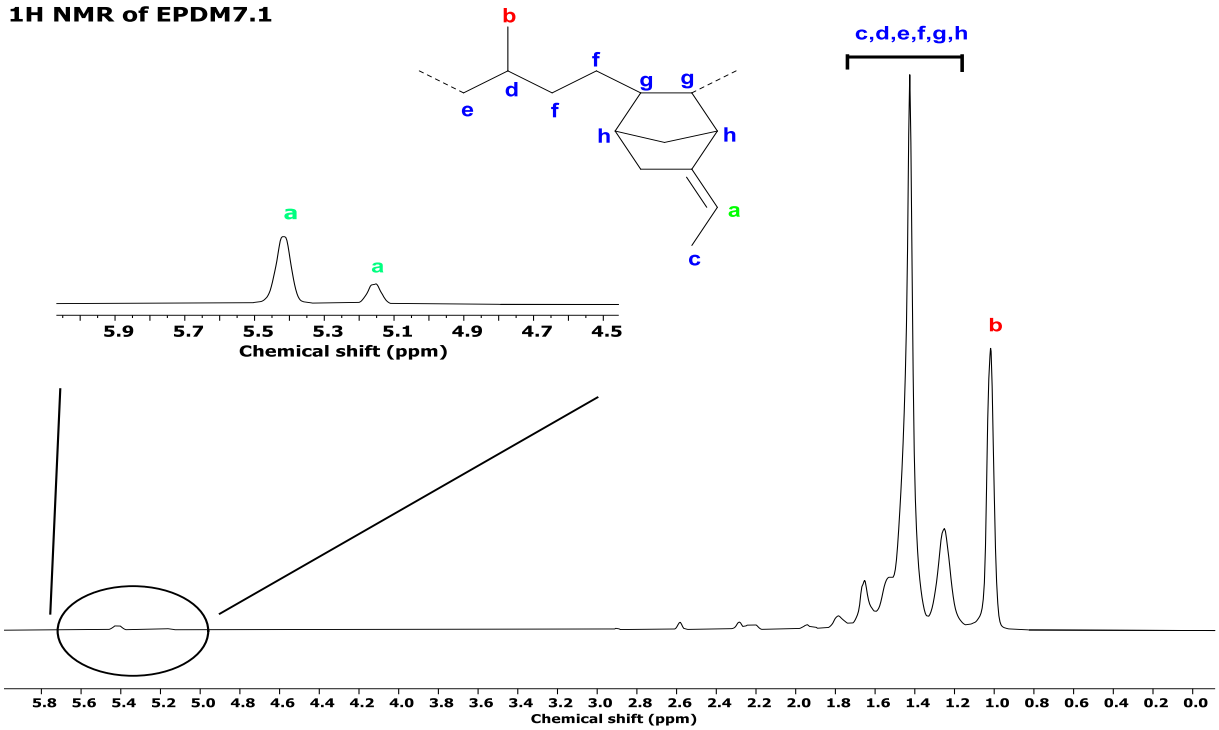

Fig. 4.37 ^{1}H NMR spectrum of EPDM$_{2.1}$ with assignment of the signals [225].

b = 0.4-0.9 ppm 3 H of P (CH_3)

c, d, e, f, g, h = 0.9-2.8 ppm 3 H of P (–CH_2–CH–) + 4 H of E (–CH_2–CH_2–) + 11 H of ENB

a = 5-5.5 ppm 1 olefinic H of ENB (two peaks because ENB has two conformational isomers, E and Z)

To compare the ENB distribution of EPDM$_{1.8, 2.1}$ using different approaches, the content of ENB was calculated for each elution volume using the calibration lines in **Fig. 4.38a,** and the distribution is shown in **Fig. 4.38b**.

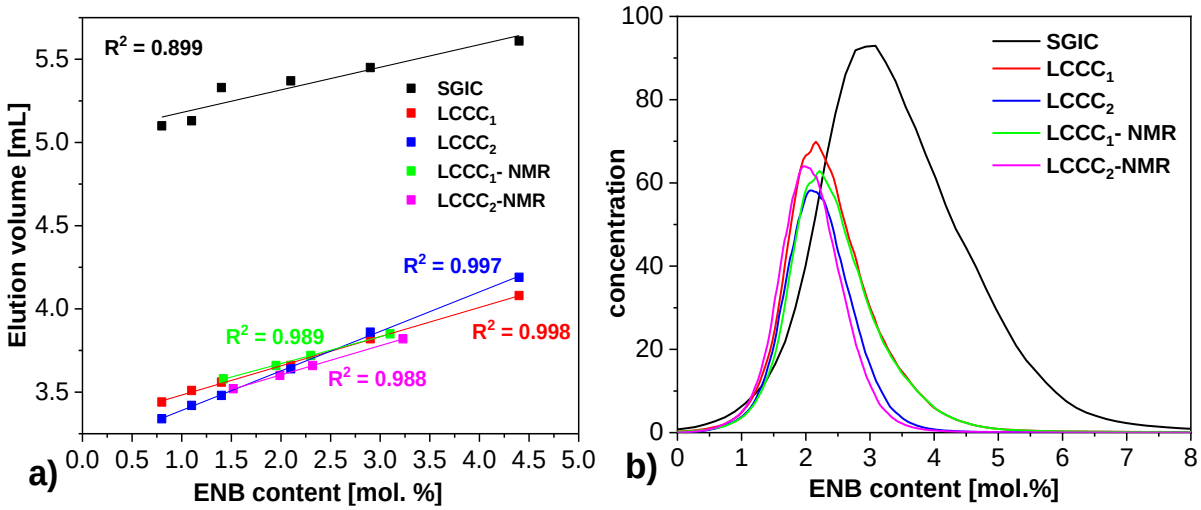

Fig 4.38a) Comparison between calibrations obtained based on different chromatographic methods; **b)** Comparison of the distribution of diene in $EPDM_{1.8,\ 2.1}$ using different procedures. $LCCC_1$: mixed eluent and $LCCC_2$: single eluent; c) Comparison of the distribution of diene using $LCCC_1$ and SGIC for three EPDM samples [225].

As reflected in **Fig. 4.38a**, there is a good agreement between the two methods and their hyphenation with NMR, thus providing validation to the CC approach. It can be implied that the separation of EPDM is solely a function of ENB content given the goodness of the fit i.e., R^2 values. This contrasts with the SGIC method as in this case the separation is influenced by two independent parameters, ethylene and diene content.

In **Fig. 4.38b**, the distribution of ENB in $EPDM_{1.8,\ 2.1}$ using the SGIC differs considerably from that obtained using both CC methods. After fractionation and following offline hyphenation, the CCD calculated by using the calibration in **Fig. 4.38a** is in good agreement with the CC approaches. Minor differences between the two procedures are expected due to instrumental/practical differences.

It should be mentioned that these CCs have been identified for polymers with a similar microstructure as they have been prepared using the same catalyst. If a different catalyst is used for synthesis, the microstructure will not be the same. For example, it may be blockier or have more alternating sequences. In such a scenario, the presence of single CC would not be possible as only homopolymers and statistical copolymers have a single CPA. Copolymers with a predominant alternating and blocky structure may have more than one CPA as explained by Brun [222, 223].

4.4 In-depth characterization of EPDM terpolymers by high temperature two-dimensional liquid chromatography

4.4.1 Abstract

High-temperature two-dimensional liquid chromatography (HT 2D-LC) using HT-HPLC as first dimension and HT-SEC as the second dimension holds enormous potential to investigate the distribution according to molar mass and chemical composition of polyolefin elastomers such as EPDM. This enables detection by using a suitable quantitative detector for monitoring the eluting polymer. Experimental data obtained from HT 2D-LC are generally presented as contour plots, which mathematically can be expressed in a matrix form.

Quantitative data about chemical composition, molar mass and concentration of all the segments, which are present in an analyte, can be obtained, after calibrating the HPLC separation (HPLC elution volume vs. chemical composition), SEC separation (SEC elution volume vs. molar mass) and the response of the detector (detector response vs. mass of the polymer).

A procedure based on subtraction and addition of matrices is described, which enables quantitative comparison of different polymer materials. This procedure enables to determine, which components are present in both materials (i.e., identical components or segments) and which are present only in one from both materials (i.e., unique segments). Moreover, molar mass distribution, as well as chemical composition distribution of both identical and unique segments is evaluated from experimental data. The procedure was applied to different EPDM samples.

4.4.2 Polymer samples

Table 4.10 Ethylene-propylene copolymers

E [mol. %]	P [mol. %]	M_w [kg/mol]	Đ
42.7	57.3	1405	2.1
52.6	47.4	2270	2.0
55.3	44.7	1160	1.9
58.3	41.7	405	2.2
60.1	39.9	2075	2.2
62.7	37.3	755	2.2
66.2	33.8	1136	2.1

67.3	32.7	1528	2.2
69.7	30.3	288	2.2
72.2	27.8	1565	2
74.4	25.6	647	2.1
80.8	19.2	2062	2.1

Table 4.11 EPDM terpolymers

ENB [mol. %]	**E [mol. %]**	**P [mol. %]**	**M_w [kg/mol]**	**Đ**
0.8	62.2	37.0	530	2.2
1.1	60.2	38.7	515	2.1
1.4	59.7	38.9	353	2.6
2.1	62.9	35.0	503	2.7
2.9	61.4	35.7	394	2.7
4.4	62.7	32.9	395	2.6

4.4.3 Optimization of the solvent flow rate in the first dimension of HT 2D-LC

Interference of the solvent peak with the polymer peak may become a problem when using IR-detection in HT 2D-LC. This solvent peak could be eliminated from the chromatograms if an IR transparent solvent which is used which simultaneously supports the adsorption of the analyte. Based on our work on LAC of EPDM, possible adsorption promoting solvent candidates belong to the class to benzene derivatives like 1,3,5-trimethylbenzene, xylene and cumene [215]. The other option is to improve the separation between the peak of the solvent and analyte. Therefore, the HPLC flow rate must be optimized to separate the solvent and the analyte peak from each other in the SEC column.

SEC-traces obtained from HT 2D-LC analysis of $EPDM_{2.1}$, using different chromatographic parameters, are shown in **Fig. 4.39**.

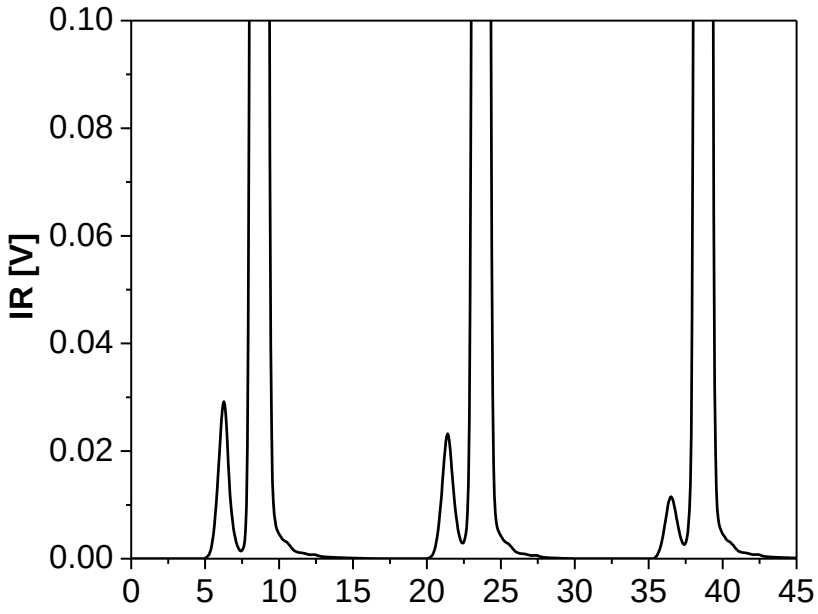

Fig. 4.39 SEC-traces of $EPDM_{2.1}$ recorded with IR5 detector (IR conc. signal) at the following flow rate in HPLC column: 0.01 mL/ min.

The peaks corresponding to 1-decanol and the polymer were well separated from each other when the HPLC flow rate was reduced to 0.01 mL/min (**Fig. 4.39b**), as this increases the time interval between two injections into the SEC column.

4.4.4 Representation of the quantitative data as a contour plot

$EPDM_{2.1}$ was analyzed with HT 2D-LC and the SEC traces are shown in **Figure 4.40a, b**. The solvent peaks were excluded and only the SEC-traces corresponding to the polymer were selected (**Fig. 4.40c**) to generate a color-coded contour plot (**Fig. 4.40d**).

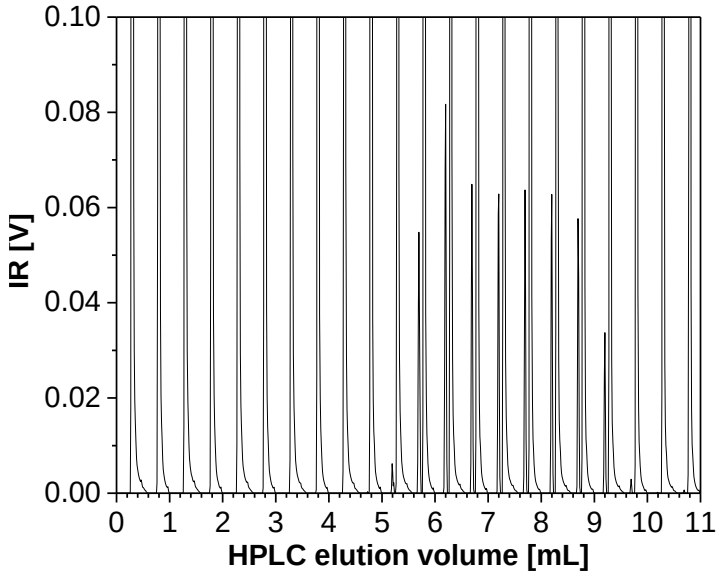

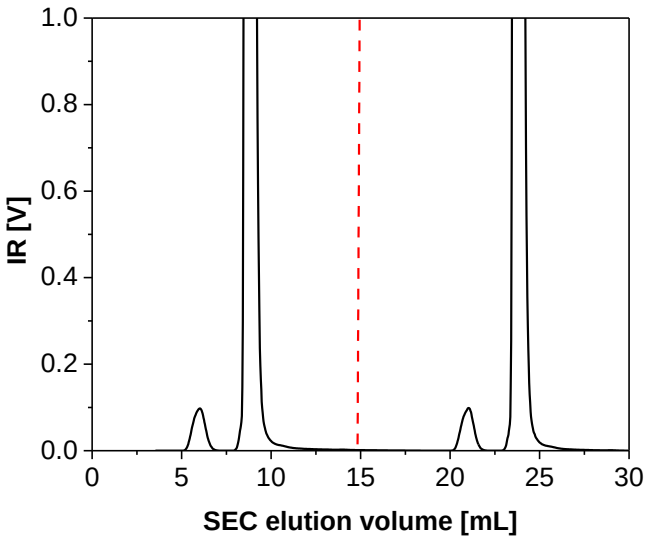
IR [V]
SEC elution volume [mL]

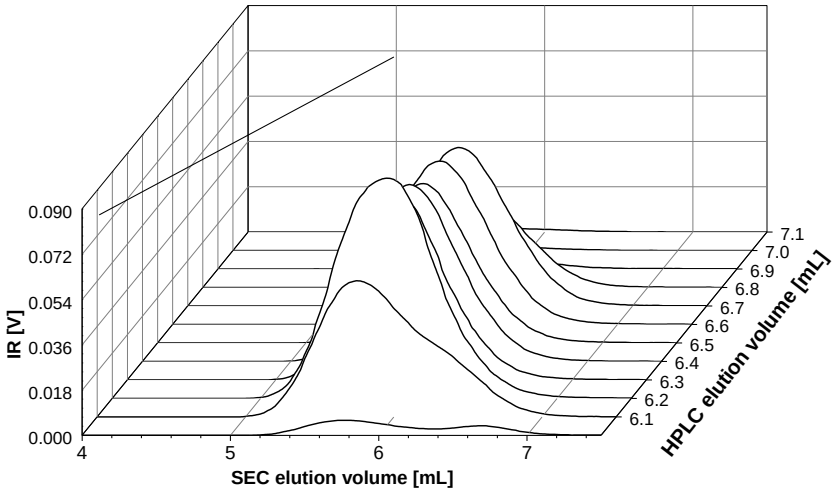
IR [V]
SEC elution volume [mL]
HPLC elution volume [mL]

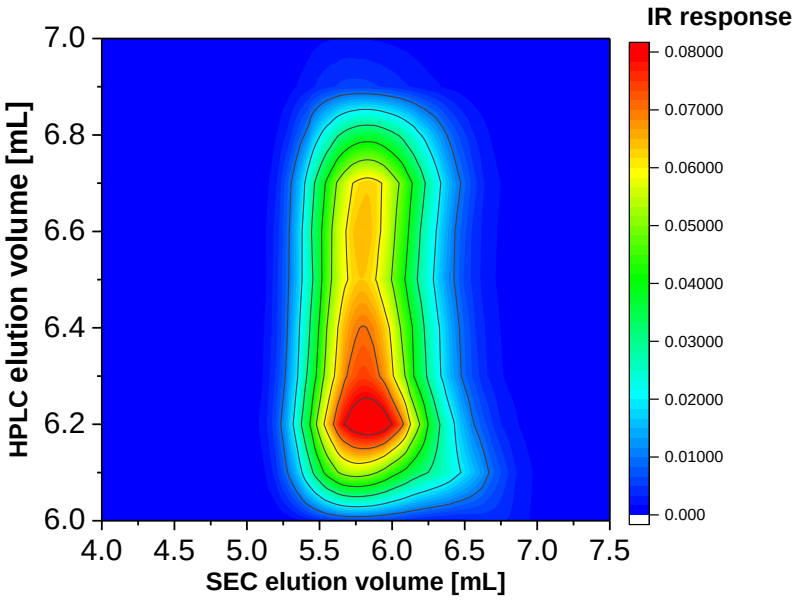
IR response
HPLC elution volume [mL]
SEC elution volume [mL]

Fig. **4.42** SEC-traces for sample $EPDM_{2.1}$: (a) Response of the IR6 (IR conc. signal); (b) zoomed at the central peaks; (c) stacked SEC-traces (fraction 61 – 72); (d) color coded contour plot. Concentration: 2 mg/mL, HPLC flow rate: 0.01 mL/min, SEC flow rate: 1.5 mL/min. 2D-LC method No. 2 was used.

$EPDM_{2.1}$ eluted in 12 fractions (fractions 61 – 72) from the HPLC column i.e., 12 SEC analyses were used for construction of the contour plot (**Fig. 4.40d**). This contour plot can be represented as a matrix with i number of rows (number of rows equal to number of points or the IR responses from one SEC analysis) and with j number of columns (number of columns equal to number of the HPLC fractions) i.e., with i × j number of elements ($E_{i,j}$). The mass of polymer, the average molar mass, and the average ENB content corresponding to each element $E_{i,j}$ as well as to each HPLC fraction can be calculated by applying corresponding calibrations (concentration of polymer vs. response of the IR detector, average molar mass vs. SEC elution volume and average ENB vs. HPLC elution volume) [224].

4.4.5 Calibrations

The mass of polymer in each element of the matrix can be calculated from a calibration, which provides the dependence between mass of the polymer and response of the IR detector. Such a calibration can be obtained by injecting solutions with different concentrations of the polymer and plotting the IR response with respect to the injected concentration. An alternate way is to inject a polymer solution with a known concentration and partition the SEC chromatogram into identical slices (e.g., 100 μL). The average IR response of the individual slice can then be plotted against the mass of analyte eluting in that slice, which can be derived from the total injected mass of the polymer.

An advantage of this approach is that only a single injection is required. A solution of sample $EPDM_{2.1}$ in 1,2,4-TCB was injected into the SEC column and the elugram of the sample is shown in **Fig. 4.41**

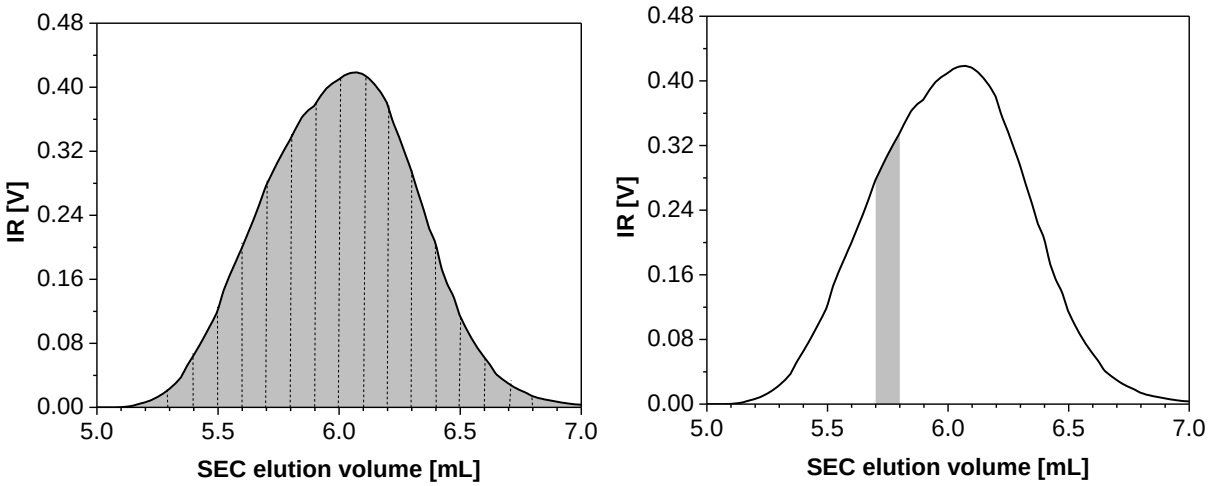

Fig. 4.41 SEC chromatogram for sample $EPDM_{2.1}$: (a) Area of the peak, (b) Area corresponding to 100µL in the 6th fraction of the chromatogram. Solvent flow rate in SEC: 1.5 mL/min, injection loop: 100 µL.

The total area of the polymer peak (**Fig. 4.41a**) corresponds to the mass of the polymer injected into the SEC column and eluted over a volume of 1200 µL. This elugram was divided into 100 µL slices (the volume of the injection loop), and the area corresponding to each volume fraction was calculated and compared with the total area of the elugram to obtain the mass of polymer eluting in each fraction (**Fig. 4.41b**). Using this method, a relation between the IR response and the mass of polymer eluted was obtained (**Fig. 4.42**).

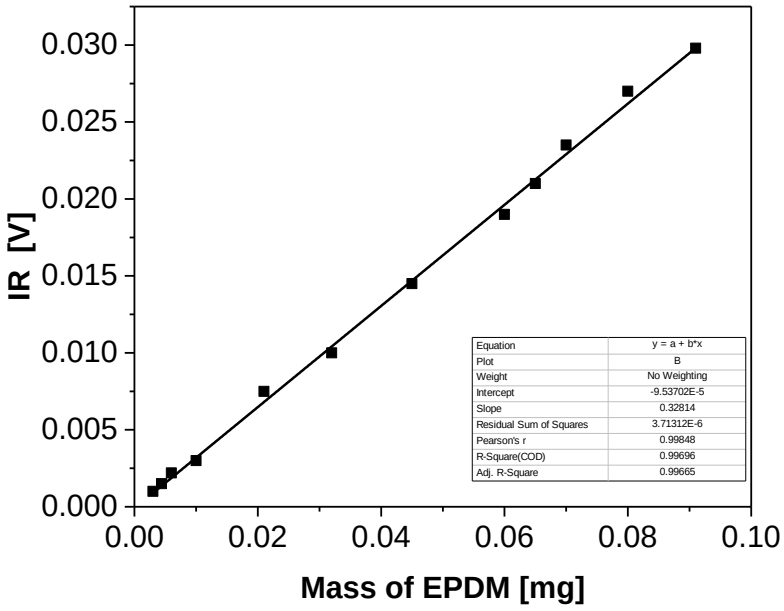

Fig. 4.42 Relation between the IR response (peak height) and the mass of sample $EPDM_{2.1}$

$$H_{i,j} = 0.3237 * m_{i,j} \quad (4.17)$$

$$m_{i,j} = H_{i,j} /(0.3237) \quad (4.18)$$

Equation 4.18 enables to calculate $m_{i,j}$, i.e., the mass of the polymer in an element $E_{i,j}$ of the matrix (i.e., in volume of one HPLC fraction = 100 μL), when an IR response ($H_{i,j}$) for that element is known.

It is crucial to know the lowest concentration of polymer which can be reliably detected to do a quantitative analysis. Thus, the limit of blank (LoB), the limit of detection (LoD) and limit of quantification (LoQ) were measured. LoB is defined as the highest apparent analyte concentration expected to be found when replicates of a sample containing no analyte are tested. Although the samples tested to define LoB do not contain analyte, a blank sample can produce an analytical signal that might otherwise be consistent with an analyte of low concentration. The LoB was estimated by measuring replicates of a blank sample (n=10) and calculating the mean value and the standard deviation (SD) [183]:

$$LoB = mean_{blank} + 1.645 \times SD_{blank} \quad (4.19)$$

Similarly, LoD was determined by using both the measured LoB and replicates of a sample known to contain a low concentration of analyte [0.1 g/L]. The median and SD of the low concentration sample is then calculated according to the following equation [183] :

$$LoD = LoB + 1.645 \times SD_{low\ concentration\ sample} \quad (4.20)$$

A Gaussian distribution of the low concentration samples was observed, 95 % of values exceeded the previously defined LoB, and only 5 % of low-concentration samples produced values below the LoB and erroneously appear to contain no analyte.

LoD was converted from absorbance [V] to concentration [mg/mL] via the calibration line, **equation 4.21** .

$$LoD\ [mg/mL] = 0.004\ mg/mL \quad (4.21)$$

LoQ is the lowest concentration at which the analyte can not only be reliably detected but at which some predefined goals for bias and imprecision are met. The LoQ may be equivalent to the LoD or it could be at a much higher concentration. For our analysis, we assumed LoQ ~ LoD [183].

The relation between the SEC elution volume and the molar mass at peak maximum (M_p) was obtained by analyzing PE standards (dissolved in 1,2,4-TCB) with the SEC column (**Fig. 4.43**).

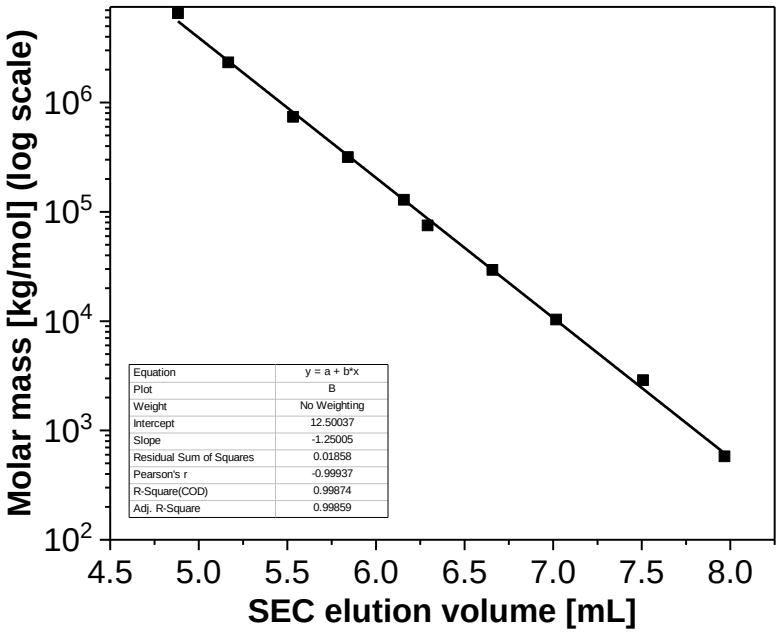

Fig 4.43 Calibration of the SEC separation with PE standards obtained with HT-SEC/IR6 (IR conc. signal): The M_p of PE standards versus elution volume. Concentration: 2 mg/mL. SEC solvent flow rate: 1.5 mL/min.

The calibration of the SEC separation is presented in **Fig.4.43** and is expressed with **equation 4.22** ($R^2 = 0.998$):

$$M_p = 12.5 - 1.25*V_{SEC} \quad (4.22)$$

Unlike the EP copolymers, the elution volume of EPDM samples is dependent on both ethylene and diene content [190, 191, 225]. For accurately characterizing the CCD of EPDM terpolymers, it is important to determine the contribution of the ENB and ethylene units to the total retention. Therefore, the SGIC approach needs to be modified in such a way as to single out the retention from the monomeric units.

Studies have shown that the content of ethylene governs the elution behavior of EP copolymers and that the retention increases linearly with the ethylene content in solvent gradient interaction chromatography, unaffected by the molar mass if it is greater than 20 kg/mol [190]. EP copolymers of varying ethylene content were injected in a 1-decanol→1,2,4-TCB gradient (**Fig. 4.44**).

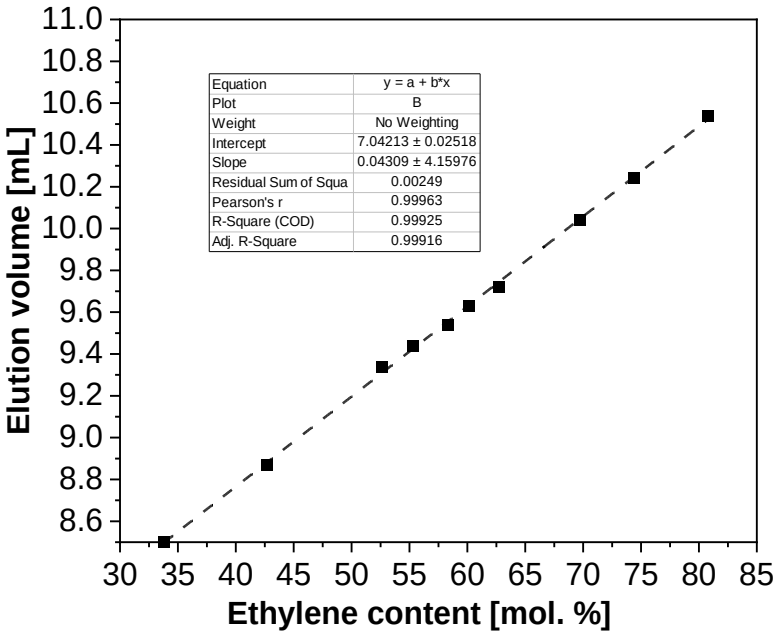

Fig. 4.44 Dependence between the elution volume and the average ethylene content in mol % of the EP copolymers. Mobile phase: 1-decanol →1,2,4-TCB.

The linear equation governing the retention of EP copolymers is valid over the entire range of chemical composition (ethylene content). Based on the equation in **Fig. 4.44**, it can be confirmed that the retention increases by 0.04309 mL when adding one mole of ethylene. Therefore, the contribution of ethylene to the total retention in an EP copolymer can be calculated by multiplying the slope of the equation (0.04309) by the mol. % of ethylene. Consequently, the contribution of ethylene to the total retention in an EPDM sample can be calculated as the ethylene content is known. It is thus postulated that the EPDM samples can be separated according to the ENB content and the distribution of ENB can be calculated. For EPDM terpolymers, it is assumed that the contribution of the ethylene units is independent from that of the diene units.

In accordance with the above discussion, the contribution of ethylene to the total retention of EPDM is subtracted. A calibration curve displaying the retention of EPDM terpolymers as a function of ENB content is shown in **Fig. 4.45**.

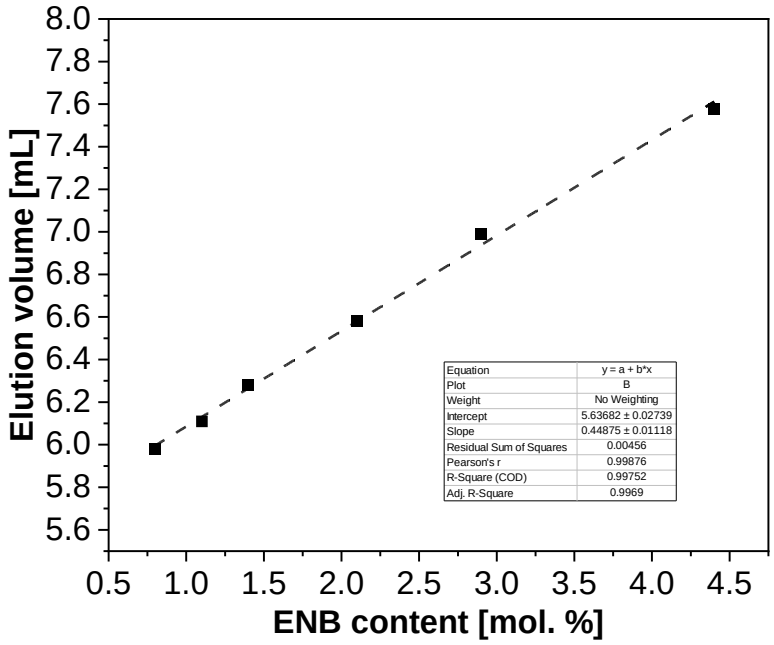

Fig. 4.45 Dependence between the modified elution volume and the average ENB content in mol. % of the EPDM terpolymers. Mobile phase: 1-decanol→1,2,4-TCB.

As seen in **Fig. 4.45**, the elution volume of EPDM samples increases linearly with ENB content with a coefficient of determination (R^2 = 0.993). This equation describes the separation of EPDM according to ENB content.

4.4.6 Matrix corresponding to a contour plot

The data presented in the form of matrices enable to perform mathematical operations with the aim to investigate differences in the molecular heterogeneities of polymers, which is not possible from the contour plots. Using the SEC and HPLC calibrations, the x and y-axes were recalculated for the contour plots of $EPDM_{2.1}$ and $EPDM_{1.4}$. In the same sense the IR response was also recalculated to the mass of polymer.

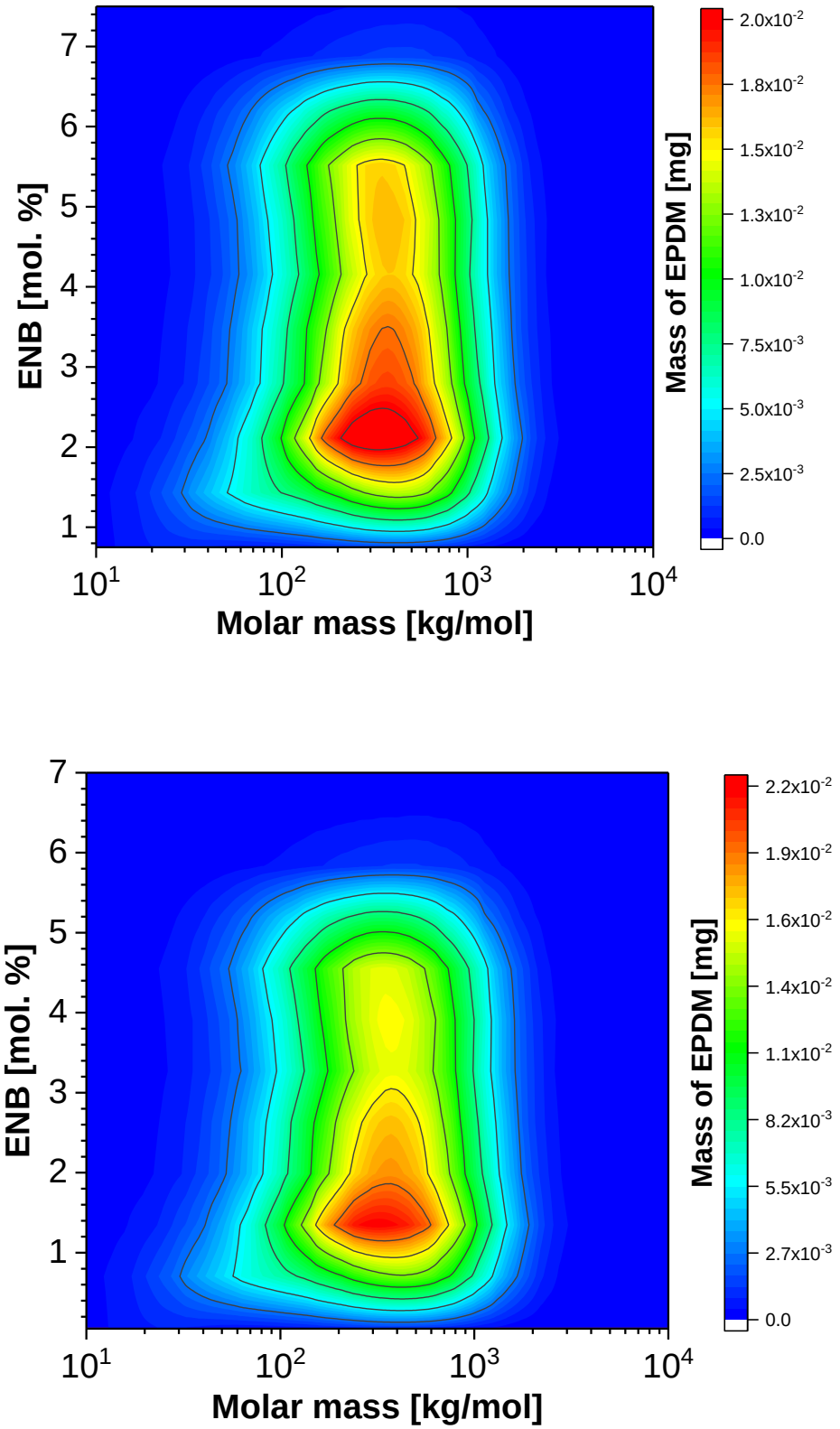

Fig. 4.46 2D-contour plot with recalculated values for (a) $EPDM_{2.1}$ (b) $EPDM_{1.4}$ Concentration: 2 mg/mL, HPLC flow rate: 0.01 mL/ min, SEC flow rate: 1.5 mL/min. 2D-LC method No. 2 was used.

4.4.7 Application of the matrix approach

The EPDM terpolymers of varying average ENB content can also contain identical segments i.e., macromolecules with identical molar mass and chemical composition. The amount of the common segments could be more extensive for the broadly distributed samples. Samples $EPDM_{2.1}$ and $EPDM_{1.4}$ were analyzed using HT 2D-LC/IR. The matrix corresponding to the contour plot for sample $EPDM_{1.4}$ was subtracted from the matrix corresponding to the contour plot of sample $EPDM_{2.1}$, to obtain information about the common segments of the two copolymers. The three-dimensional surface plots generated from this for unique and identical segments in $EPDM_{2.1}$ and $EPDM_{1.4}$ are shown below.

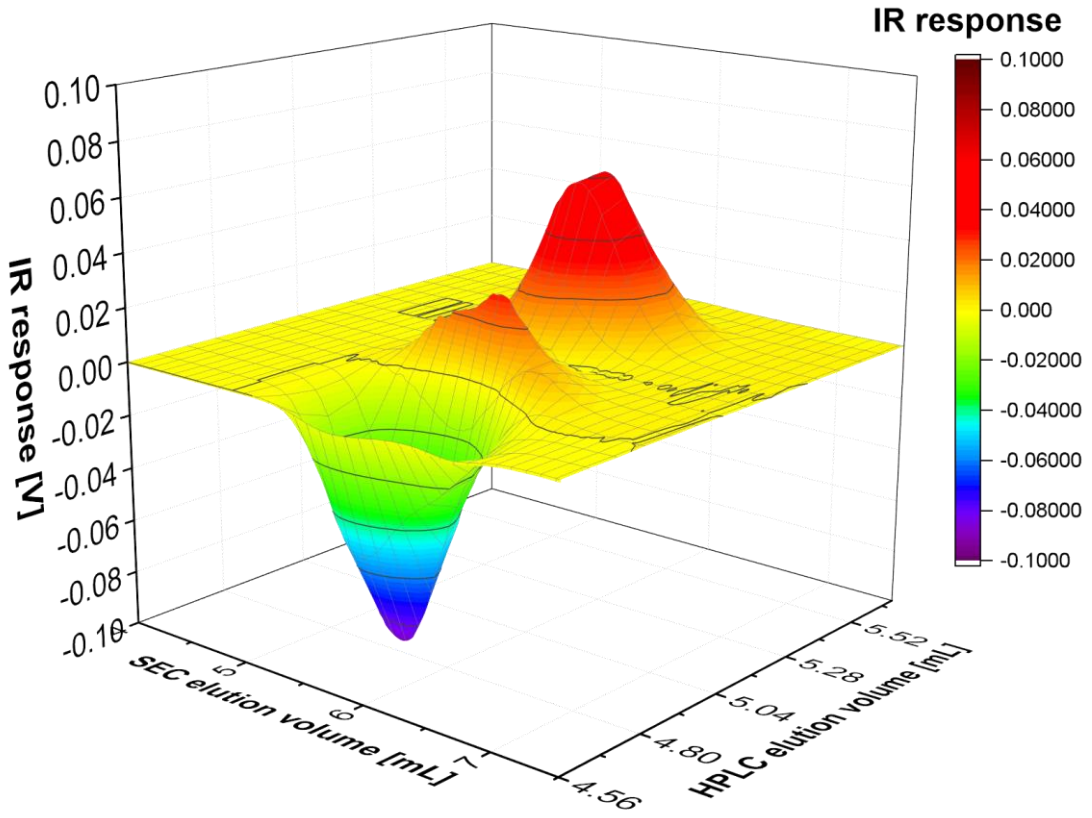

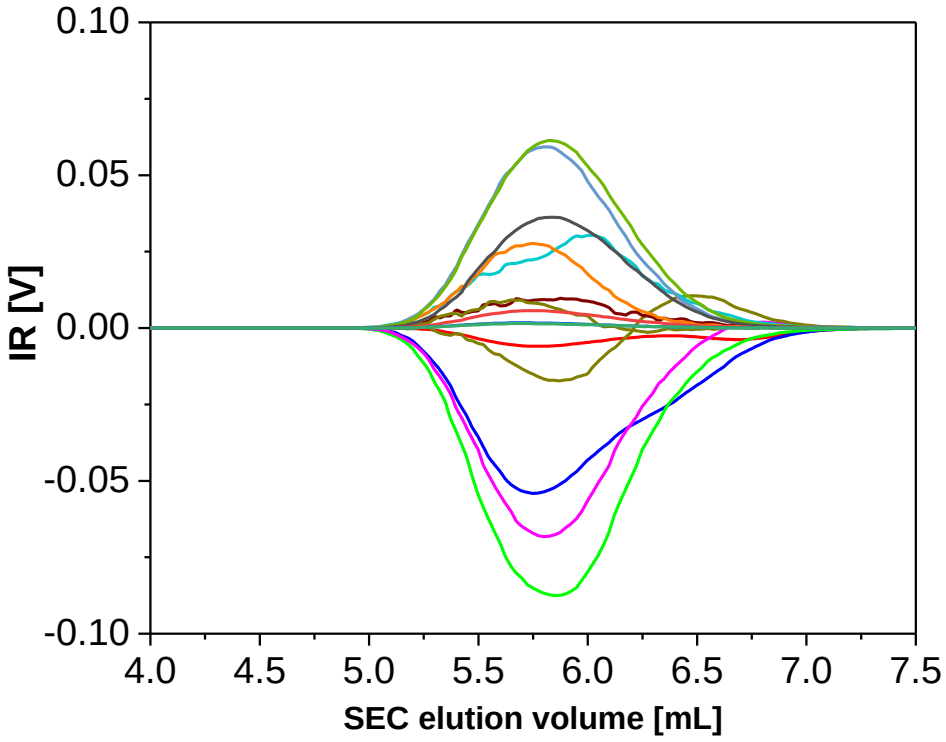

Fig. 4.47 a) Three-dimensional surface plot obtained after subtraction ($EPDM_{2.1}$ – $EPDM_{1.4}$) showing unique segments in both the terpolymers; b) Projection of the SEC elution.

The mass fraction of the identical segments in both the copolymers can be calculated by using the data from the matrices corresponding to their contour plots and the data from the subtraction matrix.

It is valid that the mass of sample $EPDM_{1.4}$ can be calculated from the corresponding matrix as sum of identical segments with mass I and unique segments with mass D1 [224]:

$$A = D_1 + I \tag{4.23}$$

The similar equation may be written for $EPDM_{2.1}$:

$$B = D_2 + I \tag{4.24}$$

where mass B may be calculated from the corresponding matrix.

Mass of both samples T may be obtained after summation of both matrices using **equation 4.24**,

$$T = A + B = D_1 + D_2 + 2I \tag{4.25}$$

while mass C can be calculated from the subtraction of matrices:

$$C = A - B = D_1 + D_2 \tag{4.26}$$

Finally, mass of the identical segments (I) in both the samples can be calculated using **equation 4.25 and 4.26**:

$$I = (T - C)/\ 2 \qquad (4.27)$$

Using **Equation 4.27** the mass fraction of identical segments in both the copolymers was determined and the corresponding contour plot is shown in **Fig. 4.48.**

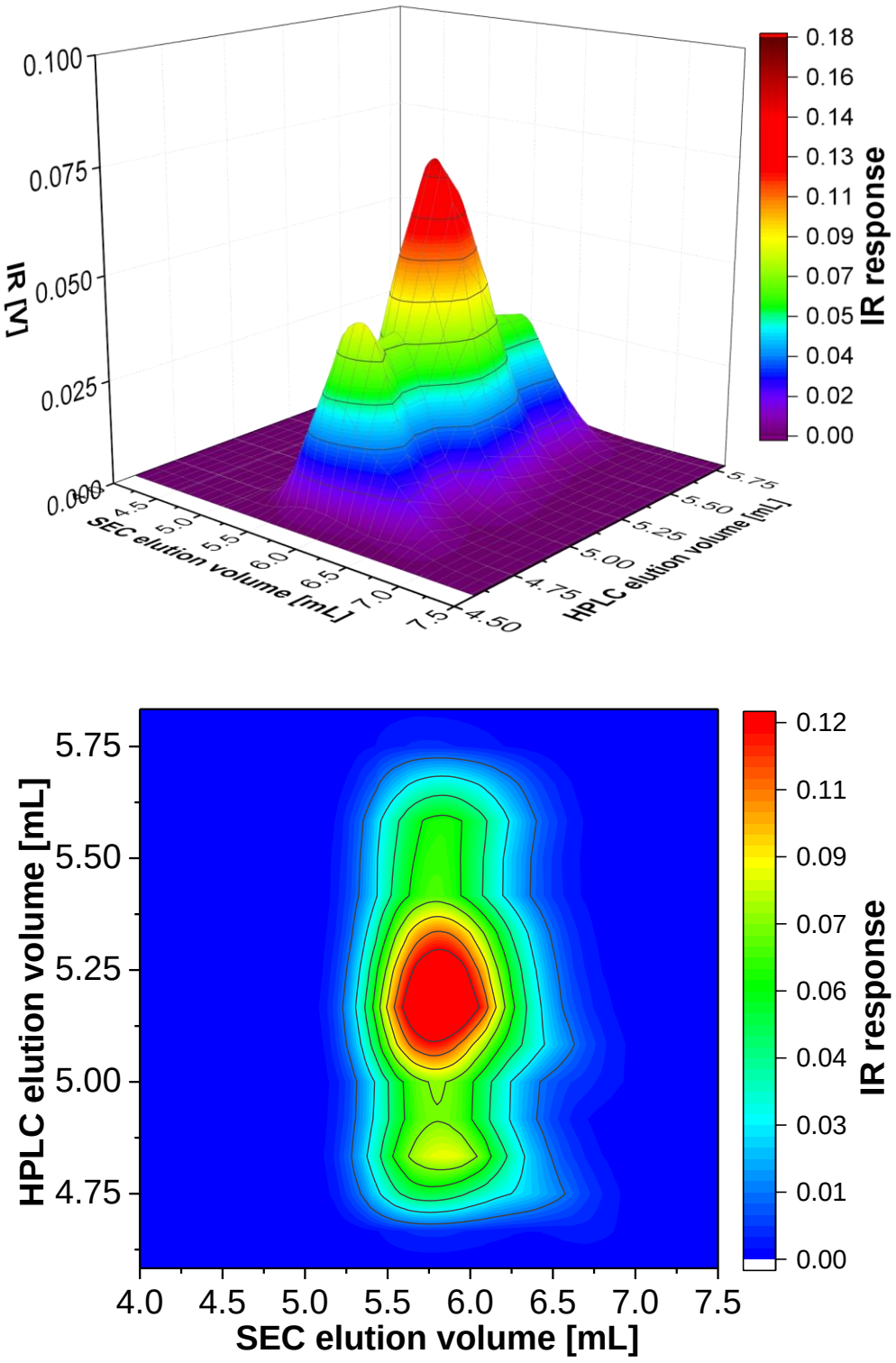

Fig. 4.48 Plots obtained after subtraction ($EPDM_{2.1} - EPDM_{1.4}$) showing the identical segments in both copolymers: (a) Three-dimensional surface plot, (b) Two-dimensional contour plot.

The number and weight average values of both the molar mass distribution (M_n, M_w) and the chemical composition distribution (ENB_n, ENB_w) were calculated using **equations 4.28- 4.31**. The Mi,j and the Hi,j values were obtained from the corresponding matrices [226].

$$M_n = [\Sigma(M)_{i,j} * H_{i,j}] / \Sigma H_{i,j} \quad (4.28)$$

$$M_w = [\Sigma(M)_{i,j}^2 * H_{i,j}] / [\Sigma(M)_{i,j} * H_{i,j}] \quad (4.29)$$

$$ENB_n = [\Sigma(ENB)_{i,j} * H_{i,j}] / \Sigma H_{i,j} \quad (4.30)$$

$$ENB_w = [\Sigma(ENB)_{i,j^2} * H_{i,j}] / [\Sigma(ENB)_{i,j} * H_{i,j}] \quad (4.31)$$

The calculated average molar mass (M) and average ENB content of the identical and unique segments are summarized in **Table 4.12**.

Polymer sample segments	$EPDM_{2.1}$ **Identical**	$EPDM_{2.1}$ **Unique**	$EPDM_{1.4}$ **Identical**	$EPDM_{1.4}$ **Unique**
Mass fraction [wt. %]	11.2	88.8	11.2	88.8
Average molar mass [kg/mol]	M_n = 122.4 M_w = 235.7	M_n = 137.9 M_w = 279.4	M_n = 122.4 M_w = 235.7	M_n = 139.6 M_w = 285.2
Average ENB [wt. %]	ENB_n = 1.42 ENB_w = 1.47	ENB_n = 2.21 ENB_w = 2.25	ENB_n = 1.42 ENB_w = 1.47	ENB_n = 1.36 ENB_w = 1.40

Data in **Table 4.12** reveal that the identical segments in both polymers have lower average molar mass compared to the unique parts. The unique segment in $EPDM_{2.1}$ has larger average chemical composition, while the unique segment of $EPDM_{1.4}$ has a lower average chemical composition in comparison with the identical segments.

The matrix approach enables to identify the identical and the unique segments within two polymers quantitatively. In this way differences in both CCD and MMD of complex polymer samples may be quantitatively visualized, evaluated and compared. Such quantitative data about differences in molecular heterogeneities are an important step towards establishing structure-property relationships.

5 Experimental

5.1 HT SEC-IR

SEC-IR analyses for the determination of the MM of the EPDM terpolymers were performed using a PolymerChar (Valencia, Spain) SEC-IR, equipped an IR 5 detector at 150 °C. The mobile phase was 1,2,4-trichlorobenzene (TCB) (Acros Organics, Schwerte, Germany) containing ~ 0.5 g/L 2,6-di-*tert*-butyl-4-methylphenol (BHT, Merck, Darmstadt, Germany) at a flow rate of 1 mL/min. Three PSS (Polymer Standards Service GmbH, Mainz, Germany) POLEFIN analytical linear XL columns (300 × 8.0 mm, L. × I.D.) were used. The molar masses have not been corrected for chemical heterogeneity. Polymer samples are separated in SEC according to their hydrodynamic volume and although the values of MW (relative to PE standards) may not be the real ones, the samples are correctly separated according to their hydrodynamic volume.

The data were evaluated using a polyethylene calibration (EasiCal PS-1, Agilent, Waldbronn, Germany) and WinGPC software version 8 (Polymer Standards Service GmbH, Mainz, Germany). For each measurement, approx. 6 mg polymer were automatically mixed with 6 mL mobile phase in an autosampler. Simultaneously, the vials were flushed with nitrogen. Each sample was dissolved under shaking in the autosampler for at least 1 h at 150 °C before injection. The resulting solutions were injected using a sample loop of 100 µL.

5.2 HT SEC – full spectrum IR

Online SEC – full spectrum IR investigations were conducted using a PL SEC 120 high temperature liquid chromatograph (Polymer Laboratories, Church Stretton, UK) equipped with an in-house built manual injection system, in which a 1 mL sample loop was installed. The mobile phase was tetrachloroethylene (purity ≥ 99 %, Merck, Darmstadt, Germany) at a flow rate of 1 mL/min. The stationary phase was one PLgel Olexis column (300 x 7.8 mm, L. x I.D., Agilent Technologies, Waldbronn, Germany). Detection was realized with a Nicolet 8700 IR (Thermo Fisher Scientific, Darmstadt, Germany) equipped with a PL-HTSEC/IR Interface (Polymer Laboratories, Church-Stretton, UK). The latter encompasses a 70 µL flow cell with CaF_2 windows. Elution times were calibrated with PS standards (Easical PS-1, Agilent, Waldbronn, Germany). A background (32 scans) was recorded before injection. Starting with injection, spectra (each encompassing 4 scans) were recorded continuously and automatically attributed to the corresponding elution times.

All components of the system were heated to 110 °C. Samples were preheated to 110 °C in an external heater and transferred to the injection system with a preheated glass syringe. Data were recorded using Omnic software (Thermo Fisher Scientific GmbH, Dreieich, Germany).

Samples were prepared at a concentration of approx. 2 g/L and later 10 g/L. For each analysis, 2 mL of the respective sample solution were introduced to the injection system. Analyses were repeated twice with independently prepared solutions to check repeatability.

5.3 High Temperature SEC-UV

High Temperature SEC-UV measurements were performed using a PolymerChar 2D-LC high-temperature chromatograph (Valencia, Spain), equipped with a 200 µL sample loop. Decahydronaphthalene (decalin, mixture of cis and trans isomers) ≥ 99 % and cyclohexane ≥ 99.7 % (VWR Chemicals, Darmstadt, Germany) were used as mobile phase at a flow rate of 1 mL/min. A PLgel Olexis column (300 × 7.8 mm, L. × I.D.), Polymer Lab., Shropshire, England) and a Perfectsil 300 Sil 5 µm silica gel column (250 × 4.6 mm, L. × I.D., MZ Analysentechnik, Mainz, Germany) was used as stationary phase.

UV spectra were recorded with an Azura DAD 2.1L UV detector (Knauer, Berlin, Germany). A UV flow cell (path length = 10 mm) was placed in the column oven heated to the selected temperature and light was transferred from/to the UV-detector via fiber optic cables. The detector measures the absorption of the sample in the region 190-400 nm at 1 Hz. For UV measurements, the sample concentration was varied from 0.05 to 10 g/L. The solvent (6 mL) was added to the solid polymer sample by the injector. Sample solutions were flushed with nitrogen and heated for 2 hours at 140 °C (decalin) or at 70 °C (cyclohexane). Most of the room temperature SEC instruments function between room temperature to 50 °C. Hence, in this regard a temperature of 70 °C is considered as high relative to the heating capability of room temperature GPC instruments. The data from the UV detector were collected and evaluated with ClarityChrom software (Knauer, Berlin, Germany).

An evaporative light scattering detector (ELSD), model Agilent 1260 Infinity II HT, was coupled to the UV detector flow cell. The nebulizer temperature and the evaporation temperature were set to 120 and 160 °C, respectively, and a nitrogen flow rate of 0.4 L/min was applied. The data from the ELSD were collected with WinGPC software (UniChrom version 8 Polymer Standards Service, Mainz, Germany). The SEC column was calibrated with polystyrene standards (EasiCal PS-1, Agilent, Waldbronn, Germany).

5.4 Sample preparation for measuring the limit of detection (LoD)

The following procedure was used to convert the LoD in absorbance units [AU] to concentration units [g/L]. Stock solutions of sample # 10 in **Table 4.1** in decalin were prepared and aliquots were pipetted out in different amounts so as to obtain concentrations ranging from 0.15 g/L to 2 g/L. For each concentration of the sample solutions, the instrument's response (peak height) was recorded.

5.5 Room temperature HPLC

The measurements were realized using a chromatographic system Agilent 1100 (Agilent, Waldbronn, Germany), comprising of an autosampler and a pump equipped with a vacuum degasser (Agilent, Waldbronn, Germany). Injection of sample solutions was performed at room temperature. For HPLC, a Hypercarb^{TM} column (100 x 4.6 mm L. x I.D., packed with porous graphite particles having diameter of 5 μm, a surface area of 120 m^2 g^{-1} and a pore size of 250 Å (Thermo Scientific, Dreieich, Germany) was used.

For sample detection, an evaporative light scattering detector (ELSD), model PL-ELS 1000 (Polymer Laboratories, Stretton, UK), was used. The nebulizer temperature and the evaporation temperature were set to 130 and 260 °C, respectively and a nitrogen flow rate of 1.5 L/min. was applied. For HPLC investigations, the following gradient was programmed: 0–3 min. 0% desorli, 3–13 min. linear gradient from 0 % to 100 % desorli, 13–15 min. 100 % desorli, 15–17 min. linear gradient from 100 % to 0 % desorli. Afterwards the column was flushed with adsorli for 25 min. to reestablish the initial adsorption conditions in the column.

The column was placed in a column oven (Waters, Milford, USA), which enables maintaining the column at temperatures up to 150 °C. The column temperature was kept at 70 °C for all HPLC measurements. A flow rate was set at 0.8 mL/min. and an ELS detector (PL ELS 1000) was used for monitoring the composition of the effluent.

To check the repeatability of LAC measurements, the five EPDM samples were 5x analyzed using a toluene→1,2,4-TCB gradient. The standard deviation of the elution volume was between ±0.0049 mL and ±0.0055, indicating good reproducibility of LAC based separations. Thus, one measurement per sample using specific experimental parameters (mobile phase, temperature, length of the solvent gradient) was realized in this study.

5.6 Isocratic elution measurements

An Agilent 1100 series HPLC system (Agilent, Waldbronn, Germany), consisting of a vacuum degasser, a quaternary gradient pump, an autosampler, a column oven and a UV-Vis diode array

detector was used for the analyses of aromatic solvents. A Hypercarb^{TM} column (100 × 4.6 mm, L. × I.D., particle diameter 5 μm, pore size 250 Å) obtained from Thermo Fisher Scientific (Dreieich, Germany) was thermostated at 30 °C. The wavelength of the UV detector was set to 254 nm. A flow rate of 1 ml/min. was used.

Solutions of the solvents with concentrations between 0.01 – 0.1 g/L were used depending on the solvent type. Each injection was measured in triplicate to check for repeatability. Retention data were repeatable to better than 2 % from run to run provided that an entire set of data were obtained over a period of 20 h. The column was checked several times by injecting a standard mixture of toluene, xylene, and 1,3,5-trimethylbenzene and monitoring their elution volume.

5.7 Raman spectroscopy

A confocal Raman microscope (WITec Alpha 500) with a frequency-doubled Nd:YAG green laser (532 nm) and a 50 × 0.8 NA objective (Zeiss EC Epiplan-Neofluar) was applied for recording the Raman spectra. The powder of neat HypercarbTM was exposed to a 5 mW laser focus and spectra were recorded with 10 accumulations of 1 s integration time. The powder loaded with solvent was drop-casted on a glass sample holder, and a glass slide cover was applied on top to prevent evaporation of the solvent. Here, 20 accumulations and 5 s integration time were used to obtain a better signal-to-noise ratio. For each sample, three Raman spectra were recorded. Cosmic ray artifacts were removed and spectra were normalized using a minmax metric, followed by smoothing with a 2nd-order Savitzky-Golay filter with a window length of 7 pixels. Then, average and standard deviation for each group of three spectra were calculated for each spectrometer channel. To accurately determine the position of carbon G bands in the Raman spectra, a Gaussian-Lorentzian sum was fitted to the peaks. The standard deviation of three independent fit positions was used as the error of position determination.

5.8 Sample preparation for Raman spectroscopy

A solution was prepared by adding the aromatic solvent into methanol. The solution was stirred for two hours with Hypercarb^{TM} particles at room temperature. The concentration of the particles and solvent was adjusted such that the final sample had high viscosity to avoid Brownian motion of the particles. The sorbent material used in the sorption experiments is the same as the one in commercial Hypercarb^{TM} HPLC columns. After the adsorption of the solvents on the Hypercarb^{TM} material was complete the solution was filtered and kept at ambient conditions for several hours.

5.9 Preparative fractionation

Fractionations were performed using a PL GPC 120 high-temperature liquid chromatograph (Polymer Laboratories, Church Stretton, England) oven. The oven was connected to an in-house built heated manual injection system consisting of a Rheodyne valve and a transfer line. The injection system was equipped with a 1000 µL sample loop. While elution times were initially determined using an ELSD, for fractionation the ELSD was replaced by an in-house built heated portable automatic fraction collector (PAFC) [227].

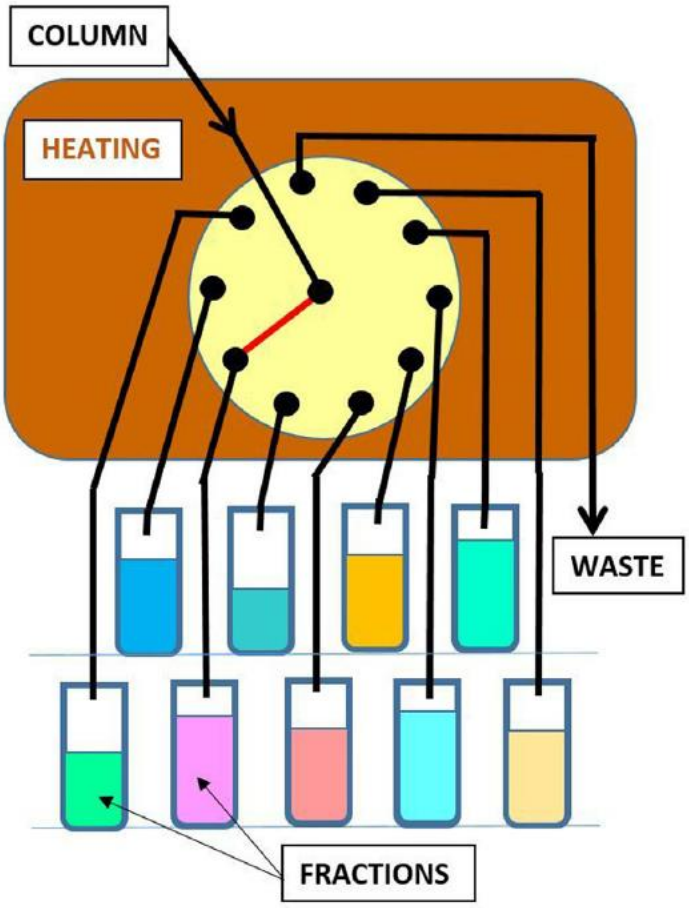

Fig. 5.1 Schematic of PAFC, based on a ten port, high temperature enabled, automatic valve, used for the fractionation of the samples [227].

Differences in capillary volume between ELSD and PAFC were found to be negligible, which enabled us to set the fractionation limits according to previously determined SGIC elution times. Fractionations were performed using concentrations of 6 g/L and the concentrations were chosen based on sample solubility. 100 injections were performed per sample and material collected from all injections was combined.

From fractionation, mixtures of polymer and solvents (1,3,5-TMB/1,2,4-TCB) were obtained. To isolate the polymer from fractionated sample solutions, ice-cold methanol was added to the

polymer-solvent mixtures. The precipitate was washed by decantation and the addition of fresh methanol (thrice) and then filtered through a 0.45 μm pore size PTFE filter. Finally, the residue was dried for three hours in vacuo (at 40 °C).

5.10 ^{1}H-NMR

^{1}H-NMR measurements were carried out using a Varian Mercury-VX 400 NMR spectrometer (9.4 Tesla, Palo Alto, US) using a 5 mm inverse probe. For bulk samples, ca. 15 mg of each EPDM terpolymer was dissolved in 0.6 mL deuterated 1,2-dichlorobenzene (ODCB- d4) at 140 °C. The ^{1}H-NMR spectra were acquired at a Larmor frequency of 400.11 MHz using a 90° excitation pulse, 64k time domain points (corresponding to an acquisition time of 2.6 s at a spectral width of 6.4 kHz), 5 s relaxation delay, and 64 scans at 120 °C. Fourier transformation was done after zero-filling the data to 64 data points in the frequency domain and exponential filtering of 0.3 Hz. For each fraction, the available amount of material was dissolved in 0.6 mL of ODCB-d_4. The number of scans was chosen based on the concentration, to achieve an acceptable signal-to-noise ratio (SNR). The other parameters were kept as stated above.

Since the intensity of the aliphatic peaks of ENB is very low, a large number of scans need to be acquired. Looking at the olefinic bond of ENB is also an option, however, longer relaxation time is needed which makes the analysis lengthier. It is thus more convenient and faster to use the ^{1}H-NMR for calculating the ENB content because of low relaxation times and a quantitative spectrum is easier/faster to obtain.

5.11 2D-LC

2D-LC measurements were conducted using a prototype instrument from PolymerChar (Valencia, Spain) equipped with an integrated IR6 detector PolymerChar (Valencia, Spain), an evaporative light scattering detector (model PL ELS 1000, Polymer Labs, Church Stretton, UK), and a binary gradient pump as well as an isocratic pump (both model 1200, Agilent, Waldbronn, Germany). Sample concentrations of 1-2 g/L in 1-decanol were used for all measurements. To achieve initial dissolution, the samples were heated in an external heater to 160 °C for about four hours. Before injection, the samples were again heated to 160 °C for 2 h in the autosampler.

The following experimental parameters were chosen. Elution temperature: 160 °C, SGIC flow rate: 0.02 mL/min, injection loop: 200 μL, SGIC stationary phase: Hypercarb^{TM} (particle ∅: 5 μm, column dimensions: 100 x 4.6 mm (L. x I.D.) (ThermoFisher Scientific, Dreieich, Germany)). A gradient 1-decanol → TCB was used with the following program: 0-200 min pure 1-decanol, 200-700 min linear gradient from 1-decanol to TCB. Then the column was

purged for 40 min with 1-decanol at a flow velocity of 0.8 mL/min in order to establish the original adsorption equilibrium in the column again. The mobile phase eluting from the Hypercarb^{TM} column was collected in 100 µL sample loops, which were injected into the SEC column (PLgel Mixed B, 300 x 7.8 mm (L. x I.D.) (Agilent Technologies, Waldbronn, Germany) in 5-minute intervals. SEC was realized in TCB at 160 °C, using a flow rate of 1.5 mL/min. Data collection was performed with WinGPC-software (version 7) from PSS (Mainz, Germany) and data evaluation with OriginPro software (version 9.2) (OriginLab Corporation, Northhampton, MA, USA).

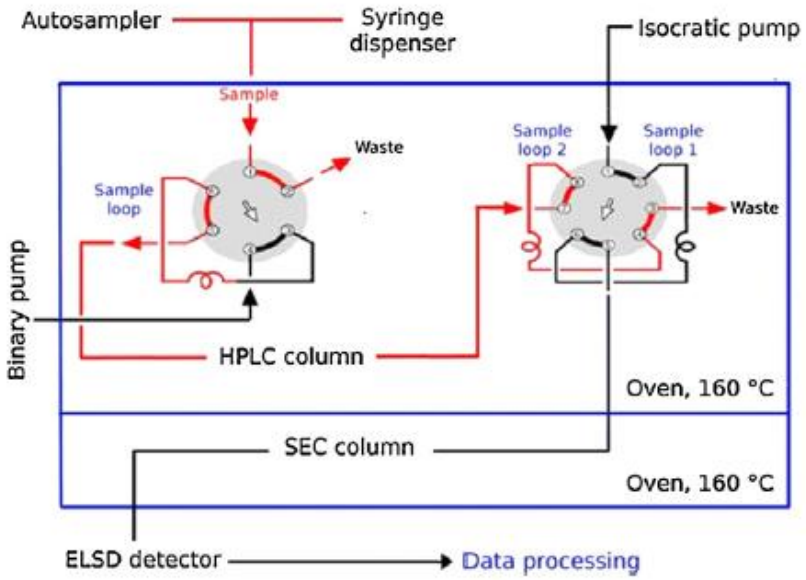

Fig. 5.2 Schematic setup of the instrument for HT 2D-LC [228]

The parameters summarized in **Table 5.1** were calculated according to the equations 5.4-5.6:

$$V_{TL} = F_{HPLC} * \Delta t \quad (5.4)$$

$$N_{HPLC} = V_{grad} / V_{TL} \quad (5.5)$$

$$t_{HT\ 2D\text{-}LC} = N_{HPLC} * \Delta t \quad (5.6)$$

Table 5.1 Parameters of HT 2D-LC measurements.

2D-LC method	F_{HPLC} [mL/min]	SEC flow rate [mL/min]	Δt [min]	V_{TL} [µL]	N_{HPLC}	$t_{HT\ 2D\text{-}LC}$ [min]
1	0.04	1.5	2.5	100	100	250
2	0.02	1.5	5	100	100	500
3	0.01	1.5	10	100	100	1000

where V_{TL} is the transfer loop volume, Δt is interval between two SEC injections, F_{HPLC} is the solvent flow rate in HPLC column, N_{HPLC} is number of HPLC fractions, V_{grad} is volume of the gradient and $t_{HT\ 2D\text{-}LC}$ is time required for one HPLC analysis.

The volume of the gradient 1-decanol → 1,2,4-TCB was kept constant (10 mL), which ensures constant selectivity of the HPLC separation. Data were collected with WinGPC unity software (PSS, Mainz, Germany) and the contour plots and matrices were generated with Origin 9.1 software.

5.12 Solvents

Decalin (mixture of *cis* and *trans* isomers, purity ≥ 99 %), cyclohexane (purity ≥ 99.7 %), 1-decanol (purity ≥ 98 %). 2-octanol (purity ≥ 98 %), n-decane (purity ≥ 95 %), n-dodecane (purity ≥ 99 %), chloroform (purity ≥ 98 %) (VWR Chemicals, Darmstadt, Germany) were used as received. Toluene, xylene isomers, 1,3,5-trimethylbenzene (1,3,5-TMB), ethylbenzene (EB), diethylbenzene (DEB), n-propylbenzene (PB), butylbenzene, amylbenzene, hexylbenzene, heptylbenzene, octylbenzene, nonylbenzene, decylbenzene. isopropylbenzene (IB), tert-butylbenzene (TB), chlorobenzene (CB), 1,3-dichlorobenzene (MDCB), 2-chlorotoluene (2-CT), 4-chlorotoluene (4-CT), tetralin, 1-chloronaphthalene (1-CN), 1,2,4-trimethylbenzene (1,2,4-TMB), 1,2,3-trimethylbenzene (1,2,3-TMB), nitrobenzene, benzaldehyde, phenol, anisole, diphenylmethane, benzonitrile, diphenyl ether were used as received. 1,2-dichlorobenzene (ODCB) and 1,2,4-trichlorobenzene (1,2,4-TCB) (for synthesis, Merck, Darmstadt, Germany) were distilled prior to use. Deuterated 1,2-dichlorobenzene (ODCB) (Eurisotop, Saint-Aubin Cedex, France) were used as received.

6 Conclusions

In the first part of this work, ethylene-propylene-diene (EPDM) terpolymers were characterized using high temperature-size exclusion chromatography coupled with an ultraviolet detector. It was observed that the double bond exhibited a UV absorbance in the 200-230 nm region with a maximum at 209 nm under the conditions employed.

The UV absorbance of $EPDM_{ENB}$ was significantly more intense $EPDM_{VNB}$ and $EPDM_{DCPD}$ at equal operating conditions, which was explained by ring strain present in the ENB comonomer. The limit of detection and the limit of quantification were calculated to demonstrate the capabilities of the UV detector in quantifying the unsaturation.

Hyphenating an evaporative light scattering detector to monitor the analyte concentration to the UV detector enabled to quantitatively profile the of unsaturation along the MMD. Monitoring the UV/ELSD ratio revealed a homogeneous distribution of ENB along the MMD as would be expected for a single site made polymer. The applicability of the dual detection technique was also demonstrated by accurately determining the ENB distribution in a polymer blend.

The second part of the investigation focused on the method development for solvent selection for liquid adsorption chromatography of EPDM terpolymers. To the best of our knowledge, this is the first time the effect of the molecular structure of the adsorption/desorption promoting solvents has been studied and comprehensively explained.

Sequential methyl substitution on the different carbon atoms of the benzene ring of the adsorli diminished the adsorption promoting capability. Furthermore, an increase in desorption strength with an increase in the number of chlorine atoms was noted. Additional substituents (di and tri) on the aromatic ring of an adsorli or desorli resulted in stronger interaction with the stationary phase and consequently reduced the retention of EPDM molecules. It was observed that the separation of samples was inversely proportional to the desorption strength of the desorli.

Additionally, the solvent-stationary phase interactions were quantified by evaluating the retention relative to benzene i.e., retention factor (log k). A retention factor, $\log k < -0.18$ was estimated for solvents to qualify as an adsorli, whereas a value higher than -0.18 indicated that the solvent is a desorli. Raman spectroscopy was employed as a supplementary tool to determine the strength of interaction between the adsorli or desorli and PGC. Based on the values of the mean G-band shift, the interactions of the benzene derivatives with PGC were as follows: 1,2,4-TCB > ODCB ~ 1,3,5-TMB > xylene > toluene.

Finally, by combining the solvent-stationary phase interaction (log k) and the solvent-polymer interactions (RED), a tool for simplifying solvent selection for LAC of EPDM was developed. For the first time, non-chlorinated solvents like tetralin, 1,2,4-trimethylbenzene and 1,2,3-trimethylbenzene were identified. The log k vs RED (SRR-HSP) plot can be customized and executed on a broader scale for solvent selection of LAC based polyolefins separation.

The third section of this work elaborated a comprehensive method to characterize the CCD of EPDM terpolymers. So far experimental conditions for liquid chromatography at critical conditions (LCCC) have never been established beyond homopolymers or block copolymers. Mobile phases for critical conditions (CC) of statistical EP copolymers were identified by employing our previous approach based on structure retention relationships and a simplified form of the Hansen solubility parameters (RED). Initially, CCs were identified by varying the composition of the binary mobile phase consisting of 1,2,4-trichlorobenzene (desorli) and 1,3,5-trimethylbenzene (adsorli).

Alternatively, by employing a single eluent, 2-chlorotoluene, the chromatographic mode of EP copolymers was modulated by varying the adsorption-desorption temperature. It was hypothesized that solvents having a retention factor between that of an adsorli and desorli were best suited for determining CC using the single-eluent approach. The identified CC were verified by the method of Cools et al., which was previously used to obtain critical conditions for polymers analyzed at ambient conditions. The critical mobile phase composition (or critical temperature) was calibrated using EP copolymers of different chemical composition.

The distribution of the pendant double bonds in the polymer chains affects the vulcanization and mechanical properties of EPDM terpolymers. While the evaluation of CCD is an ideal task for liquid chromatography of copolymers, no such method exists for terpolymers. Using the identified critical conditions based on the calibration curves, EPDM terpolymers could for the first time be separated according to their ENB content. Finally, the distribution of diene was verified through offline hyphenation of LCCC with ^{1}H NMR spectroscopy.

HT 2D-LC with IR detection was used for the quantitative analysis of EPDM terpolymer samples. The adsorption promoting solvent used in the first dimension of the HT 2D-LC was not IR transparent and gave intensive solvent peaks, which overlapped with the peaks of polymer. This problem was overcome by optimizing the solvent flow rate in the first dimension of the separation. The experimental data from 2D-LC: elution volume in HPLC, elution volume in SEC and response of the IR detector, were organized into a matrix. Calibrations of the HPLC separation with respect to chemical composition, SEC separation with respect to molar mass

and the response of IR detector with respect to mass of polymer injected were plotted to use them for quantitative analysis.

Subtraction of matrices corresponding to different EPDM terpolymer samples enabled to identify the identical and the unique segments present in the EPDM samples. Summation and subtraction of both matrices were used to calculate the mass fraction of the identical segments. MMD, CCD as well as average molar masses and average chemical compositions corresponding to the identical and unique segments were calculated and presented in numerical and graphical forms.

The described procedure holds a promise for practical application of HT 2D-LC of polyolefins, because the differences between several polymer materials with identical types of comonomers and microstructures (one sample from a set of samples of interest is chosen as a reference sample) can be compared qualitatively and quantitatively. Quantification of the common and unique segments for series of polymer samples can lead to better understanding of their structure-property relationships as well as the selectivity of catalysts.

7 Abbreviations and Symbols

CC	Critical Condition
CCD	Chemical Composition Distribution
MMD	Molar Mass Distribution
PGC	Porous graphitic carbon
ENB	2-Ethylidene-5-norbornene
VNB	Vinyl norbornene
DCPD	Dicyclopentadiene
PE	Polyethylene
PP	Polypropylene
*i*PP	Isotactic Polypropylene
*s*PP	Syndiotactic Polypropylene
*a*PP	Atactic Polypropylene
EP	Ethylene-Propylene copolymer
EPDM	Ethylene-Propylene-Diene
EO	Ethylene-Octene copolymer
PS-DVB	Poly (styrene-divinylbenzene)
HPLC	High Performance Liquid Chromatography
LAC	Liquid Adsorption Chromatography
HT-HPLC	High Temperature High Performance Liquid Chromatography
HT-LAC	High Temperature Liquid Adsorption Chromatography
SEC	Size Exclusion Chromatography
HT-SEC	High Temperature Size Exclusion Chromatography
TREF	Temperature Rising Elution Fractionation
CRYSTAF	Crystallization Analysis Fractionation
CEF	Crystallization elution fractionation

HT 2D-LC	High-Temperature Two-Dimensional Liquid Chromatography
TGIC	Temperature gradient interaction chromatography
TCB	1,2,4-trichlorobenzene
ODCB	o-dichlorobenzene
2E1H	2-ethyl-1-hexanol
IR	Infrared Detector
ELSD	Evaporative Light Scattering Detector
FTIR	Fourier Transform Infrared Spectroscopy
LCB	Long Chain Branching
SCB	Short Chain Branching
HDPE	High Density Polyethylene
EMMA	Ethylene Methyl Methacrylate
M	Molar mass
M_n	Number average molar mass
M_w	Weight average molar mass
M_p	Molar mass at peak maximum
Đ	Dispersity Index
V_R	Retention volume
K	Distribution (partition) equilibrium coefficient
ΔG	Gibbs free energy change
ΔH	Enthalpy change
ΔS	Entropy change
VTL	Transfer loop volume
F_{LAC}	Solvent flow rate in HT-LAC column
Δt	Interval between two SEC injections
N_{LAC}	Number of HT-LAC fractions

V_{grad}	Volume of the gradient
$t_{HT\ 2D\text{-}LC}$	Time required for one HT-LAC analysis
S	Standard deviation
μ	Average of the data set
N	Total number of points in the data set
$E_{i,j}$	Element of the matrix
$H_{i,j}$	IR response in an element Ei,j of the matrix
$m_{i,j}$	Mass of the polymer in an element Ei,j
$M_{i,j}$	Molar mass of the polymer in an element Ei,j
LoQ	Limit of quantification
LoB	Limit of Blank
LoD	Limit of Detection
V_{SEC}	Elution volume in SEC
D1	Mass of unique segments calculated from the matrix corresponding to EP39.8
D2	Mass of unique segments calculated from the matrix corresponding to EP59.7
ENB_n	Number average ethylene content
ENB_w	Weight average ethylene content

8 References

[1] van Doremaele, G.; van Duin, M.; Valla, M.; Berthoud, A. Kautsch. Gummi Kunstst. 70, 2017, 14-23.

[2] Ravishankar, P. S. Rubber Chem. & Technol. 85, 2012, 327-349.

[3] M. van Duin, H. Dikland, T. Früh, T. Groß, C. Haßmann, N. Sary, R. Schmidt, Eds., Handbook of synthetic rubber, ARLANXEO Deutschland, Dormagen, 2020.

[4] Morton, M. (Ed). Rubber Technology (3rd Edition), Springer, Netherlands, 1999.

[5] Allen, R.D. J. Elastom. Plast. 15, 1983, 19-32.

[6] Imanishi, Y.; Naga, M. Progr. Polym. Sci. 26, 2001, 1147-1198.

[7] Kaminsky, W.; Miri, M. J. Polym. Sci: Part A, 26, 1985, 2151-2164.

[8] van Duin M. Rub. Chem. and Tech. 74, 2001, 138-150.

[9] Dees, M.; Duin, M. Rubber World. 238, 2008, 19-25.

[10] van Doremaele, G.; van Duin, M.; Valla, M.; Berthoud, A. J. Polym. Sci., Part A, 55, 2017, 2877–2891.

[11] Ning, N., Li, S., Wu, H., Tian, H., Yao, P., Guo-Hua, H. U.; Zhang, L. Progress in Polymer Science, 79, 2018, 61-97.

[12] W. Kaminsky. J. Chem. Soc. Dalton Trans. 9, 1998, 1413-1418.

[13] Coates, J. W. Chem. Rev. 100, 2000, 1223-125.

[14] McKnight, A. L.; Waymouth, R. M. Chem. Rev. 1998, 98, 2587-2598.

[15] Kolthammer, B.W.S.; Cardwell, R.S.; Parikh, D.R. ; Edmondson, M.S.; Smith, S.W. U.S. Pat. 2003, 6,545,088.

[16] Bolton, P. D.; Mountford, P. Adv. Synth. Catal. 347, 2005, 355-366.

[17] Soares, J.B.P.; Hamielec, A.E. Polym. React. Eng. 3, 1995, 131-200.

[18] Nomura, K. Dalton Trans., 41, 2009, 8811-8823.

[19] H. Pasch, Advances in Polymer Science 128 (1997) 1.

[20] J.B.P. Soares, Fractionation, Wiley-VCH, Weinheim, 2004.

[21] W.W. Yau, D. Gillespie, Polymer 42 (2001) 8947.

[22] S. Mori, H.G. Barth, Size Exclusion Chromatography, Springer, Berlin, 1999.

[23] A.M. Striegel, W.W. Yau, J.J. Kirkland, D.D. Bly, Modern Size Exclusion Liquid Chromatography, John Wiley & Sons, Hoboken, New Jersey, 2009.

[24] H. Pasch, B. Trathnigg, HPLC of polymers, Springer, Berlin, 1997.

[25] G. Glöckner, Gradient HPLC of copolymers and chromatographic cross fractionation, Springer, Berlin, 1991.

[26] W. Radke, Structure-Property Correlation and Characterization Techniques, Wiley, Weinheim, 2007.

[27] Chitta, R., Development of High Temperature Liquid Chromatography for Chemical Composition Separation of Polyolefins. Darmstadt, Technische Universität, 2014 [Dissertation]

[28] W.W. Yau, J.J. Kirkland, D.D. Bly, Modern Size-Exclusion Liquid Chromatography, Wiley, New York, 1979.

[29] Macko, T.; Pasch, H. Macromolecules 42, 2009, 6063.

[30] B.G. Belenky, M.D. Valchikhina, I.A. Vakhtina, E.S. Gankina, O.G. Tarakanov, Journal of Chromatography 129 (1976) 115.

[31] B.G. Belenky, E.S. Gankina, M.B. Tennikov, L.Z. Vilenchik, Journal of Chromatography 147 (1978) 99.

[32] M.B. Tennikov, P.P. Nefedov, M.A. Lazareva, S.Y. Frenkel, Vysokomolekulyarnye Soedineniya, Seriya A 19 (1977) 657.

[33] H. Pasch, C. Brinkmann, Y. Gallot. (1993). Polymer, 34, 4100-4104.

[34] Hiller, W., Pasch, H., Sinha, P., Wagner, T., Thiel, J., Wagner, M., Müllen, K. (2010). Macromolecules, 43, 4853-4863.

[35] Mekap, D., Macko, T., Brüll, R., Cong, R., DeGroot, A. W., Parrott, A., Yau, W. (2013). Polymer, 54, 5518-5524.

[36] Bhati, S. S., Macko, T., Brüll, R. (2016). Journal of Chromatography A, 1451, 91-96.

[37] Bhati, S. S., Macko, T., Brüll, R., Mekap, D. (2015). Macromolecular Chemistry and Physics, 216(22), 2179-2189.

[38] L.R. Snyder, J.J. Kirkland, Introduction to Modern Liquid Chromatography, John Wiley & Sons Inc., New York, 1979.

[39] Berek, D. (1999). Macromolecules, 32(11), 3671-3673.

[40] H. Pasch, B. Trathnigg, HPLC of polymers, Springer, Berlin, 1997.

[41] B. Trathnigg, Encyclopedia of Analytical Chemistry, John Wiley & Sons Ltd., Chichester, 2000.

[42] P. Tackx, S. Bremmers, Polymeric Materials: Science and Engineering 78 (1998) 50.

[43] P.J. DesLauriers, D.C. Rohlfing, E.T. Hsieh, Polymer 43 (2002) 159.

[44] K. Ute, R. Niimi, K. Hatada, A.C. Kolbert, International Journal of Polymer Analysis and Characterization 5, 1999, 47.

[45] W. Hiller, H. Pasch, T. Macko, M. Hofmann, J. Ganz, M. Spraul, U. Braumann, R. Streck, J. Mason, F.A. Van Damme, Journal of Magnetic Resonance 183, 2006, 290.

[46] Macko, T.; Brüll, R.; Pasch, H. Chromatographia 2003, 57, S39-S43.

[47] Macko, T.; Pasch, H.; Kazakevich, Y. V.; Fadeev, A. Y. J. Chromatogr. A 2003, 988, 69-76.

[48] Mirabella, F. M.; Ford, E. A. J. Polym. Sci., Part B: Polym. Phys. 1987, 25, 777-790.

[49] Macko, T.; Pasch, H.; Denayer, J. F. J. Chromatogr. A 2003, 1002, 55-62.

[50] Heinz, L. C.; Pasch, H. Polymer 2005, 46, 12040-12045.

[51] Heinz, L. C.; Graef, S.; Macko, T.; Brull, R.; Balk, S.; Keul, H.; Pasch, H. e-Polymers 2005, 1-17.

[52] Heinz, L. C.; Macko, T.; Pasch, H.; Weiser, M. S.; Mulhaupt, R. Int. J. Polym. Anal. Charact. 2006, 11, 47-55.

[53] Cong, R.; Cheatham, C. M.; Parrott, A.; Yau, W. W.; Hazlitt, L. G.; Zhou, Z.; deGroot, A. W.; Miller, M. D. WO2012167035A2, US2011493121P, WO2012US40402A.

[54] van Damme, F.; Lyons, J.; Winniford, W. A.; deGroot, A. W.; Miller, M. D. US patent: 8076147.

[55] Winniford, W. L.; Cong, R.; Stokich, T. M.; Pell, R. J.; Miller, M.; Roy, A.; van Damme, F.; deGroot, A. W.; Lyons, J. W.; Meunier, D. M. US patent: 8318896.

[56] Macko, T.; Brüll, R.; Alamo, R. G.; Thomann, Y.; Grumel, V. Polymer 2009, 50, 5443-5448.

[57] Macko, T.; Pasch, H. Macromolecules 2009, 42, 6063-6067.

[58] Knox, J. H.; Kaur, B.; Millward, G. R. J. Chromatogr. A 1986, 352, 3-25.

[59] Berek, D. Macromol. Symp., 110 1996, 33-56.

[60] Gorshkov, A.; Much, H.; Becker, H.; Pasch, H.; Evreinov, V.; Entelis, S. J. Chromatogr. 1990, 523 91-102.

[61] Lee, W.; Cho, D.; Chang, T.; Hanley, K.; Lodge, T. Macromolecules 2001, 34, 2353-2358.

[62] van Hulst, M.; van der Horst, A.; Kok, W.; Schoenmakers, P. J. Separ. Sci. 2010, 33, 1414-1420.

[63] Sinha, P.; Hiller, W.; Bellas, V. J. Separ. Sci. 2012, 35, 1731-1740.

[64] Hehn, M.; Wagner, T.; Hiller, W. Anal. Chem. 2014, 86, 490-497.

[65] Falkenhagen, J.; Much, H.; Stauf, W.; Müller, A. Macromolecules 2000, 33, 3697-3693.

[66] Malik, M.; Sinha, P.; Bayley, G.; Mallon, P.; Pasch, H. Macromol. Chem. Phys. 2011, 212, 1221-1228.

[67] Heinz, L.; Macko, T.; Pasch, H. Int. J. Polym. Anal. Charact. 2006, 11, 47-55.

[68] Petit, C.; Luneau, B.; Beaudoin, E.; Gigmes, D.; Bertin, D. J. Chromatogr. A 2007, 1163, 128-137.

[69] Baran, K.; Laugier, S.; Cramail, H. J. Chromatogr. B 2001, 753, 139-149.

[70] Biela, T.; Duda, A.; Rode, K.; Pasch, H. Polymer 2003, 44, 1851-1860.

[71] Lee, W.; Lee, H.; Cho, D.; Chang, T.; Gorbunov, A.; Roovers, J. Macromolecules 2002, 35, 529-538.

[72] Pasch, H.; Esser, E.; Kloninger, C.; Latrou, H.; Hadjichrististidis, N. Macromol. Chem. Phys. 2001, 202, 1424-1429.

[73] Pasch, H.; Deffieux, A.; Henze, I.; Schappacher, M.; Rique-Lurbet, L. Macromolecules 1996, 29, 8776-8782.

[74] S.T. Balke, Separation and Purification Methods 11, 1982, 1.

[75] J. Adrian, E. Esser, G. Hellmann, H. Pasch, Polymer 41, 2000, 2439.

[76] V. Mass, V. Bellas, H. Pasch, Macromolecular Chemistry and Physics 209, 2008, 2026.

[77] P. Kilz, R.P. Krueger, H. Much, G. Schulz, Advances in Chemistry Series 247, 1995, 223.

[78] P. Kilz, Chromatographia 59, 2004, 3.

[79] M.I. Malik, B. Trathnigg, K. Bartl, R. Saf, Analytica Chimica Acta 658, 2010, 217.

[80] G. Glöckner, Trends in Analytical Chemistry 7, 1988, 169.

[81] D. Lee, I. Teraoka, Polymer 43, 2002, 2691.

[82] T. Lindemann, H. Hintelmann, Analytical Chemistry 74, 2002, 4602.

[83] J.P.C. Vissers, R.E.J. van Soest, J.P. Chervet, C.A. Cramers, Journal of Microcolumn Separations 11,1999, 277.

[84] J.A. Raust, A. Bruell, P. Sinha, W. Hiller, H. Pasch, Journal of Separation Science 33, 2010, 1375.

[85] A. van der Horst, P.J. Schoenmakers, Journal of Chromatography A 1000, 2003, 693.

[86] S.J. Kok, T. Hankemeier, P.J. Schoenmakers, Journal of Chromatography A 1098, 2005 104.

[87] L. Coulier, E.R. Kaal, T. Hankemeier, Journal of Chromatography A 1070, 2005, 79.

[88] R. Edam, D.M. Meunier, E.P.C. Mes, F.A. Van Damme, P.J. Schoenmakers, Journal of Chromatography A 1201, 2008, 208.

[89] J.A. Raust, A. Brüll, C. Moire, C. Farcet, H. Pasch, Journal of Chromatography A 1203, 2008, 207.

[90] B. Winther, J.L.E. Reubsaet, Journal of Separation Science 28 (2005) 477.

[91] X. Jiang, A. van der Horst, V. Lima, P.J. Schoenmakers, Journal of Chromatography A 1076, 2005, 51.

[92] S. Moyses, Journal of Separation Science 33, 2010, 1480.

[93] A. Ginzburg, T. Macko, V. Dolle, R. Brüll, Journal of Chromatography A 1217, 2010, 6867.

[94] A. Roy, M.D. Miller, M.D. Meunier, W. deGroot, W.L. Winniford, F.A. Van Damme, R.J. Pell, J.W. Lyons, Macromolecules 43, 2010, 3710.

[95] A. Ginzburg, T. Macko, V. Dolle, R. Brüll, European Polymer Journal 47, 2011, 319.

[96] D. Lee, M.D. Miller, D.M. Meunier, J.W. Lyons, J.M. Bonner, R.J. Pell, C. Li Pi Shan, T. Huang, Journal of Chromatography A 1218, 2011, 7173.

[97] Harris, R. K.; Becker, E. D.; De Menezes, S. M. C.; Goodfellow, R.; Granger, P. Pure Appl. Chem. 2001, 73, 1795-1818.

[98] Malz, F.; Jancke, H. J. Pharm. Biomed. Anal. 2005, 38, 813-823.

[99] Albrecht, A.; Brüll, R.; Macko, T.; Malz, F.; Pasch, H. Macromol. Chem. Phys. 2009, 210, 1319-1330.

[100] Zhou, Z.; Cong, R.; He, Y.; Paradkar, M.; Demirors, M.; Cheatham, M.; deGroot, A. W. Macromol. Symp. 2012, 312, 88-96.

[101] Busico, V.; Cipullo, R.; Friederichs, N.; Linssen, H.; Segre, A.; Van Axel Castelli, V.; van der Velden, G. Macromolecules 2005, 38, 6988-6996.

[102] He, Y.; Qiu, X.; Klosin, J.; Cong, R.; Roof, G. R.; Redwine, D. Macromolecules 2014, 47, 3782-3790.

[103] Busico, V.; Cipullo, R. Prog. Polym. Sci. 2001, 26, 443-533.

[104] Zhou, Z.; Stevens, J. C.; Klosin, J.; Kümmerle, R.; Qiu, X.; Redwine, D.; Cong, R.; Taha, A.; Mason, J.; Winniford, B.; Chauvel, P.; Montañez, N. Macromolecules 2009, 42, 2291-2294.

[105] Randall, J. C. J. Macromol. Sci. Part C 1989, 29, 201-317.

[106] Qiu, X.; Zhou, Z.; Gobbi, G.; Redwine, O. D. Anal. Chem. 2009, 81, 8585-8589.

[107] Wood-Adams, P. M.; Dealy, J. M.; deGroot, A. W.; Redwine, O. D. Macromolecules 2000, 33, 7489-7499.

[108] Shroff, R. N.; Mavridis, H. Macromolecules 1999, 32, 8454-8464.

[109] Shroff, R. N.; Mavridis, H. Macromolecules 2001, 34, 7362-7367.

[110] J. Hodkiewiez, Thermofischer Scientific Application note: 51946, 2012.

[111] Y. Wang, D.C. Alsmeyer, R.L. McCreery, Chemistry of Materials 2, 1990, 557.

[112] S. Reich, C. Thomsen, Philosophical Transactions of the Royal Society of London A: Mathematical, Physical and Engineering Sciences 362, 2004, 2271.

[113] J. Hodkiewiez, Thermofischer Scientific Application note: 51901, 2012.

[114] A. Sanoria, T. Schuster, R. Brüll, Analytical Methods, 2015.

[115] A.C. Ferrari, Solid state communications 143, 2007, 47.

[116] J.A. Ewen, Journal of the American Chemical Society 106, 1984, 6355.

[117] H.S. Zijlstra, S. Harder, European Journal of Inorganic Chemistry 2015, 19.

[118] G. Odian, Principles of Polymerization, Wiley, 2004.

[119] J.B. Soares, T.F. McKenna, Polyolefin Reaction Engineering, John Wiley & Sons, 2013.

[120] A. Winter, M. Antberg, V. Dolle, J. Rohrmann, W. Spaleck, Process for the preparation of an olefin polymer using metallocenes having specifically substituted indenyl ligands, US5304614 A, 1994.

[121] H. Kreyenschulte, S. Richter, T. Götze, D. Fischer, D. Steinhauser, M. Klüppel, G. Heinrich, Carbon 50, 2012, 3649.

[122] K. Subramaniam, A. Das, G. Heinrich, Composites Science and Technology 71, 2011, 1441.

[123] J.P. RABE, S. BUCHHOLZ, Science 253, 1991, 424.

[124] R. Hentschke, B.L. Schürmann, J.P. Rabe, The Journal of Chemical Physics 96, 1992, 6213.

[125] L. Askadskaya, J.P. Rabe, Physical Review Letters 69, 1992, 1395.

[126] G.T. Austin, Shreve's Chemical Process Industries, McGraw-Hill, Singapore, 1984.

[127] A. Di Corcia, S. Marchese, R. Samperi, Journal of Chromatography A 642, 1993, 163.

[128] A. Di Corcia, R. Samperi, A. Marcomini, S. Stelluto, Analytical Chemistry 65, 1993, 907.

[129] A.V. Kiselev, J.P. Jashin, Gas Adsorption Chromatography, Plenum Publishing, New York, 1969.

[130] A.V. Kiselev, N.V. Kovaleva, Y.S. Nikitin, Journal of Chromatography 58, 1971, 19.

[131] H. Colin, C. Eon, G. Guiochon, Journal of Chromatography 119, 1976, 41.

[132] H. Colin, C. Eon, G. Guiochon, Journal of Chromatography 122, 1976, 223.

[133] E. Smolková, J. Zima, F.P. Dousek, J. Jansta, Z. Plzák, Journal of Chromatography 191, 1980, 61.

[134] M.T. Gilbert, J.H. Knox, B. Kaur, Chromatographia 16, 1982, 138.

[135] P. Ciccioli, R. Tappa, A. di Corcia, A. Liberti, Journal of Chromatography 206, 1981, 35.

[136] A. Gierak, R. Leboda, Journal of Chromatography 483, 1989, 197.

[137] K. Unger, P. Roumeliotis, H. Mueller, H. Goetz, Journal of Chromatography 202, 1980, 3.

[138] D. Berek, I. Novák, Chromatographia 30, 1990, 582.

[139] T.P. Weber, P.W. Carr, Analytical Chemistry 62, 1990, 2620.

[140] T.P. Weber, P.W. Carr, E.F. Funkenbusch, Journal of Chromatography 519,1990, 31.

[141] C. Liang, S. Dai, G. Guiochon, Analytical Chemistry 75, 2003, 4904.

[142] N. Tanaka, T. Tanigawa, K. Kimata, K. Hosoya, T. Araki, Journal of Chromatography 549, 1991, 29.

[143] O. Chiantore, I. Novak, D. Berek, Analytical Chemistry 60, 1988, 638.

[144] R. Leboda, Chromatographia 13, 1980, 703.

[145] J. Kriz, E. Adamcova, J.H. Knox, J. Hora, Journal of Chromatography A 663, 1994, 151.

[146] F. Belliardo, O. Chiantore, D. Berek, I. Novak, C. Lucarelli, Journal of Chromatography 506, 1990, 371.

[147] T. Teutenberg, J. Tuerk, M. Holzhauser, S. Giegold, Journal of Separation Science 30, 2007, 1101.

[148] L. Pereira, S. Aspey, H. Ritchie, Journal of Separation Science 30, 2007, 1115.

[149] K.K. Unger, Porous Silica: Its properties and use as support in column liquid chromatography, Elsevier, Amsterdam, 1979.

[150] J.H. Knox, P. Ross, Advances in Chromatography 37, 1997, 73.

[151] M.A. Castro, S.M. Clarke, A. Inaba, R.K. Thomas, T. Arnold, Journal of Physical Chemistry B 105, 2001, 8577.

[152] P. Chaimbault, C. Elfakir, M. Lafosse, Journal of Chromatography A 797, 1998, 83.

[153] L. Pereira, Journal of Liquid Chromatography and Related Technologies 31, 2008, 1687.

[154] V. Coquart, M.C. Hennion, Journal of Chromatography 600, 1992, 195.

[155] Q.H. Wan, M.C. Davies, P.N. Shaw, D.A. Barrett, Analytical Chemistry 68, 1996, 437.

[156] E. Forgács, K. Valkó, T. Cserháti, Journal of Liquid Chromatography 14, 1991, 3457.

[157] E. Forgács, T. Cserháti, Journal of Pharmaceutical and Biomedical Analysis 10, 1992, 861.

[158] E. Forgács, T. Cserháti, Journal of Chromatography 600, 1992, 43.

[159] E. Forgács, T. Cserháti, B. Bordás, Chromatographia 36, 1993, 19.

[160] E. Forgács, T. Cserháti, Trends in Analytical Chemistry 14, 1995, 23.

[161] M.C. Hennion, V. Coquart, S. Guenu, C. Sella, Journal of Chromatography A 712, 1995, 287.

[162] P.T. Jackson, P.W. Carr, Journal of Chromatography A 958, 2002, 121.

[163] ASTM D6047-17, ASTM International, West Conshohocken, PA, 2017 10.1520/D6047-17.

[164] Deshmukh, S., Brüll, R., Macko, T., Arndt, J. H., Bernardo, R., & Niessen, S. Polymer, 242, 2022, 124585.

[165] Micheli, R.A.; Applewhite, T.H.; J. Org. Chem. 27, 1962, 345-353.

[166] Wheeler, O. H.; Mateos, J. L. The ultraviolet absorption of isolated double bonds1. J. Org. Chem., 21, 1956, 1110-1112.

[167] Dorfman, L. Ultraviolet absorption of steroids. Chem. Reviews 53, 1953, 47-144.

[168] Kirumakki, S. R.; Shpeizer, B. G.; Sagar, G. V.; Chary, K. V.; Clearfield, A. J. Catal. 242, 2006, 319-331.

[169] Gejo, J. L.; Kunjappu, J. T.; Conley, W. E., Zimmerman, P. A.; Turro, N. J. J. Micro/Nanolith., MEMS & MOEMS, 6, 2007, 033003.

[170] Zhou, Z.; Janco, M.; Cong, R.; Lee, D.; Shan, C. L.P.; Boopalachandran, P.; Shi, Z.; Miller, M. D.; Winniford, B.; Huang, T.; Herceg, E.; Salazar, I.; Pangburn, T.; Sandlin, A.; Fan, L.; Wu, J. J. Appl. Polym. Sci. 133, 2016, 43911-43921.

[171] Airinei, A.; Homocianu, M.; Dorohoi, D. O. J. Mol. Liq., 157, 2010, 13-17.

[172] Gobrecht, A.; Bendoula, R.; Roger, J. M.; Bellon-Maurel, V. Anal. Chim. Acta, 853, 2015, 486-494.

[173] Berger, S. A. Spectroscopy Letters, 1990, 23, 783-790.

[174] Tolbin, A. Y.; Pushkarev, V. E.; Tomilova, L.G.; Zefirov, N. S. Phys. Chem. & Chem. Phys. 19, 2017, 12953-12958.

[175] Moore, J.C. Separation Science, 5, 1970, 723-730.

[176] Cantow, M. J. R.; Porter, R. S.; Johnson, J. F. J. Polym. Sci., Part B, 4, 1966, 707-711.

[177] Collins, R. E. Flow of fluids through porous materials, Reinhold Publishing, New York 8, 1961, 196-200.

[178] Garcia-Rubio, G.H. Macromolecules 25, 1992, 2608-2613.

[179] Ito, M. J. Mol. Spectr. 4, 1960, 106-124.

[180] Yarborough, V. A.; Haskin, J. F.; Lambdin, W. J. Anal. Chem. 26, 1954, 1576–1578.

[181] Belter, M.; Sajnóg, A.; Barałkiewicz, D. . Talanta, 129, 2014, 606-616.

[182] Boqué, R.; Heyden, Y.V. LCGC Europe 22, 2009, 82–85.

[183] Armbruster, D. A.; Pry, T. Clin Biochem Rev.29, 2008, 49-52.

[184] Arndt, J.H.; Macko, T.; Brüll, R. J. Chromatogr. A 1310, 2013 1–14.

[185] Megoulas, N.C.; Koupparis, M.A., Crit. Rev. Anal. Chem. 35, 2005, 301–316.

[186] Jiang, X.; Lima, V.; Schoenmakers, P.J. J. Chromatogr. A 1018, 2003, 19-27.

[187] Boborodea, A.; O'Donohue, S. Int. J. Polym. Anal. & Charact. 22, 2017, 631–638.

[188] Hansen, C. M.; Durkee, J.; Kontogeorgis, G.; Panayiotou, C.; Willliams, L.; Poulsen, T.; Priebe, H.; Redelius, P. Hansen solubility parameters, 2nd ed.; Hansen, C. M., Ed.; CRC Press: Boca Raton, FL, 2007.

[189] Nielsen, T. B.; Hansen, C. M. Poly. Test. 24, 2005, 1054-1061.

[190] Chitta, R.; Macko, T.; Brüll, R.; Van Doremaele, G.; Heinz, L. C. Journal of Polymer Science Part A: Polymer Chemistry, 49, 2011, 1840-1846.

[191] Chitta, R., Ginzburg, A., van Doremaele, G., Macko, T., Brüll, R. Polymer 52, 2011, 5953-5960.

[192] Monrabal, B.; López, E.; Romero, L. Macromol. Symp. 2013, 330, 9−21.

[193] Ndiripo, A.; Albrecht, A.; Pasch, H. Anal. Chem., 92, 2020, 7325-7333.

[194] Plüschke, L.; Ndiripo, A.; Mundil, R.; Merna, J.; Pasch, H.; Lederer, A. Macromolecules, 53, 2020, 3765-3777.

[195] Arndt, J. H.; Brüll, R.; Macko, T.; Garg, P.; Tacx, J. C. J. F. Polymer 156, 2018, 214-221.

[196] Yau, W. W.; Kirkland, J. J.; Bly, D. D. Modern size-exclusion liquid chromatography: Practice of gel permeation and gel filtration chromatography; Wiley: New York, 1979.

[197] Dolan, J. W. LCGC North Am., 20, 2002 430-433.

[198] Cozzi. F.; Cinquini, M.; Annuziata, R.; Siegel, J.S. J. Am. Chem. Soc. 115, 1993, 5330-5331

[199] Hunter, C. A. Angew. Chem. Int. Ed. 32, 1993, 1584-1586.

[200] Rochefort, A.; Wuest, J. D. Langmuir, 25, 2009, 210-215.

[201] Zhou, P. P.; Zhang, R. Q. Phy. Chem. Chem. Phy., 17, 2015, 12185-12193.

[202] Elstner, M.; Hobza, P.; Frauenheim, T.; Suhai, S.; Kaxiras, E. J. of Chem. Phy. 114, 2001, 5149-5155.

[203] Wang, Y.; Alsmeyer, D. C.; McCreery, R. L. Chem. Mater. 2, 1990, 557–563.

[204] Reich, S.; Thomsen, C. Phil. Trans. R. Soc. Lond. A 362, 2004, 2271–2288.

[205] Kreyenschulte, H.; Richter, S.; Götze, T.; Fischer, D.; Steinhauser, D.; Klüppel, M.; Heinrich, G. Carbon 50,2012, 3649–3658.

[206] Subramaniam, K.; Das, K.; Heinrich, G. Compos. Sci. Tech. 71, 2011, 1441–1449.

[207] Jorio, A.; Pimenta, M. A.; Souza Filho, A. G.; Saito, R.; Dresselhaus, G.; Dresselhaus, M. S. New J. Phys. 5, 2003, 1–17.

[208] Utracki, L.; Simha, R. Poly. Int. 286, 2003, 279−286.

[209] Yu, H.; Hu, J.; Chang, J. Ind. Eng. Chem. Res. 50, 2011, 7513−7519.

[210] Cheruthazhekatt, S.; Pasch, H. Anal. Bioanal. Chem. 405, 2013, 8607–8614.

[211] Lee, D.; Miller, M. D.; Muenier, D. M; Lyons, J. W.; Bonner, J. M.; Pell, R. J. J. of Chrom. A 1218, 2011,7173-7179.

[212] Lipatov, Y. S.; Sergeeva, L. M. Adsorption of polymers. New York: John Wiley & Sons; 1974.

[213] Brun, Y. Journal of liquid chromatography related technologies, 22, 1999, 3027-3065.

[214] Brun, Y. Journal of liquid chromatography related technologies, 22, 1999, 3067-3090.

[215] S. Deshmukh, T. Macko, J.H. Arndt, B. Barton, R. Bernardo, G. van Doremaele, R. Brüll, Ind. Eng. Chem. Res. 6, 2022, 5672–5683.

[216] P.J.C.H. Cools, A.M. Van Herk, A.L. German, W. Staal, J. Liq. Chromatogr. 17, 1994, 3133-43.

[217] H.J.A. Philipsen, B. Klumperman, A.M. van Herk, A.L. German, J. Chromatogr. A 727, 199613–25.

[218] Casassa, E. F. Journal of Polymer Science Part B: Polymer Letters, 5, 1967, 773-778.

[219] Berek, D., Jančo, M., Meira, G. R. Journal of Polymer Science Part A: Polymer Chemistry, 36, 1998, 1363-1371.

[220] L.R. Snyder, J.J. Kirkland, Solvents. Introduction to Modern Liquid Chromatography, 1979.

[221] Leone, G., Zanchin, G., Di Girolamo, R., De Stefano, F., Lorber, C., De Rosa, C., ... & Bertini, F. Macromolecules, 53, 2020, 5881-5894.

[222] Y. Brun, P. Foster, J. Separ. Sci. 33, 2010, 3501–3510.

[223] Y. Brun, P. Alden, J. Chromatogr. A 966, 2002, 25–40.

[224] Bhati, S., Macko, T., & Brüll, R. Polyolefins Journal, 3, 2016, 119-133.

[225] Deshmukh, S., Macko, T., Arndt, J. H., Malz, F., Bernardo, R., Niessen, S., ... & Brüll, R. Analytica Chimica Acta, 2023, 340856.

[226] Kebritchi A, Nekoomanesh M, Mohammadi F, Khonakdar H. A. Polyolefins J, 1, 2014 117-129

[227] Arndt, J. H., Brüll, R., Macko, T., Garg, P., & Tacx, J. C. J. F. Journal of Chromatography A, 1621, 2020, 461081.

[228] Prabhu, K. N., Brüll, R., Macko, T., Remerie, K., Tacx, J., Garg, P., & Ginzburg, A. Journal of Chromatography A, 1419, 2015, 67-80.

9 Copyrights and Permissions

“Portions of **chapter 4**, **section 4.1, Figures 4.1 - 4.15** and **Table 4.1 - 4.2** were published in Polymer, Vol number 242, Subrajeet Deshmukh, Robert Brüll, Tibor Macko, Jan-Hendrik Arndt, Raffaele Bernardo, Sander Niessen. Characterization of ethylene-propylene-diene terpolymers using high-temperature size exclusion chromatography coupled with an ultraviolet detector, Page No. 124585, Copyright Elsevier, 2022/3/1.”

“Portions of **chapter 4, section 4.2, Figures 4.16 - 4.28** and **Table 4.3 - 4.5** were published in Industrial and Engineering Chemistry Research, Vol number 61, Subrajeet Deshmukh, Tibor Macko, Jan-Hendrik Arndt, Bastian Barton, Raffaele Bernardo, Gerard van Doremaele, Robert Brüll. Solvent Selection for Liquid Adsorption Chromatography of Ethylene–Propylene–Diene Terpolymers by Combining Structure–Retention Relationships and Hansen Solubility Parameters, Page No. 5672-5683, Publisher American Chemical Society, 2022/4/13.”

“Portions of **chapter 4, section 4.3, Figures 4.29 - 4.38** and **Table 4.6 - 4.9** were published in Analytica Chimica Acta, Vol number 1246, Subrajeet Deshmukh, Tibor Macko, Jan-Hendrik Arndt, Frank Malz, Raffaele Bernardo, Sander Niessen, Gerard van Doremaele, Robert Brüll. Critical conditions for liquid chromatography of statistical polyolefins: Evaluation of diene distribution in EPDM terpolymers, Page No. 340856, Copyright Elsevier, 2023/1/20.”

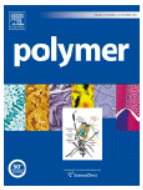

Characterization of ethylene-propylene-diene terpolymers using high-temperature size exclusion chromatography coupled with an ultraviolet detector

Author:
Subrajeet Deshmukh,Robert Brüll,Tibor Macko,Jan-Hendrik Arndt,Raffaele Bernardo,Sander Niessen

Publication: Polymer

Publisher: Elsevier

Date: 1 March 2022

Journal Author Rights

Please note that, as the author of this Elsevier article, you retain the right to include it in a thesis or dissertation, provided it is not published commercially. Permission is not required, but please ensure that you reference the journal as the original source. For more information on this and on your other retained rights, please visit: https://www.elsevier.com/about/our-business/policies/copyright#Author-rights

BACK CLOSE WINDOW

Solvent Selection for Liquid Adsorption Chromatography of Ethylene–Propylene–Diene Terpolymers by Combining Structure–Retention Relationships and Hansen Solubility Parameters

ACS Publications
Most Trusted. Most Cited. Most Read.

Author: Subrajeet Deshmukh, Tibor Macko, Jan-Hendrik Arndt, et al
Publication: Industrial & Engineering Chemistry Research
Publisher: American Chemical Society
Date: Apr 1, 2022

PERMISSION/LICENSE IS GRANTED FOR YOUR ORDER AT NO CHARGE

This type of permission/license, instead of the standard Terms and Conditions, is sent to you because no fee is being charged for your order. Please note the following:

- Permission is granted for your request in both print and electronic formats, and translations.
- If figures and/or tables were requested, they may be adapted or used in part.
- Please print this page for your records and send a copy of it to your publisher/graduate school.
- Appropriate credit for the requested material should be given as follows: "Reprinted (adapted) with permission from {COMPLETE REFERENCE CITATION}. Copyright {YEAR} American Chemical Society." Insert appropriate information in place of the capitalized words.
- One-time permission is granted only for the use specified in your RightsLink request. No additional uses are granted (such as derivative works or other editions). For any uses, please submit a new request.

If credit is given to another source for the material you requested from RightsLink, permission must be obtained from that source.

BACK CLOSE WINDOW

Critical conditions for liquid chromatography of statistical polyolefins: Evaluation of diene distribution in EPDM terpolymers

Author:
Subrajeet Deshmukh,Tibor Macko,Jan-Hendrik Arndt,Frank Malz,Raffaele Bernardo,Sander Niessen,Gerard van Doremaele,Robert Brüll

Publication: Analytica Chimica Acta

Publisher: Elsevier

Date: 15 March 2023

Journal Author Rights

Please note that, as the author of this Elsevier article, you retain the right to include it in a thesis or dissertation, provided it is not published commercially. Permission is not required, but please ensure that you reference the journal as the original source. For more information on this and on your other retained rights, please visit: https://www.elsevier.com/about/our-business/policies/copyright#Author-rights

ACS Publications
Most Trusted. Most Cited. Most Read.

Preferential Adsorption from Binary Mixtures of Short Chain n-Alkanes; The Octane−Decane System

Author: Miguel A. Castro, Stuart M. Clarke, Akira Inaba, et al
Publication: The Journal of Physical Chemistry B
Publisher: American Chemical Society
Date: Sep 1, 2001

PERMISSION/LICENSE IS GRANTED FOR YOUR ORDER AT NO CHARGE

This type of permission/license, instead of the standard Terms and Conditions, is sent to you because no fee is being charged for your order. Please note the following:

- Permission is granted for your request in both print and electronic formats, and translations.
- If figures and/or tables were requested, they may be adapted or used in part.
- Please print this page for your records and send a copy of it to your publisher/graduate school.
- Appropriate credit for the requested material should be given as follows: "Reprinted (adapted) with permission from {COMPLETE REFERENCE CITATION}. Copyright {YEAR} American Chemical Society." Insert appropriate information in place of the capitalized words.
- One-time permission is granted only for the use specified in your RightsLink request. No additional uses are granted (such as derivative works or other editions). For any uses, please submit a new request.

If credit is given to another source for the material you requested from RightsLink, permission must be obtained from that source.

BACK CLOSE WINDOW

In-depth characterization of polyolefin plastomers/elastomers (ethylene/1-octene copolymers) through hyphenated chromatographic techniques

Author: J.-H. Arndt,R. Brüll,T. Macko,P. Garg,J.C.J.F. Tacx
Publication: Journal of Chromatography A
Publisher: Elsevier
Date: 21 June 2020

Saved Quote

This quote will be kept until the Expiration Date listed below. You may complete the purchase of this Saved Quote by selecting the "Complete Purchase" option below or visiting MyAccount.copyright.com at a later time. If no action is taken before the expiration deadline this quote will expire.

Quote Number	501794144
Quote Date	Feb 16, 2023
Expiration Date	Apr 17, 2023

Licensed Content

Licensed Content Publisher	Elsevier
Licensed Content Publication	Journal of Chromatography A
Licensed Content Title	In-depth characterization of polyolefin plastomers/elastomers (ethylene/1-octene copolymers) through hyphenated chromatographic techniques
Licensed Content Author	J.-H. Arndt,R. Brüll,T. Macko,P. Garg,J.C.J.F. Tacx
Licensed Content Date	21 June 2020
Licensed Content Volume	1621
Licensed Content Issue	n/a
Licensed Content Pages	1

Order Details

Type of Use	reuse in a thesis/dissertation
Portion	figures/tables/illustrations
Number of figures/tables/illustrations	1
Format	both print and electronic
Are you the author of this Elsevier article?	No
Will you be translating?	No

About Your Work

Title	Development of new chromatographic methods for the characterization of the chemical composition distribution of EPDM copolymers
Institution name	TU Darmstadt
Expected presentation date	Jun 2023

Additional Data

Portions	Figure 1

Requestor Location

	Mr. Subrajeet Deshmukh Goethestarße
Requestor Location	Darmstadt, Hessen 64285 Germany Attn: Mr. Subrajeet Deshmukh

Price

Total	0.00 EUR

Tax Details

Publisher Tax ID	GB 494 6272 12

Quote Total: 0.00 EUR

CLOSE WINDOW COMPLETE PURCHASE

Separation of bimodal high density polyethylene using multidimensional high temperature liquid chromatography

Author: K.N. Prabhu,R. Brüll,T. Macko,K. Remerie,J. Tacx,P. Garg,A. Ginzburg
Publication: Journal of Chromatography A
Publisher: Elsevier
Date: 6 November 2015

Order Completed

Thank you for your order.

This Agreement between Subrajeet Deshmukh ("You") and Elsevier ("Elsevier") consists of your order details and the terms and conditions provided by Elsevier and Copyright Clearance Center.

License number	Reference confirmation email for license number
License date	Feb, 16 2023

Licensed Content

Licensed Content Publisher	Elsevier
Licensed Content Publication	Journal of Chromatography A
Licensed Content Title	Separation of bimodal high density polyethylene using multidimensional high temperature liquid chromatography
Licensed Content Author	K.N. Prabhu,R. Brüll,T. Macko,K. Remerie,J. Tacx,P. Garg,A. Ginzburg
Licensed Content Date	6 November 2015
Licensed Content Volume	1419
Licensed Content Issue	n/a
Licensed Content Pages	14

Order Details

Type of Use	reuse in a thesis/dissertation
Portion	figures/tables/illustrations
Number of figures/tables/illustrations	1
Format	both print and electronic
Are you the author of this Elsevier article?	No
Will you be translating?	No

About Your Work

Title	Development of new chromatographic methods for the characterization of the chemical composition distribution of EPDM copolymers
Institution name	TU Darmstadt
Expected presentation date	Jun 2023

Additional Data

Portions	Figure 2

Requestor Location

	Mr. Subrajeet Deshmukh Goethestarße
Requestor Location	Darmstadt, Hessen 64285 Germany Attn: Mr. Subrajeet Deshmukh

Tax Details

Publisher Tax ID	GB 494 6272 12

Billing Information

Billing Type	Invoice
Billing address	Mr. Subrajeet Deshmukh Goethestarße Darmstadt, Germany 64285 Attn: Mr. Subrajeet Deshmukh

Price

Total	0.00 EUR

Total: 0.00 EUR

CLOSE WINDOW

Erklärungen

§8 Abs. 1 lit. c der Promotionsordnung der TU Darmstadt

Ich versichere hiermit, dass die elektronische Version meiner Dissertation mit der schriftlichen Version übereinstimmt und für die Durchführung des Promotionsverfahrens vorliegt.

§8 Abs. 1 lit. d der Promotionsordnung der TU Darmstadt

Ich versichere hiermit, dass zu einem vorherrigen Zeitpunkt noch keine Promotion versucht wurde und zu keinem früheren Zeitpunkt an einer in- oder ausländischen Hochschule eingereicht wurde. In diesem Fall sind nähere Angaben über Zeitpunkt, Hochschule, Dissertationsthema und Ergebnis dieses Versuchs mitzuteilen.

§9 Abs. 1 der Promotionsordnung der TU Darmstadt

Ich versichere hiermit, dass die vorliegende Dissertation selbstständig und nur unter Verwendung der angegebenen Quellen verfasst wurde.

§9 Abs. 2 der Promotionsordnung der TU Darmstadt

Die Arbeit hat bisher noch nicht zu Prüfungszwecken gedient.

Darmstadt, 24 March 2023

Subrajeet Deshmukh